Stationary and oscillatory patterns of a food chain model with diffusion and predator-taxis

Renji Han[1] and Gergely Rost[2]

[1]Zhejiang University of Science and Technology
[2]University of Szeged

August 29, 2022

Abstract

In this paper, we investigate pattern dynamics in a reaction-diffusion-chemotaxis food chain model with predator-taxis, which enriches previous studies about diffusive food chain models. By virtue of diffusion semigroup theory, we first show the global classical solvability and uniform boundedness of the considered model over a bounded domain [?] R N (N [?] 1) with smooth boundary. Then the linear stability analysis for the considered model shows that chemotaxis can induce the unique positive spatially homogeneous steady state loses its stability via Turing bifurcation and Turing-spatiotemporal Hopf bifurcation, which results in the formation of two kinds of important spatiotemporal patterns: stationary Turing pattern and oscillatory pattern. Simultaneously, the threshold values for Turing bifurcation and Turing-spatiotemporal Hopf bifurcation are given explicitly. In addition, the existence and stability of non-constant positive steady state that bifurcates from the positive constant steady state is investigated by the abstract bifurcation theory of Crandall-Rabinowitz and eigenvalue perturbation theory. Finally, numerical simulations are performed to verify our theoretical results, and some interesting non-Turing pattern are found in temporal Hopf parameter space by numerical simulation.

Stationary and oscillatory patterns of a food chain model with diffusion and predator-taxis *

Renji Han[a,b]†, Gergely Röst[b]
[a] School of Science,
Zhejiang University of Science and Technology,
Hangzhou 310023, P. R. China
[b] Bolyai Institute,
University of Szeged,
Szeged H-6720, Hungary

Abstract

In this paper, we investigate pattern dynamics in a reaction-diffusion-chemotaxis food chain model with predator-taxis, which extends previous studies of reaction-diffusion food chain model. By virtue of diffusion semigroup theory, we first prove the global existence and uniform boundedness of non-negative classical solution of the model over a bounded domain $\Omega \subset \mathbb{R}^N$ $(N \geq 1)$ with smooth boundary for arbitrary predator-taxis sensitivity coefficient. Then the linear stability analysis for the considered model shows that chemotaxis can induce the unique positive spatially homogeneous steady state loses its stability via Turing bifurcation and Turing-spatiotemporal Hopf bifurcation, which results in the formation of two kinds of important spatiotemporal patterns: stationary Turing pattern and oscillatory pattern. Simultaneously, the threshold values for Turing bifurcation and Turing-spatiotemporal Hopf bifurcation are given explicitly. In addition, the existence and stability of non-constant positive steady state that bifurcates from the positive constant steady state is investigated by the abstract bifurcation theory of Crandall-Rabinowitz and eigenvalue perturbation theory. Finally, numerical simulations are performed to illustrate and support our theoretical findings, and some interesting non-Turing pattern are found in temporal Hopf parameter space by numerical simulation.

*Supported by Youth Foundation of Zhejiang University of Science and Technology (Grant No. 2021QN001), the National Research, Development and Innovation Fund of Hungary grants KKP 129877, NKFIH FK 124016, and 2020-2.1.1-ED-2020-0000.

†Corresponding author: rjhan@zust.edu.cn; rost@math.u-szeged.hu

Keywords: Reaction-diffusion food chain model; Predator-taxis; Stationary Turing pattern; Oscillatory pattern; non-constant positive steady state.

MSC(2010): 35K57, 35K59, 35B32, 35B45, 35B10, 92D25; 92D30

1 Introduction

Predation is one of the basic interspecies relationships in biology and ecology, and various mathematical models have been established to describe predator-prey interaction to predict long term outcome and impact on the entire ecosystem (see, for example, Murray[1]). Mathematical models of many biological control processes naturally require ordinary differential systems with three equations describing the growth of plant, pest and top predator (control agent), respectively. One important mathematical model of these three species is the so-called food chain model. Many papers on food chain model have been published to illustrate the importance of this multiple species interaction (see e.g. [2, 3, 4] and the related references therein).

By Fick's law, the species are distributed unevenly over space and interact with each other within the spatial domain [6, 7, 8]. Recently, spatially heterogeneous distribution of many species have been observed in some ecological systems, for example, patchiness of plankton in a minimal phytoplankton-zooplankton interaction model [9, 10], spatiotemporal pattern formation in a nutrient-plankton-fish coupled model [11].One important question is that what are the mechanisms behind the spatially heterogeneous distribution of species in a homogeneous environment? Generally, there are two categories of important mechanisms: one category is that spatial patterns emerge from locally stable kinetic dynamics due to the presence of self-diffusion [12], cross-diffusion [13, 14, 15, 16], nonlocal interactions [17, 18] and advection [19]; the other category is that spatial patterns emerge from locally unstable kinetic dynamics (such as limit cycle oscillation, chaos) through spatially inhomogeneous perturbations [20, 21].

The diffusive predator-prey model mentioned above is based on the assumption that preys and predators move randomly in their habitats, which is undirected. In reality, in addition to pure random movement of preys and predators, directed movement of predators and preys often occurs, which is reflected in the two aspects: predators pursuing preys and preys escaping from predators. As we know, the directed spatial movement of predators and preys can be classified into two kinds: one is predators move toward the gradient direction of prey distribution (called "prey-taxis"), the other is prey move opposite to the gradient of predator distribution (called "predator-taxis"). Prey-taxis problem has attracted many scholar's attention in recent years and has inspired numerous research about it. In [22], the global existence and boundedness of the solution were proved in a Keller-Segel-type chemotaxis model. In [23], the authors proved the global existence of weak solution and classical solution, respectively. Uniform persistence are proved in [25]. Boundedness and global existence or blow-up are given in [24]. A necessary conditions for pattern formation in prey-taxis system was given in [26], In [27], steady-state bifurcations and their stability results were given in a prey-taxis system with herd behaviour. In [30], the existence of non-constant positive steady states and their stability in chemotaxis model with prey-taxis in 1D were proved. Besides the fact that predators forage prey, prey may evade predators and move away from the direction of the higher predator density due to the anti-predator behaviors [32]. Very recently, Wu et. al. [31] investigated the global existence and boundedness in a reaction-diffusion predator-prey equations model with predator-taxis, and it was shown that the presence of predator-taxis can induce disappearance of spatial pattern. In [32], the authors studied pattern formation of a predator-prey model with the cost of anti-predator behavior and predator-taxis through mathematical and numerical analyses. Dai and Liu investigated global solvability for a general cross-diffusion predator-prey system with predator-taxis [33].

Functional response describes how the consumption rate of individual consumers changes with respect to resource density, and is often used to model predator-prey interactions. Recently there is a growing evidences [34, 35] that in some circumstance, especially when predator have to search for food, a more suitable mathematical model that depicts predator-prey interactions should be based on the so called ratio-dependent theory, which can be stated as that the per capita predator growth rate should be a function of prey to predator abundance, i.e., if we substitute this ratio-dependence into the standard Holling II functional response we obtain

$$f(u,v) = \frac{u/v}{u/v + c} = \frac{u}{u + cv},$$

where c is a half saturation constant.

Motivated by the above discussions, in this paper, we consider the following reaction-diffusive-chemotaxis food chain model with predator-taxis and ratio-dependent functional response:

$$\begin{cases} \frac{\partial S1}{\partial t} = D_1 \Delta S_1 + \frac{e_1 c_1 S_2 S_1}{S_2 + aS_1} - m_1 S_1, & \mathbf{x} \in \Omega,\ t > 0, \\ \frac{\partial S2}{\partial t} = \nabla \cdot (D_2 \nabla S_2 + \bar{\chi} S_2 \nabla S_1) + \frac{e_2 c_2 S_2 S_3}{S_3 + bS_2} - \frac{c_1 S_2 S_1}{S_2 + aS_1} - m_2 S_2, & \mathbf{x} \in \Omega,\ t > 0, \\ \frac{\partial S3}{\partial t} = D_3 \triangle S_3 + r_0 S_3 (1 - \frac{S_3}{K_0}) - \frac{c_2 S_2 S_3}{S_3 + bS_2}, & \mathbf{x} \in \Omega,\ t > 0, \\ \frac{\partial S_1(\mathbf{x},t)}{\partial \nu} = \frac{\partial S_2(\mathbf{x},t)}{\partial \nu} = \frac{\partial S_3(\mathbf{x},t)}{\partial \nu} = 0, & \mathbf{x} \in \partial\Omega,\ t > 0, \\ S_1(\mathbf{x}, 0) = S_{10}(\mathbf{x}) \geq 0\, S_2(\mathbf{x}, 0) = S_{20}(\mathbf{x}) \geq 0,\ S_3(\mathbf{x}, 0) = S_{30}(\mathbf{x}) \geq 0, & \mathbf{x} \in \Omega, \end{cases} \tag{1.1}$$

where $S_1(\mathbf{x}, t), S_2(\mathbf{x}, t), S_3(\mathbf{x}, t)$ represent the densities of the top predator, the predator and the prey at time t and location $\mathbf{x}$, respectively; the habitat of the three species Ω is a bounded domain in $\mathbb{R}^N$ $(N \geq 1)$ with boundary $\partial\Omega \in \mathcal{C}^1$; the homogeneous Neumann boundary conditions indicate the region with a no-flux boundary environment; $D_i, i = 1, 2, 3$ are the respective diffusion coefficients of the three species; $\bar{\chi}$ represents predator-taxis rate which reflects the repulsion effect of the predator-taxis; r_0 is the intrinsic growth rate of the prey S_3 in the absence of the predator S_2 and the top predator S_1, K_0 represents the carrying capacity of environment of the prey; $c_i, i = 1, 2, 3$ are the predation rates of the three interaction species; $e_i, i = 1, 2, 3$ are the conversion rates of the three species; a, b are half saturation constants; m_1 and m_2 are density-independent morality rates of the top predator and the predator, respectively.

To reduce the number of parameters, we start by non-dimensionalizing. Let

$$\begin{array}{c} u = \frac{abS_1}{K_0}, \quad v = \frac{bS_2}{K_0}, \quad w = \frac{S_3}{K_0}, \\ \beta_1 = \frac{e_1 c_1}{r_0}, \quad \gamma_1 = \frac{m_1}{r_0}, \quad \beta_2 = \frac{c_1}{ar_0}, \quad \gamma_2 = \frac{m_2}{r_0}, \\ \delta_1 = \frac{c_2}{br_0}, \quad \delta_2 = \frac{e_2 c_2}{r_0}, \quad \chi = \frac{K_0 \bar{\chi}}{abr_0 L^2}, \quad \hat{\mathbf{x}} = \frac{\mathbf{x}}{L}, \\ d_1 = \frac{D_1}{r_0 L^2}, \quad d_2 = \frac{D_2}{r_0 L^2}, \quad d_3 = \frac{D_3}{r_0 L^2}, \quad \hat{t} = tr_0. \end{array} \tag{1.2}$$

Here L is the spatial size of bounded domain Ω. Then the non-dimensionalized form of model (1.1), dropping the hats for $\hat{t}$ and $\hat{\mathbf{x}}$, is

$$\begin{cases} \frac{\partial u}{\partial t} = d_1 \Delta u + f(u, v, w), & \mathbf{x} \in \Omega,\ t > 0, \\ \frac{\partial v}{\partial t} = \nabla \cdot (d_2 \nabla v + \chi v \nabla u) + g(u, v, w), & \mathbf{x} \in \Omega,\ t > 0, \\ \frac{\partial w}{\partial t} = d_3 \triangle w + h(u, v, w), & \mathbf{x} \in \Omega,\ t > 0, \\ \frac{\partial u(\mathbf{x},t)}{\partial \nu} = \frac{\partial v(\mathbf{x},t)}{\partial \nu} = \frac{\partial w(\mathbf{x},t)}{\partial \nu} = 0, & \mathbf{x} \in \partial\Omega,\ t > 0, \\ u(\mathbf{x}, 0) = u_0(\mathbf{x}) \geq 0\, v(\mathbf{x}, 0) = v_0(\mathbf{x}) \geq 0,\ w(\mathbf{x}, 0) = w_0(\mathbf{x}) \geq 0, & \mathbf{x} \in \Omega, \end{cases} \tag{1.3}$$

where

$$
\begin{aligned}
f(u,v,w) &= \frac{\beta_1 vu}{v+u} - \gamma_1 u,\\
g(u,v,w) &= \frac{\delta_2 vw}{v+w} - \frac{\beta_2 vu}{u+v} - \gamma_2 v,\\
h(u,v,w) &= w(1-w) - \frac{\delta_1 vw}{v+w}.
\end{aligned}
$$

Taking $\chi = 0$ in model (1.3), Ko and Ahn [36] investigated the large time behavior of all non-negative equilibria and studied the existence of non-constant positive steady states and demonstrated the Turing pattern formation arising from diffusion-driven instability. Subsequently, the existence and non-existence of coexistence states and global attractor of unique coexistence state are proved [37]. Other work for the ratio-dependent food chain model and spatial diffusion can be found in [38, 39, 40].

An origin of reaction-diffusion-chemotaxis model (1.3) is the following non-dimensionalized ODE system suggested by S.B. Hsu et al. in [4]:

$$
\begin{cases}
\dot{x}(t) = \frac{\beta_1 xy}{x+y} - \gamma_1 x, & x(0) > 0,\\
\dot{y}(t) = \frac{\delta_2 yz}{y+z} - \frac{\beta_2 xy}{x+y} - \gamma_2 y, & y(0) > 0,\\
\dot{z}(t) = z(1-z) - \frac{\delta_1 yz}{y+z}, & z(0) > 0,
\end{cases}
$$

where x, y, z are the population densities of top predator, predator and prey respectively. The other parameters have the same meanings as those in model (1.3). The authors studied rich dynamics of boundary equilibria and unique coexist equilibrium, and multiple attractor scenario was found.

The rest of the paper is organized as follows. In Section 2 and Section 3, local and global existence and boundedness of non-negative classical solution of the considered model is established. Then linear stability analysis is carried out to interpret Turing pattern formation mechanism via Turing bifurcation and Turing-spatiotemporal Hopf bifurcation, respectively in Section 4. In Section 5, we study the existence and stability of non-constant positive solution by abstract bifurcation theory. Eventually, numerical simulations are carried out to illustrate the effectiveness of our theoretical results, and some interesting non-Turing patterns are found near temporal Hopf bifurcation threshold. In the rest of the paper, we use abbreviated notations like $\|z(t)\|_p = \|z(\cdot,t)\|_p = \|z(\cdot,t)\|_{L^p(\Omega)} = (\int_\Omega |z(x,t)|^p)^{\frac{1}{p}}$ for $p \in [1,\infty)$, $\|z(t)\|_\infty = \|z(\cdot,t)\|_\infty = \|z(\cdot,t)\|_{L^\infty(\Omega)} = \operatorname*{esssup}_{x\in\Omega} |z(x,t)|$ and $\|\cdot\|_{m,p}$ as the norm of $W^{m,p}$ with $m = 1, 2, 1 \le p \le \infty$.

2 Local Existence and Preliminaries

Let $\rho \in (N, \infty)$, then $W^{1,\rho}(\Omega, \mathbb{R}^3)$ is continuously embedded in $C(\bar{\Omega}, \mathbb{R}^3)$. We consider solutions of (1.3) in $X = \left\{\omega \in W^{1,\rho}(\Omega, \mathbb{R}^3) \middle| \frac{\partial \omega}{\partial \nu} = 0 \text{ on } \partial\Omega\right\}$. Then we have the following lemma.

Lemma 2.1 *Assume that the nonnegative initial data $(u_0, v_0, w_0) \in X$ for some $\rho > N$, and $u_0, v_0, w_0 \not\equiv 0$ in Ω. Then:*

(i) There exists a positive constant T_{max} (the maximal existence time) such that the system (1.3) has a unique classical solution $((u(\mathbf{x}, t), v(\mathbf{x}, t), w(\mathbf{x}, t)) \in X$ defined on $\Omega \times (0, T_{max})$ satisfying $(u, v, w) \in C([0, T_{max}), X) \bigcap C^{2,1}(\overline{\Omega} \times (0, T_{max}), \mathbb{R}^3)$.

(ii) There exist constants $C_1 > 0, C_2 > 0, C_3 > 0$ such that the solution of system (1.3) defined on $\Omega \times (0, T_{max})$ satisfies

$$\|u(.,t)\|_1 \leq C_1, \quad \|v(.,t)\|_1 \leq C_2, \quad \|w(.,t)\|_1 \leq C_3 \quad \text{for} \, \forall \, t \in (0, T_{max}). \tag{2.1}$$

Furthermore, there exists two constants $M_u > 0$ and $M_w > 0$ such that u, v, w satisfy

$$0 \leq u(\mathbf{x}, t) \leq M_u, \quad v(\mathbf{x}, t) \geq 0, \quad 0 \leq w(\mathbf{x}, t) \leq M_w \quad \text{for} \, \forall \, (\mathbf{x}, t) \in \Omega \times (0, T_{max}). \tag{2.2}$$

Proof Let $\mathbf{u} = (u, v, w)^T$. Then system (1.3) can be rewritten as

$$\begin{cases} \mathbf{u}_t = \nabla \cdot (\alpha(\mathbf{u}) \nabla \mathbf{u}) + \mathbf{f}(\mathbf{u}) & \text{in } \Omega \times (0, \infty), \\ \frac{\partial \mathbf{u}}{\partial \nu} = 0 & \text{on } \partial\Omega \times (0, \infty), \\ \mathbf{u}(\cdot, 0) = (u_0, v_0, w_0)^T & \text{in } \Omega, \end{cases} \tag{2.3}$$

where

$$\alpha(\mathbf{u}) = \begin{pmatrix} d_1 & 0 & 0 \\ \chi v & d_2 & 0 \\ 0 & 0 & d_3 \end{pmatrix}, \quad \mathbf{f}(\mathbf{u}) = \begin{pmatrix} u(\frac{\beta_1 v}{u+v} - \gamma_1) \\ v(\frac{\delta_2 w}{v+w} - \frac{\beta_2 u}{u+v} - \gamma_2) \\ w(1 - w - \frac{\delta_1 v}{v+w}) \end{pmatrix}. \tag{2.4}$$

Because eigenvalues of $\alpha(\mathbf{u})$ are all positive and $\alpha(\mathbf{u})$ is a triangular matrix, then system (2.3) is normally elliptic [42]. Hence local existence in (i) follows from Theorem 7.3 in [42].

Next we prove (ii). Define the operator

$$\mathcal{L}v = v_t - d_2 \Delta v - \chi \nabla \cdot (v \nabla u) - \frac{\delta_2 v w}{v + w} + \frac{\beta_2 v u}{u + v} + \gamma_2 v.$$

Because $v_0 \geq 0$ and $\frac{\partial v}{\partial \nu} = 0$, $v = 0$ is a lower solution of the v equation. Similarly, we get $u = 0$ and $w = 0$ are two lower solutions of the u and w equations, respectively. Hence

$$u(\mathbf{x}, t) \geq 0, \quad v(\mathbf{x}, t) \geq 0, \quad w(\mathbf{x}, t) \geq 0 \quad \text{for } \forall \ (\mathbf{x}, t) \in \Omega \times (0, T_{max}). \tag{2.5}$$

To further estimate $u(\mathbf{x},t), v(\mathbf{x},t)$ and $w(\mathbf{x},t)$, letting $\int_\Omega u(\mathbf{x},t) = U(t)$, $\int_\Omega v(\mathbf{x},t) = V(t)$, $\int_\Omega w(\mathbf{x},t) = W(t)$. Noting the Neumann boundary condition, we get

$$\begin{aligned}
\frac{dU}{dt} &= \int_\Omega \frac{\partial u(\mathbf{x},t)}{\partial t} = \int_\Omega u(\frac{\beta_1 v}{u+v} - \gamma_1),\\
\frac{dV}{dt} &= \int_\Omega \frac{\partial v(\mathbf{x},t)}{\partial t} = \int_\Omega v(\frac{\delta_2 w}{v+w} - \frac{\beta_2 u}{u+v} - \gamma_2),\\
\frac{dW}{dt} &= \int_\Omega \frac{\partial w(\mathbf{x},t)}{\partial t} = \int_\Omega w(1 - w - \frac{\delta_1 v}{v+w}).
\end{aligned} \tag{2.6}$$

From the third equation of (2.6), we have

$$\frac{dW}{dt} = \frac{d}{dt}\int_\Omega w(\mathbf{x},t) \le \int_\Omega (w - w^2) \le \int_\Omega w - \frac{1}{|\Omega|}\left(\int_\Omega w\right)^2, \tag{2.7}$$

which gives

$$\int_\Omega w(\mathbf{x},t) \le \max\left\{\int_\Omega w_0(\mathbf{x}), |\Omega|\right\} := C_3. \tag{2.8}$$

Since

$$\begin{cases}
\frac{\partial w}{\partial t} = d_3\triangle w + w(1 - w - \frac{\delta_1 v}{v+w}) \le d_3\triangle w + w, & \mathbf{x}\in\Omega,\ t\in(0,T_{max}),\\
\frac{\partial w}{\partial \nu} = 0, & \mathbf{x}\in\partial\Omega,\ t\in(0,T_{max}),\\
w(\mathbf{x},0) = w_0(\mathbf{x}) \ge 0, & \mathbf{x}\in\Omega.
\end{cases} \tag{2.9}$$

In view of [41, Theorem 3.1], we obtain there exists positive constant C_0 such that

$$w(\mathbf{x},t) \le C_0 \max\{1, \sup_{0\le t<T_{max}} \|w(\cdot,t)\|_1, \|w_0\|_\infty\} := M_w. \tag{2.10}$$

Then it follows from (2.6) that

$$\begin{aligned}
\frac{d(\frac{\beta_2}{\beta_1}U(t) + V(t) + W(t))}{dt} &= \int_\Omega w(1-w) + (\delta_2 - \delta_1)\int_\Omega \frac{vw}{v+w} - \gamma_2\int_\Omega v - \frac{\beta_2\gamma_1}{\beta_1}\int_\Omega u\\
&\le \frac{|\Omega|}{4} + \delta_2 M_w - \gamma_2 V(t) - \frac{\beta_2\gamma_1}{\beta_1}U(t)\\
&\le \frac{|\Omega|}{4} + \delta_2 M_w + \kappa M_w|\Omega| - \kappa(\frac{\beta_2}{\beta_1}U(t) + V(t) + W(t)),
\end{aligned}$$

where $\kappa = \min\{\gamma_1, \gamma_2\}$. This implies that

$$\frac{\beta_2}{\beta_1}U(t) + V(t) + W(t) \le \frac{|\Omega|}{4\kappa} + \frac{\delta_2 M_w}{\kappa} + M_w|\Omega| := C_2, \tag{2.11}$$

and hence

$$\|v(\cdot,t)\|_1 = V(t) \le C_2, \text{ for } \forall\, t\in(0,T_{max}). \tag{2.12}$$

We also get that there exists positive constant C_1 such that

$$\|u(\cdot,t)\|_1 = U(t) \le C_1, \text{ for } \forall\, t\in(0,T_{max}). \tag{2.13}$$

Combing (2.8), (2.12) and (2.13), it gives rise to (2.1).

Similarly, it follows from the first equation of (1.3) that

$$\begin{cases} \frac{\partial u}{\partial t} = d_1 \triangle u + u(\frac{\beta_1 v}{u+v} - \gamma_1) \leq d_1 \triangle u + \beta_1 u, & \mathbf{x} \in \Omega,\ t \in (0, T_{max}), \\ \frac{\partial u}{\partial \nu} = 0, & \mathbf{x} \in \partial\Omega,\ t \in (0, T_{max}), \\ u(\mathbf{x}, 0) = u_0(\mathbf{x}) \geq 0, & \mathbf{x} \in \Omega. \end{cases} \tag{2.14}$$

From [41, Theorem 3.1], we obtain there exists positive constant $\tilde{C}_0$ such that

$$u(\mathbf{x}, t) \leq \tilde{C}_0 \max\{1, \sup_{0 \leq t < T_{max}} \|u(\cdot, t)\|_1, \|u_0\|_\infty\} := M_u. \tag{2.15}$$

Combing (2.5), (2.10) and (2.15), it gives rise to (2.2), and thus we complete the proof of part (ii). ■

Next we recall some preliminary results which will be used in the sequel. First we review some well-known results about the diffusion semigroup with homogeneous Neumann boundary conditions (see [22]). For $p \in (1, \infty)$, Denote by A the sectorial operator defined by

$$Au := -\Delta u \quad \text{for} \quad u \in D(A) := \left\{ \varphi \in W^{2,p}(\Omega) : \frac{\partial \varphi}{\partial \nu} = 0 \text{ on } \partial\Omega \right\}. \tag{2.16}$$

The spectrum of A is a countable set of nonnegative real numbers $0 = \lambda_1 < \lambda_2 \leq \lambda_3 \leq \cdots$ and $p-$independent. Denote $\mathbb{X} = L^p(\Omega)$ for $p \in (1, \infty)$. In view of [44, Theorem 7.3.6], $A + 1$ is a sectorial operator defined on $\mathbb{X}$ and the spectrum of $A+1$ is contained in $[1, \infty)$, and thus the operator $-(A + 1)$ is the infinitesimal generator of an analytic semigroup of contractions on $L^p(\Omega)$. Hence we can define the fractional power $(A+1)^\theta \triangleq ((A+1)^{-\theta})^{-1}$ and the fractional power space $\mathbb{X}^\theta \triangleq D((A + 1)^\theta)$ for $\theta \geq 0$ with graph norm $\|x\|_\theta = \|(A+1)^\theta x\|_{\mathbb{X}}$ for $\forall\, x \in \mathbb{X}^\theta$.

In the following, we collect some properties of A which can be found in [22], and these properties also hold for A_d which is defined as $A_d u = -d\Delta u$ with a scaling.

Lemma 2.2 *[22]*

(i) Assume that $k \in \{0, 1\}$, $p \in (1, \infty)$ and $q \in [1, \infty]$. Then there exists some positive constant C_4 such that

$$\|u\|_{k,q} \leq C_4 \|(A + 1)^\theta u\|_p, \tag{2.17}$$

for any $u \in D((A + 1)^\theta)$, where $\theta \in (0, 1)$ satisfies

$$k - \frac{n}{q} < 2\theta - \frac{n}{p},\ q \geq p.$$

(ii) $\|(A + 1)^\theta e^{-t(A+1)} u\|_{L^p(\Omega)} \leq C_5 t^{-\theta} e^{-\mu t} \|u\|_{L^p(\Omega)}$ for all $u \in L^p(\Omega)$, any $t > 0$ and some $\mu > 0$ and constant $C_5 > 0$.

(iii) For $1 \le p < q < \infty$, there exists $C_6 > 0$ and $\mu > 0$ such that for all $u \in L^p(\Omega)$ the general $L^p - L^q$ estimate

$$\|(A+1)^{\theta} e^{-t(A+1)} u\|_q \le C_6 t^{-\theta - \frac{n}{2}(\frac{1}{p} - \frac{1}{q})} e^{-\mu t} \|u\|_p, \tag{2.18}$$

holds for any $t > 0$ and $\theta \ge 0$, where the associated diffusion semigroup $\{e^{-t(A+1)}\}_{t \ge 0}$ maps $L^p(\Omega)$ into $D((A+1)^{\theta})$.

3 Global existence and boundedness

In this section, we shall prove the global existence and boundedness for the considered model (1.3). First we need to establish a uniform bound of $\nabla u(x,t)$ in $L^{\infty}(\Omega)$ for any $t \in (0, T_{max})$. Then the standard Morse-Alikakos iteration technique is employed to obtain the L^{∞} bound of $v(x,t)$. Finally, we get the global existence of the solution of system (1.3) by Amann's argument [42, 43].

Lemma 3.1 *Let (u,v,w) be a solution defined on $\Omega \times [0, T_{max})$ of system (1.3). Then there exists a positive constant M_v such that*

$$\|v(\cdot,t)\|_{\infty} \le M_v \quad \text{for } \forall\ t \in (0, T_{max}). \tag{3.1}$$

Proof We first write the third equation of (1.3) as follows

$$u_t - d_1 \Delta u + u = \varphi(u,v,w), \tag{3.2}$$

where $\varphi(u,v,w) = \frac{\beta_1 uv}{u+v} - \gamma_1 u + u$. Then applying the variation of constants formula on (3.2) gives

$$u(\cdot,t) = e^{-t(A_{d_1}+1)} u_0 + \int_0^t e^{-(t-s)(A_{d_1}+1)} \varphi(u(\cdot,s), v(\cdot,s), w(\cdot,s)) ds. \tag{3.3}$$

Choosing $p > n$ and $\theta \in (\frac{1}{2}(1 + \frac{n}{p}), 1)$ and letting $k = 1, q = \infty$ in (2.17). Let ε be fixed arbitrary positive constant. Then from (2.17) and Sobolev embedding $L^{\infty}(\Omega) \hookrightarrow L^p(\Omega)$, for all $t \in (\varepsilon, T_{max})$, there exist positive constants C_8, C_9, C_{10} and $\mu > 0$ such that

$$
\begin{aligned}
\|u(\cdot,t)\|_{1,\infty} \leq & C_4\|(A_{d_1}+1)^{\theta}u(\cdot,t)\|_p \\
\leq & C_8\int_0^t (t-s)^{-\theta}e^{-\mu(t-s)}\|u(\cdot,s)\big(\frac{\beta_1 v(\cdot,s)}{u(\cdot,s)+v(\cdot,s)}-\gamma_1\big)+u(\cdot,s)\|_p ds \\
& + C_8\|(A_{d_1}+1)^{\theta}e^{-(A_{d_1}+1)t}u_0\|_p \\
\leq & C_9\int_0^t (t-s)^{-\theta}e^{-\mu(t-s)}\|u(\cdot,s)\|_{\infty}ds + C_9 t^{-\theta}e^{-\mu t}\|u_0\|_p \\
\leq & C_{10}\int_0^{\infty} \varrho^{-\theta}e^{-\mu\varrho}d\varrho + C_{10}\varepsilon^{-\theta}\|u_0\|_p \\
\leq & C_{10}\big(\varepsilon^{-\theta}\|u_0\|_p + \frac{\Gamma(1-\theta)}{\mu^{1-\theta}}\big) := G,
\end{aligned}
\tag{3.4}
$$

which implies that $\|\nabla u(\cdot,t)\|_{L^{\infty}(\Omega)} \leq G$ for all $t \in (0, T_{max})$.

Next, for any $k \geq 2$, multiplying the second equation of (1.3) by v^{k-1} and integrating by parts and combining Young's inequality yields

$$
\begin{aligned}
& \frac{1}{k}\frac{d}{dt}\int_{\Omega} v^k + (k-1)d_2\int_{\Omega} v^{k-2}|\nabla v|^2 \\
& = -(k-1)\chi\int_{\Omega} v^{k-1}\nabla v\cdot\nabla u + \int_{\Omega} v^k\big(\frac{\delta_2 w}{v+w}-\frac{\beta_2 u}{u+v}-\gamma_2\big) \\
& \leq (k-1)\chi G\int_{\Omega} v^{k-1}|\nabla v| + \delta_2\int_{\Omega} v^k \\
& \leq \frac{(k-1)d_2}{2}\int_{\Omega} v^{k-2}|\nabla v|^2 + \frac{(k-1)\chi^2 G^2}{2d_2}\int_{\Omega} v^k + \delta_2\int_{\Omega} v^k.
\end{aligned}
\tag{3.5}
$$

From (3.5), we obtain

$$
\frac{1}{k}\frac{d}{dt}\int_{\Omega} v^k + \frac{(k-1)d_2}{2}\int_{\Omega} v^{k-2}|\nabla v|^2 \leq \frac{(k-1)\chi^2 G^2}{2d_2}\int_{\Omega} v^k + \delta_2\int_{\Omega} v^k. \tag{3.6}
$$

Finally, since $\|v(\cdot,t)\|_1 \leq C_2$, applying the standard Moser-Alikakos iteration technique [41] on (3.6), we obtain the finiteness of $\|v(\cdot,t)\|_{\infty}$ for all $t \in (0, T_{max})$, and thus the proof is completed. ■

In view of Amann's argument [42, 43], we can draw the main conclusions about the global existence and boundedness of solutions to the spatial system (1.3) as follows

Theorem 3.2 *Let Ω be a bounded domain in $\mathbb{R}^N$ with boundary $\partial\Omega \in \mathcal{C}^1$. Suppose that the conditions of Lemma 2.1 are satisfied. Then system (1.3) has a unique positive global classical solution $((u(\mathbf{x},t), v(\mathbf{x},t), w(\mathbf{x},t)) \in X$ defined on $\Omega \times [0,\infty)$ satisfying $(u,v,w) \in C([0,\infty), X)\bigcap C^{2,1}(\overline{\Omega}\times(0,\infty), \mathbb{R}^3)$, and $(u(\mathbf{x},t), v(\mathbf{x},t), w(\mathbf{x},t))$ is bounded in $\Omega \times (0,\infty)$, that is, there exists a positive constant M_0 such that $\|u(\cdot,t)\|_{\infty} + \|v(\cdot,t)\|_{\infty} + \|w(\cdot,t)\|_{\infty} \leq M_0$.*

4 Stability of spatially homogeneous steady state

4.1 Stability analysis of the corresponding ODE

To investigate Turing instability of the spatial system (1.3), it is necessary to analyze the stability of the corresponding temporal system:

$$\begin{cases} \dot{u}(t) = u(\frac{\beta_1 v}{u+v} - \gamma_1), \\ \dot{v}(t) = v(\frac{\delta_2 w}{v+w} - \frac{\beta_2 u}{u+v} - \gamma_2), \\ \dot{w}(t) = w(1 - w - \frac{\delta_1 v}{v+w}). \end{cases} \tag{4.1}$$

4.1.1 Existence of equilibria

In this subsection, we shall give the existence and uniqueness of positive equilibrium for system (4.1) by analytical methods. Clearly system (4.1) has one extinction equilibrium $E_0 := (0,0,0)$, one semi-trivial equilibria $E_1 := (0,0,1)$, one boundary equilibrium $E_2 := \left(0, \frac{(\delta_2-\gamma_2)(\delta_2-\delta_1\delta_2+\delta_1\gamma_2)}{\gamma_2\delta_2}, \frac{\delta_2-\delta_1\delta_2+\delta_1\gamma_2}{\delta_2}\right)$ with $\delta_2 > \max\{\gamma_2, \delta_1\delta_2 - \delta_1\gamma_2\}$. Biologically, we are interested in positive equilibrium. In view of [4], system (4.1) has a unique positive equilibrium $E_* := (u_*, v_*, w_*) = (\frac{\beta_1-\gamma_1}{\gamma_1}, \frac{w_*(1-w_*)}{\delta_1-(1-w_*)}, \frac{1}{\alpha}(\delta_1+\alpha(1-\delta_1)))$ if and only if the following assumption is satisfied:

$$(\mathbf{A_1}) : \beta_1 > \gamma_1, \quad \alpha > 1, \quad 0 < \delta_1 < \frac{\alpha}{\alpha-1},$$

where $\alpha = \frac{\beta_1\delta_2}{\beta_1\beta_2+\beta_1\gamma_2-\beta_2\gamma_1}$.

4.1.2 Stability of positive equilibrium E_*

The necessary condition on the occurrence of Turing instability for the positive equilibrium E_* requires that it is stable for the corresponding non-spatial system (4.1). The stability of E_* is determined by the nature of eigenvalues of the following Jacobian matrix

$$J = \begin{pmatrix} -\frac{\beta_1 u_* v_*}{(u_*+v_*)^2} & \frac{\beta_1 u_*^2}{(u_*+v_*)^2} & 0 \\ -\frac{\beta_2 v_*^2}{(u_*+v_*)^2} & \frac{\beta_2 u_* v_*}{(u_*+v_*)^2} - \frac{\delta_2 v_* w_*}{(v_*+w_*)^2} & \frac{\delta_2 v_*^2}{(v_*+w_*)^2} \\ 0 & -\frac{\delta_1 w_*^2}{(v_*+w_*)^2} & \frac{\delta_1 v_* w_*}{(v_*+w_*)^2} - w_* \end{pmatrix} := \begin{pmatrix} J_{11} & J_{12} & J_{13} \\ J_{21} & J_{22} & J_{23} \\ J_{31} & J_{32} & J_{33} \end{pmatrix}. \tag{4.2}$$

The associate characteristic equation of (4.2) is given by

$$\lambda^3 + s_1\lambda^2 + s_2\lambda + s_3 = 0, \tag{4.3}$$

where

$$\begin{aligned} s_1 &= w_* + \frac{(\delta_2-\delta_1)v_*w_*}{(v_*+w_*)^2} + \frac{(\beta_1-\beta_2)u_*v_*}{(u_*+v_*)^2}, \quad s_3 = \frac{\beta_1\delta_2 u_* v_*^2 w_*^2}{(u_*+v_*)^2(v_*+w_*)^2}, \\ s_2 &= \frac{(\beta_1(\delta_2-\delta_1)+\beta_2\delta_1)u_*v_*^2w_*}{(u_*+v_*)^2(v_*+w_*)^2} + \frac{(\beta_1-\beta_2)u_*v_*w_*}{(u_*+v_*)^2} + \frac{\delta_2 v_* w_*^2}{(v_*+w_*)^2}. \end{aligned} \tag{4.4}$$

Clearly $s_3 > 0$. Then from $s_1 > 0, s_1s_2 - s_3 > 0$ we conclude that $s_2 > 0$.

Theorem 4.1 *Assume that* $(\mathbf{A_1})$ *holds.*

(i) If

$$(\mathbf{A_2}) : s_1 > 0, \quad s_1s_2 - s_3 > 0$$

is satisfied, then all roots of characteristic Eq. (4.3) have negative real parts and thus the unique positive equilibrium E_* of the non-spatial system (4.1) is locally asymptotically stable. And vice versa.

(ii) If

$$s_1 > 0, \quad s_1s_2 - s_3 < 0.$$

is satisfied, then characteristic Eq. (4.3) has one negative real root and a pair of complex roots with positive real parts and thus E_* is unstable.

(iii) If

$$s_1 > 0, \quad s_1s_2 - s_3 = 0.$$

is satisfied, then characteristic Eq. (4.3) has a negative real root and a pair of simple purely imaginary roots $\pm \mathrm{i}\xi$ $(\xi > 0)$. Furthermore, if transversality condition

$$\left\{ \frac{(s_3 - s_1s_2)'}{2(s_1^2 + s_2)} \right\}_{\delta_1 = \delta_1^H} \neq 0$$

is satisfied, then system (4.1) undergoes temporal Hopf bifurcation near the unique positive equilibrium E_* when parameter value δ_1 crosses its critical value δ_1^H. Here δ_1^H can be determined by the equation $s_1s_2 - s_3 = 0$.

Proof (i) and (ii) follow directly from Routh-Hurwitz stability criterion. Next we shall prove (iii). Since $s_1 > 0, s_3 > 0, s_1s_2 - s_3 = 0$, it follows from the properties of roots of cubic equation we get characteristic Eq. (4.3) has a pair of simple purely imaginary roots $\pm\mathrm{i}\xi$. Moreover, from Vieta's formula, we get $\xi^2 = \frac{s_3(\delta_1^H)}{\delta_1^H} = s_2(\delta_1^H)$. Next we check the transversality condition at the critical value δ_1^H. Let $\lambda = \xi_1(\delta_1) \pm \mathrm{i}\xi_2(\delta_1)$ be a pair of complex conjugate roots of (4.3) satisfying $\xi_1(\delta_1^H) = 0$. Then substituting it into (4.3), separating real and imaginary parts and differentiating yields

$$\left\{\frac{d\xi_1(\delta_1)}{d\delta_1}\right\}_{\delta_1=\delta_1^H} = \left\{\frac{(s_3 - s_1 s_2)'}{2(s_1^2 + s_2)}\right\}_{\delta_1=\delta_1^H} \neq 0,$$

where $'$ denotes the derivative with respect to δ_1. Therefore the transversality condition is satisfied, which implies that the proof of (iii) is complete. ■

Remark 4.2 *There exists parameter values such that the assumptions* $(\mathbf{A_1})$ *and* $(\mathbf{A_2})$ *hold. For example, let* $\beta_1 = 10/3, \beta_2 = 10, \gamma_1 = 1, \gamma_2 = 1, \delta_1 = 1, \delta_2 = 10$. *A direct calculation gives the unique positive equilibrium* $(0.4667, 0.2, 0.8)$ *and* $s_1 = 0.84 > 0, s_3 = 0.896 > 0, s_1 s_2 - s_3 = 0.3674 > 0$, *which implies the unique positive equilibrium* E_* *of system (4.1) is locally asymptotically stable according to Theorem 4.2. In addition, there also exist several sets of parameters such that system* (4.1) *is unstable via Hopf bifurcation (see the numerical simulations of Section 6.3).*

4.2 Turing instability of spatially homogeneous steady state E_*

Clearly, $(u(x,t), v(x,t), w(x,t) = (u_*, v_*, w_*)$ satisfies spatial system (1.3) and the associated boundary conditions, we refer it to be the spatially homogeneous steady state of system (1.3). To interpret spatially heterogeneous distribution of the interaction species over the habitat, we shall study the Turing instability of the spatial system (1.3) when the temporally stable equilibrium E_* loses its stability due to small amplitude heterogeneous perturbations around E_* [45]. In what follows, we always assume that $(\mathbf{A_1})$ and $(\mathbf{A_2})$ are satisfied.

Now, we mainly focus on such pattern formation is due to joint effect of spatial diffusion and predator-taxis, which doesn't exclude Turing pattern formation only induced by the chemotactic factor χ at some special cases. In what follows, for the better observation of pattern transition as time evolution on the spatial domain Ω and the simplicity of calculations, we restrict our attention to (1.3) over a typical two-dimensional rectangle region $\Omega = [0, L] \times [0, L] \subseteq \mathbb{R}^N$ with $N = 2$. Linearizing (1.3) around the spatially homogeneous steady state (u_*, v_*, w_*) yields

$$\begin{cases} \frac{\partial \mathbf{Z}}{\partial t} = J\mathbf{Z} + D\Delta\mathbf{Z}, & \mathbf{x} \in \Omega,\ t > 0, \\ \frac{\partial \mathbf{Z}}{\partial \nu} = 0, & \mathbf{x} \in \partial\Omega,\ t > 0, \\ \mathbf{Z}(\mathbf{x}, 0) = \mathbf{Z_0}(\mathbf{x}), & \mathbf{x} \in \Omega, \end{cases} \tag{4.5}$$

where $\mathbf{x} = (\tilde{x}, \tilde{y})$, $\mathbf{Z} = (u - u_*, v - v_*, w - w_*)^{\mathbb{T}}$ and $D = \alpha(\mathbf{u})_{\mathbf{u}=(u_*, v_*, w_*)}$.

Since Ω is a square domain given by $[0, L] \times [0, L]$, the solutions to the linearized system (4.5) with Neumann boundary conditions are:

$$\mathbf{Z} = \sum_{(m,n)\in\mathbb{N}^2} \mathbf{c}_{mn} e^{\lambda t} \cos(\frac{m\pi\tilde{x}}{L}) \cos(\frac{n\pi\tilde{y}}{L}), \quad k^2 \triangleq (\frac{m\pi}{L})^2 + (\frac{n\pi}{L})^2 \equiv k_{\tilde{x}}^2 + k_{\tilde{y}}^2, \tag{4.6}$$

where $\mathbf{c}_{mn}$ are the Fourier coefficients of the initial conditions; λ is the growth rate of perturbation in time t; $k_{\tilde{x}}$ and $k_{\tilde{y}}$ represent the wave numbers of the solutions on horizontal direction and vertical direction, respectively; $\mathbb{N}$ represents nonnegative integer set. Substituting (4.6) into (4.5) leads to the following characteristic equation

$$\lambda^3 + r_1(\chi, k)\lambda^2 + r_2(\chi, k)\lambda + r_3(\chi, k) = 0, \tag{4.7}$$

where

$$\begin{aligned}
r_1(\chi, k) =& d_1k^2 + d_2k^2 + d_3k^2 + s_1, \\
r_2(\chi, k) =& (d_1d_2 + d_2d_3 + d_3d_1)k^4 + \left(w_* + \frac{(\delta_2 - \delta_1)v_*w_*}{(v_* + w_*)^2} - \frac{\beta_2u_*v_*}{(u_* + v_*)^2}\right) d_1k^2 + \\
& \left(w_* - \frac{\delta_1v_*w_*}{(v_* + w_*)^2} + \frac{\beta_1u_*v_*}{(u_* + v_*)^2}\right) d_2k^2 + d_3k^2 \left(\frac{(\beta_1 - \beta_2)u_*v_*}{(u_* + v_*)^2} + \frac{\delta_2v_*w_*}{(v_* + w_*)^2}\right) \\
& + \chi\frac{\beta_1u_*^2v_*}{(u_* + v_*)^2}k^2 + s_2, \\
r_3(\chi, k) =& d_1d_2d_3k^6 + \left(w_* - \frac{\delta_1v_*w_*}{(v_* + w_*)^2}\right) d_1d_2k^4 + \left(\frac{\delta_2v_*w_*}{(v_* + w_*)^2} - \frac{\beta_2u_*v_*}{(u_* + v_*)^2}\right) d_1d_3k^4 \\
& + \frac{\beta_1u_*v_*d_2d_3}{(u_* + v_*)^2}k^4 + \frac{\chi d_3\beta_1u_*^2v_*}{(u_* + v_*)^2}k^4 + \frac{d_1\delta_1\delta_2v_*^2w_*^2}{(v_* + w_*)^4}k^2 + \frac{\beta_1\delta_2u_*v_*^2w_*d_3}{(u_* + v_*)^2(v_* + w_*)^2}k^2 \\
& + \left(w_* - \frac{\delta_1v_*w_*}{(v_* + w_*)^2}\right) \left(d_1 \left(\frac{\delta_2v_*w_*}{(v_* + w_*)^2} - \frac{\beta_2u_*v_*}{(u_* + v_*)^2}\right) + d_2\frac{\beta_1u_*v_*}{(u_* + v_*)^2}\right) k^2 \\
& + \frac{\chi\beta_1u_*^2v_*}{(u_* + v_*)^2} \left(w_* - \frac{\delta_1v_*w_*}{(v_* + w_*)^2}\right) k^2 + s_3
\end{aligned}$$

with s_1, s_2 and s_3 are given in (4.4).

The stability of the spatially homogeneous steady state E_* to perturbations of wavenumber k is determined by the signs of the real parts of λ in the characteristic Eq. (4.7). Solving the cubic equation for λ we get three branches of solutions $\lambda_1(k), \lambda_2(k)$ and $\lambda_3(k)$. In view of the principle of the linearized stability, $E_* = (u_*, v_*, w_*)$ is locally asymptotically stable if and only if all eigenvalues of the characteristic Eq. (4.7) have negative real part. Then according to the Routh-Hurwitz stability criteria, the steady state $E_* = (u_*, v_*, w_*)$ of system (1.3) is locally asymptotically stable if and only if the following conditions hold for each wave number k given by (4.6)

$$r_1(\chi, k) > 0, \quad r_3(\chi, k) > 0, \quad r_1(\chi, k)r_2(\chi, k) - r_3(\chi, k) > 0. \tag{4.8}$$

while (u_*, v_*, w_*) is linearly unstable if one of the conditions above fails for some wave number k. Note that $r_1(\chi, k) > 0$ for all wave numbers k under the assumption $(\mathbf{A_2})$. Therefore we get the necessary and sufficient condition for Turing instability is either

$$\begin{aligned} &P(\chi, k) \equiv r_3(\chi, k) < 0 \quad \text{or} \\ &Q(\chi, k) \equiv r_1(\chi, k) r_2(\chi, k) - r_3(\chi, k) < 0 \end{aligned} \tag{4.9}$$

for some nonzero wavenumber k. For convenience, we rewrite $P(\chi, k)$ and $Q(\chi, k)$ as the following forms, respectively:

$$P(\chi, k) = P_0 k^6 + P_1(\chi) k^4 + P_2(\chi) k^2 + P_3 \tag{4.10}$$

$$Q(\chi, k) = Q_0 k^6 + Q_1(\chi) k^4 + Q_2(\chi) k^2 + Q_3, \tag{4.11}$$

where the coefficients $P_i, Q_i, i = 0, 1, 2$ are given in Appendix A. In the following, we choose χ as a bifurcation parameter to study the two types of primary instability.

4.2.1 Turing bifurcation

As we know, below (above) the Turing bifurcation threshold value, the spatially homogeneous steady state is stable and thus all the eigenvalues have negative real parts. At the Turing bifurcation threshold, exactly one eigenvalue becomes zero at the critical value χ_c^T with non-zero critical wavenumber k_{cT}, while the other two sets of eigenvalues still have negative real parts [46, 47]. Since $\lambda_1(k), \lambda_2(k), \lambda_3(k)$ be the roots of the characteristic Eq. (4.7). Then from the properties of the roots of a cubic equation we have the following equalities:

$$\begin{cases} \lambda_1(k) + \lambda_2(k) + \lambda_3(k) = -r_1(\chi, k), \\ \lambda_1(k)\lambda_2(k) + \lambda_2(k)\lambda_3(k) + \lambda_3(k)\lambda_1(k) = r_2(\chi, k), \\ \lambda_1(k)\lambda_2(k)\lambda_3(k) = -r_3(\chi, k), \\ -(\lambda_1(k) + \lambda_2(k))(\lambda_2(k) + \lambda_3(k))(\lambda_3(k) + \lambda_1(k)) = r_1(\chi, k) r_2(\chi, k) - r_3(\chi, k). \end{cases}$$

Since at critical wavenumber k_{cT} there exists only one of the roots of characteristic Eq. (4.7) is equal to zero, without loss of generality we assume

$$\lambda_1(k) \mid_{k=k_{cT}} = 0, \quad \mathrm{Re}(\lambda_2(k)) \mid_{k=k_{cT}} < 0, \quad \mathrm{Re}(\lambda_3(k)) \mid_{k=k_{cT}} < 0. \tag{4.12}$$

Therefore at the critical wavenumber k_{cT} we have $r_3(\chi_c^T, k_{cT}) = 0$ which is equivalent to $P(\chi_c^T, k_{cT}) = 0$. Furthermore, we get $r_1(\chi_c^T, k_{cT}) > 0, r_2(\chi_c^T, k_{cT}) > 0$ and thus $Q(\chi_c^T, k_{cT}) =$

$r_1(\chi_c^T, k_{cT})r_2(\chi_c^T, k_{cT}) - r_3(\chi_c^T, k_{cT}) > 0$. Now we can identify Turing bifurcation value χ_c^T which satisfies the Turing bifurcation condition as follows:

There exists $k_{cT} > 0$ such that

$$P(\chi_c^T, k_{cT}) = 0,\ Q(\chi_c^T, k_{cT}) > 0,\ \text{and } P(\chi_c^T, k) \neq 0,\ Q(\chi_c^T, k) > 0 \quad \text{for} \quad k \neq k_{cT}.$$

According to the above conditions, to determine the Turing bifurcation boundary, we first need to find the threshold value χ_c^T for which $P(\chi_c^T, k) = 0$ holds for a unique k. Now for all χ, $P(\chi, 0) > 0$ and also $P(\chi, k) > 0$ for large values of k. At Turing bifurcation boundary, we have

$$\min_k P(\chi, k) = 0. \tag{4.13}$$

Let $z = k^2$. Then we have

$$P(\chi, z) = P_0 z^3 + P_1 z^2 + +P_2 z + P_3.$$

Solving $\frac{\partial P(\chi,z)}{\partial z} = 0$ yields the possible local extremum points of $P(\chi, k)$

$$z = \frac{-P_1 + \sqrt{P_1^2 - 3P_0P_2}}{3P_0} := z_*, \tag{4.14}$$

which requires that $P_1 < 0$, $P_1^2 > 3P_0P_2$ or $P_2 < 0$ is satisfied, and

$$\tilde{z} = \frac{-P_1 - \sqrt{P_1^2 - 3P_0P_2}}{3P_0} := z^*, \tag{4.15}$$

which requires that $P_1 < 0$, $P_1^2 > 3P_0P_2$, $P_2 > 0$ is satisfied.

A direct calculation shows that $\frac{\partial^2 P(\chi,z)}{\partial z^2}\ |_{z=z_*} = 2\sqrt{P_1^2 - 3P_0P_2} > 0$ and $\frac{\partial^2 P(\chi,z)}{\partial z^2}\ |_{z=z^*} = -2\sqrt{P_1^2 - 3P_0P_2} < 0$, which implies that z_* is a local minimum point. As $P(\chi, 0) = P_3 > 0$ and $\lim\limits_{z\to\infty} P(\chi, z) = \infty$, we infer that $z_* \in (0, \infty)$ and satisfies $\min_z P(\chi, z) = P(\chi, z_*) = 0$. Thus substituting (4.14) into (4.13) and simplifying, we get the critical value of χ should satisfy the following critical condition

$$P_3 = \frac{1}{27P_0^2}[P_1(9P_0P_2 - 2P_1^2) + 2(P_1^2 - 3P_0P_2)^{\frac{3}{2}}]. \tag{4.16}$$

Let $a_0 = 27P_0^2P_3, P_1 = a_1 + a_2\chi, P_2 = a_3 + a_4\chi$, where a_1, a_2, a_3, a_4 are given in the expressions of P_1 and P_2. Substituting them into (4.16) yields

$$G^2(\chi) = 4H^3(\chi), \tag{4.17}$$

where

$$\begin{aligned} G(\chi) =& 2a_2^3\chi^3 + (6a_1a_2^2 - 9a_2a_4P_0)\chi^2 + (6a_1^2a_2 - 9(a_1a_4 + a_2a_3)P_0)\chi \\ &+ a_0 - 9a_1a_3P_0 + 2a_1^3, \\ H(\chi) =& a_2^2\chi^2 + (2a_1a_2 - 3a_4P_0)\chi + a_1^2 - 3a_3P_0. \end{aligned}$$

Simplifying (4.17), it's a quintic equation of variable χ. Assume

$$(\mathbf{A_3}):\ a_0^2 + 4a_0a_1^3 - 18a_0a_1a_3P_0 - 27a_1^2a_3^2P_0^2 + 108a_3^3P_0^3 < 0$$

is satisfied. Then Eq. (4.17) has at least one positive root, without loss of generality, we may assume that it has five positive roots, which are denoted by $\chi_1^c, \chi_2^c, \chi_3^c, \chi_4^c, \chi_5^c$, respectively. Denote

$$\chi^T = \{\chi_1^c, \chi_2^c, \chi_3^c, \chi_4^c, \chi_5^c\}. \tag{4.18}$$

Then we get Turing bifurcation threshold value χ_c^T can be found from the set χ^T, and the positivity of the wavenumber k requires it should satisfy the following condition

$$(\mathbf{A_4}):\ P_1^c < 0,\ (P_1^c)^2 > 3P_0P_2^c \quad \text{or} \quad P_2^c < 0,$$

where $P_1^c = a_1 + a_2\chi_c^T$ and $P_2^c = a_3 + a_4\chi_c^T$ with $\chi_c^T \in \chi^T$.

The corresponding critical wave number k_{cT}^2 is given by

$$k_{cT}^2 = \frac{9P_0P_3 - P_1^cP_2^c}{2((P_1^c)^2 - 3P_0P_2^c)}. \tag{4.19}$$

Moreover, from Eq. (4.11), it is clear that $Q_0 > 0$ and $Q_3 > 0$ under the assumption $(\mathbf{A_2})$. Hence if we assume that

$$(\mathbf{A_5}): Q_1|_{\chi=\chi_c^T} > 0, \quad Q_2|_{\chi=\chi_c^T} > 0$$

is satisfied, then we obtain $Q(\chi_c^T, k) > 0$ for all wave numbers k. Therefore system (1.3) undergoes Turing bifurcation at χ_c^T near the unique positive steady state E_*.

4.2.2 Turing-spatiotemporal Hopf bifurcation

It is well known that spatiotemporal Hopf bifurcation of system (1.3) occurs when characteristic Eq. (4.7) has only a pair of simple purely imaginary eigenvalues at critical value χ_c^H with non-zero critical wavenumber k_{cH}, while the other eigenvalues have negative real parts and the corresponding transversality condition should be satisfied [48]. Since its corresponding non-spatial system (4.1) is always asymptotically stable, we call this kind of spatial Hopf bifurcation as Turing-spatiotemporal Hopf bifurcation, which breaks both spatial symmetry leading spatial pattern formation and temporal symmetry inducing periodic oscillations in time. As analyzed above, we can identify Turing-spatiotemporal Hopf bifurcation value χ_c^H

which satisfies the Hopf bifurcation condition taking the following form:

There exists $k_{cH} > 0$ such that

$Q(\chi_c^H, k_{cH}) = 0,\ P(\chi_c^H, k_{cH}) > 0,$ and $Q(\chi_c^H, k) \neq 0,\ P(\chi_c^H, k) > 0$ for $k \neq k_{cH}$;

and for the unique pair of complex eigenvalues near the imaginary axis

$\mu(\chi, k) \pm \mathrm{i}\tau(\chi, k)$ satisfying $\mu'(\chi_c^H, k_{cH}) \neq 0$ and $\tau(\chi_c^H, k_{cH}) > 0$.

To determine the Turing-spatiotemporal Hopf bifurcation boundary, it is necessary to find the threshold value χ_c^H for which $Q(\chi_c^H, k) = 0$ holds for a unique k. As $Q(\chi, 0) > 0$ and also for large value of k. At the critical case, we need to find the threshold value χ_c^H of parameter χ at which $Q(\chi, k)$ has a zero minimum at $k = k_{cH}$ and $k_{cH} \in (0, \infty)$. This implies that $Q(\chi, k)$ satisfies

$$\min_k Q(\chi, k) = 0. \tag{4.20}$$

Similar to the analyses above, we get the condition for the marginal stability as follows

$$Q_3 = \frac{1}{27Q_0^2}[Q_1(9Q_0Q_2 - 2Q_1^2) + 2(Q_1^2 - 3Q_0Q_2)^{\frac{3}{2}}]. \tag{4.21}$$

Assume that

$$(\mathbf{A_6}):\ b_0^2 + 4b_0b_1^3 - 18b_0b_1b_3Q_0 - 27b_1^2b_3^2Q_0^2 + 108b_3^3Q_0^3 < 0.$$

is satisfied. Here $b_0 = 27Q_0^2Q_3$ and b_i, $i = 1, 2, 3, 4$ are given in the expressions of $Q_1 = b_1 + \chi b_2$ and $Q_2 = b_3 + \chi b_4$. Denote

$$\chi^H = \{\hat{\chi}_1^c, \hat{\chi}_2^c, \hat{\chi}_3^c, \hat{\chi}_4^c, \hat{\chi}_5^c\}, \tag{4.22}$$

where $\hat{\chi}_i^c$, $i = 1, 2, 3, 4, 5$ are possible positive roots of the following quintic equation

$$\hat{G}^2(\chi) = 4\hat{H}^3(\chi), \tag{4.23}$$

where

$$\begin{aligned}\hat{G}(\chi) =& 2b_2^3\chi^3 + (6b_1b_2^2 - 9b_2b_4Q_0)\chi^2 + (6b_1^2b_2 - 9(b_1b_4 + b_2b_3)Q_0)\chi \\ &+ b_0 - 9b_1b_3Q_0 + 2b_1^3, \\ \hat{H}(\chi) =& b_2^2\chi^2 + (2b_1b_2 - 3b_4Q_0)\chi + b_1^2 - 3b_3Q_0.\end{aligned}$$

Then we obtain that Turing-spatiotemporal Hopf bifurcation threshold value χ_c^H should be chosen from the set χ^H, and the positivity requirement of the wavenumber k such that it should satisfy the following assumption

$$(\mathbf{A_7}):\ Q_1^c < 0,\ (Q_1^c)^2 > 3Q_0Q_2^c \quad \text{or} \quad Q_2^c < 0,$$

where $Q_1^c = b_1 + b_2\chi_c^H$ and $Q_2^c = b_3 + b_4\chi_c^H$ with $\chi_c^H \in \chi^H$.

And the corresponding critical wave number k_{cH}^2 is calculated by

$$k_{cH}^2 = \frac{9Q_0Q_3 - Q_1^cQ_2^c}{2((Q_1^c)^2 - 3Q_0Q_2^c)}. \tag{4.24}$$

Noting that $r_1(\chi_c^H, k_{cH}) > 0$ and $r_3(\chi_c^H, k_{cH}) > 0$. Since $r_1(\chi_c^H, k_{cH})r_2(\chi_c^H, k_{cH}) - r_3(\chi_c^H, k_{cH}) = 0$, we get $r_2(\chi_c^H, k_{cH}) > 0$. Therefore the characteristic equation (4.7) has a negative real root $\lambda_1^H(\chi_c^H, k_{cH})$ and a pair of purely imaginary eigenvalues $\lambda_{2,3}^H(\chi_c^H, k_{cH})$ given by

$$\lambda_1^H(\chi_c^H, k_{cH}) = -r_1(\chi_c^H, k_{cH}) < 0, \quad \lambda_{2,3}^H(\chi_c^H, k_{cH}) = \pm \mathrm{i}\sqrt{r_2(\chi_c^H, k_{cH})}.$$

Next we check the transversality condition. Let $\lambda_1^H(\chi, k)$ and $\lambda_{2,3}^H(\chi, k) = \mu(\chi, k) \pm \tau(\chi, k)$ be the unique eigenvalues of (4.7) in a neighbourhood of $\chi = \chi_c^H$. Then we know that λ_1^H, μ and τ are real analytical functions of χ satisfying $\mu(\chi_c^H, k_{cH}) = 0$ and $\tau(\chi_c^H, k_{cH}) > 0$. In the following, we need to prove the following transversality condition

$$\left.\frac{\partial \mu(\chi, k)}{\partial \chi}\right|_{\chi=\chi_c^H, k=k_{cH}} \neq 0. \tag{4.25}$$

Substituting the eigenvalues $\lambda_1^H(\chi, k)$ and $\lambda_{2,3}^H(\chi, k) = \mu(\chi, k) \pm \tau(\chi, k)$ into the characteristic Eq. (4.7) and equating the real and imaginary parts yield

$$\begin{cases} -r_1(\chi, k) = 2\mu(\chi, k) + \lambda_1^H(\chi, k), \\ r_2(\chi, k) = \mu^2(\chi, k) + \tau^2(\chi, k) + 2\mu(\chi, k)\lambda_1^H(\chi, k), \\ -r_3(\chi, k) = \lambda_1^H(\chi, k)(\mu^2(\chi, k) + \tau^2(\chi, k)). \end{cases} \tag{4.26}$$

Differentiating the equations above with respect to χ gives

$$\begin{aligned} &2\mu'(\chi, k) + \lambda_1'(\chi, k) = 0, \\ &2\mu(\chi, k)\mu'(\chi, k) + 2\tau(\chi, k)\tau'(\chi, k) + 2\mu'(\chi, k)\lambda_1(\chi, k) + 2\mu(\chi, k)\lambda_1'(\chi, k) = \frac{\beta_1 u_*^2 v_* k^2}{(u_* + v_*)^2}, \\ &\lambda_1'(\chi, k)(\mu^2(\chi, k) + \tau^2(\chi, k)) + (2\mu(\chi, k)\mu'(\chi, k) + 2\tau(\chi, k)\tau'(\chi, k))\lambda_1(\chi, k) \\ = &-\frac{\beta_1 u_*^2 v_* d_3 k^4}{(u_* + v_*)^2} - \frac{\beta_1 u_*^2 v_* k^2}{(u_* + v_*)^2}(w_* - \frac{\delta_1 v_* w_*}{(v_* + w_*)^2}). \end{aligned} \tag{4.27}$$

Since $\mu(\chi_c^H, k_{cH}) = 0$ and $\lambda_1(\chi_c^H, k_{cH}) = -r_1(\chi_c^H, k_{cH})$, solving (4.27) with $\chi = \chi_c^H$ yields

$$\begin{aligned} \mu'(\chi_c^H, k_{cH}) = -\frac{1}{2}\lambda_1'(\chi_c^H, k_{cH}) = &\frac{\beta_1 u_*^2 v_* k_{cH}^2}{(\tau^2(\chi_c^H, k_{cH}) + r_1^2(\chi_c^H, k_{cH}))(u_* + v_*)^2} \times \\ &\left(d_1 k_{cH}^2 + d_2 k_{cH}^2 + \frac{\delta_2 v_* w_*}{(v_* + w_*)^2} + \frac{(\beta_1 - \beta_2)u_* v_*}{(u_* + v_*)^2}\right). \end{aligned}$$

So if we assume that

$$(\mathbf{A_8}):\ d_1k_{cH}^2+d_2k_{cH}^2+\frac{\delta_2v_*w_*}{(v_*+w_*)^2}+\frac{(\beta_1-\beta_2)u_*v_*}{(u_*+v_*)^2}\neq 0$$

is satisfied, then the transversality condition (4.25) holds and system (1.3) undergoes spatiotemporal Hopf bifurcation at χ_c^H near the unique positive steady state E_*.

From Eq. (4.10), it is clear that $P_0>0$ and $P_3>0$. If we assume that

$$(\mathbf{A_9}):\ P_1|_{\chi=\chi_c^H}>0,\quad P_2|_{\chi=\chi_c^H}>0$$

is satisfied, then we obtain $P(\chi_c^H,k)>0$ for all wave numbers k, which indicates stationary Turing bifurcation cannot occur under this assumption when χ near χ_c^H. Hence system (1.3) undergoes Turing-spatiotemporal Hopf bifurcation at χ_c^H near the unique positive steady state E_*.

We summarize the above discussion as the following theorem.

Theorem 4.3 *Assume that* $(\mathbf{A_1})$ *and* $(\mathbf{A_2})$ *are satisfied. Then we have the following results about the Turing instability of the unique spatially homogeneous steady state* E_**:*

(i) If $(\mathbf{A_3}),(\mathbf{A_4})$ *or* $(\mathbf{A_6}),(\mathbf{A_7}),(\mathbf{A_8})$ *are satisfied, then* E_* *is linearly unstable when* χ *crosses its critical value* χ_c^T *or* χ_c^H*;*

(ii) If $(\mathbf{A_3}),(\mathbf{A_4})$ *and* $(\mathbf{A_5})$ *are satisfied, then system (1.3) undergoes Turing bifurcation at* χ_c^T *near* E_**, namely, stationary pattern forms in this case, and the critical wave number is given by (4.19);*

(iii) If $(\mathbf{A_6})$*,* $(\mathbf{A_7}),(\mathbf{A_8})$ *and* $(\mathbf{A_9})$ *are satisfied, then system (1.3) undergoes Turing-spatiotemporal Hopf bifurcation at* χ_c^H *near* E_**, namely, oscillatory pattern forms in this case, and the critical wave number is given by (4.24);*

Proof The proof of (i)-(iii) can be found from the discussion above, so we omit it here for brevity. ∎

To interpret the chemotaxis-driven stationary pattern formation, we plot the functional curve $P(\chi,k)$ as a function of the wavenumber k in Figure 1 (left) with the given parameters $\beta_1=10/3,\beta_2=10,\gamma_1=1,\gamma_2=1,\delta_1=1,\delta_2=10,d_1=3.5,d_2=0.02,d_3=0.15$. It is easy to check that the assumptions $(\mathbf{A_1}),(\mathbf{A_2})$ and $(\mathbf{A_3})$ are satisfied. A direct calculation shows that Eq. (4.17) has only one positive root $\chi_1^c=1.6563$ which satisfies the assumption $(\mathbf{A_4})$, and the critical wavenumber is $k_{cT}^2=7.2204$. Furthermore, we obtain $Q_1|_{\chi=\chi_c^T=\chi_1^c}=4.6292>0$

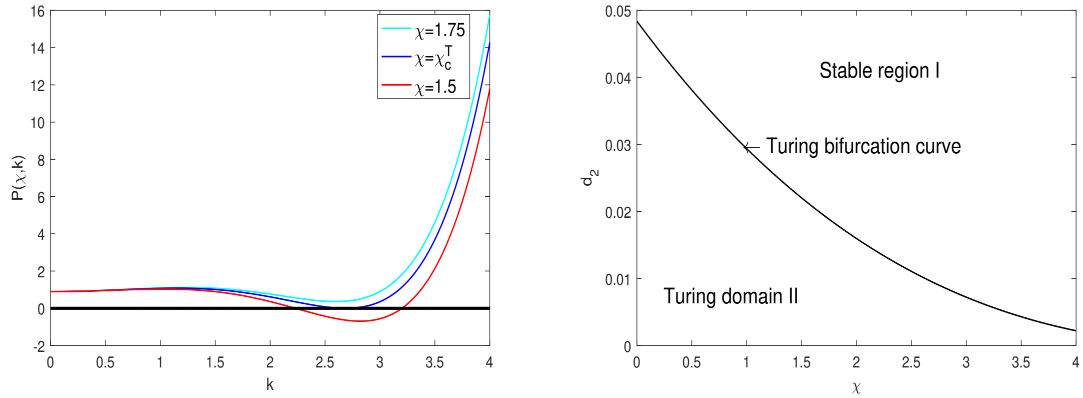

Figure 1: (Left) Plots of $P(\chi, k)$ for different values of χ against k. (Right) Turing bifurcation diagram for the system (1.3). Here the parameters are given in the text.

and $Q_2|_{\chi=\chi_c^T=\chi_1^c} = 6.3573 > 0$, which implies that the assumption $(\mathbf{A_5})$ is satisfied. Since the values of Q_1 and Q_2 are also positive for other chemotaxis factors besides $\chi = \chi_1^c$, we get spatial Hopf bifurcation cannot occur at this case by noticing that $Q_0 > 0$ and $Q_3 > 0$. Therefore from Theorem 4.3(i) and 4.3(ii) we get that the unique positive steady state E_* is linearly unstable and stationary Turing pattern arises when χ crosses its critical value $\chi_c^T = \chi_1^c = 1.6563$. As is illustrated in Figure 1 (left), the value of $P(\chi, k)$ becomes negative for a certain range of values of k when χ crosses its critical value 1.6563, which indicates spatial pattern formation arises, that is, the parameter value χ affects spatial pattern formation arises. In Figure 1 (right), we plot Turing bifurcation curve in the (χ, d_2)-parameter space for fixed $\beta_1 = 10/3, \beta_2 = 10, \gamma_1 = 1, \gamma_2 = 1, \delta_1 = 1, \delta_2 = 10, d_1 = 3.5, d_3 = 0.15$. Clearly, the assumptions $(\mathbf{A_1})$ and $(\mathbf{A_2})$ are satisfied for the set of parameters. After check carefully, we find $Q_1 > 0$ and $Q_2 > 0$ for arbitrary positive parameter values χ and d_2. Thus the assumption $(\mathbf{A_5})$ is satisfied and further we have $Q(\chi, k) > 0$ for arbitrary wavenumber k and chemotaxis coefficient χ, and thus Turing bifurcation curve is determined by solving Eq. (4.16). As can be seen from Figure 1 (right), the parameter space is divided into two distinct regions by the Turing bifurcation curve. In region I, the unique positive spatially homogeneous steady state is the stable solution of system (1.3). Domain II is the region of pure Turing bifurcation, in which Turing instability occurs and we call it Turing space.

To interpret the chemotaxis-driven oscillatory pattern formation, we plot the functional curve $Q(\chi, k)$ as k is fixed in Figure 2 (left). Here we choose system parameters to be $d_1 = 0.0001, d_2 = 0.0008, d_3 = 0.0002, \beta_1 = 3, \beta_2 = 10, \gamma_1 = 1.658, \gamma_2 = 1, \delta_1 = 0.2, \delta_2 = 8$. Clearly,

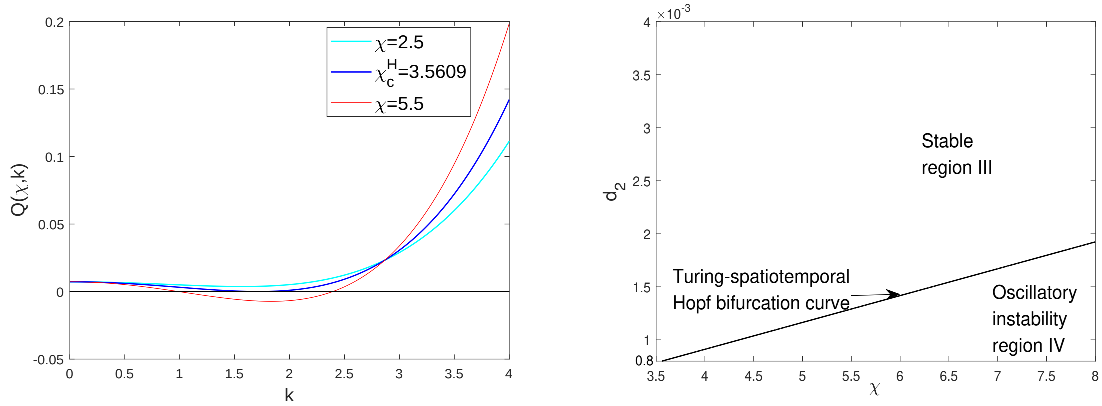

Figure 2: (Left) Plots of $Q(\chi, k)$ for different values of χ against k. (Right) Turing-spatiotemporal Hopf bifurcation diagram for the system (1.3). Here the parameters are given in the text.

the assumptions $(\mathbf{A_1})$, $(\mathbf{A_2})$ and $(\mathbf{A_6})$ are satisfied. Solving (4.23) gives a unique positive root $\hat{\chi}_1^c = 3.5609$ which satisfies the assumptions $(\mathbf{A_7})$ and $(\mathbf{A_8})$, and thus $\chi_c^H = 3.5609$. We also obtain the critical wavenumber is $k_{cH}^2 = 2.9411$. Moreover, we calculate $P_1|_{\chi=\chi_c^H=\hat{\chi}_1^c} = 1.8508 \times 10^{-4} > 0$ and $P_2|_{\chi=\chi_c^H=\hat{\chi}_1^c} = 0.8269 > 0$, which implies that the assumption $(\mathbf{A_9})$ is also satisfied. In view of Theorem 4.3(iii), system (1.3) becomes unstable and oscillatory pattern formation arises when χ crosses its critical value $\chi_c^H = 3.5609$, which is illustrated in Figure 2 (left). In Figure 2 (right), we plot Turing-spatiotemporal Hopf bifurcation curve in the (χ, d_2)-parameter space for fixed $\beta_1 = 3, \beta_2 = 10, \gamma_1 = 1.658, \gamma_2 = 1, \delta_1 = 0.2, \delta_2 = 8, d_1 = 0.0001, d_3 = 0.0002$. Clearly, the assumptions $(\mathbf{A_1})$ and $(\mathbf{A_2})$ are satisfied for the set of parameters. Additionally, we find $P_1 > 0$ and $P_2 > 0$ for $\chi \geq 3.5$ and $d_2 \geq 0.0008$. Thus the assumption $(\mathbf{A_9})$ is satisfied and further we have $P(\chi, k) > 0$ for arbitrary wavenumber k and $(\chi, d_2) \in [3.5, \infty) \times [0.0008, \infty)$, and thus Turing-spatiotemporal Hopf bifurcation curve is determined by solving Eq. (4.21). As can be seen from Figure 2 (right), the parameter space is divided into two distinct domains by the Turing-spatiotemporal Hopf bifurcation curve. In domain III, the unique positive spatially homogeneous steady state is the stable solution of system (1.3). However, Domain IV is the domain of instable domain, in which oscillatory instability occurs and we call it Turing-spatiotemporal Hopf space.

5 Existence and stability of non-constant positive steady state

5.1 Existence of non-constant positive steady state

In this subsection, we shall study non-constant positive steady states to system (1.3), which satisfy:

$$\begin{cases} d_1\Delta u + \frac{\beta_1 vu}{v+u} - \gamma_1 u = 0, & \mathbf{x} \in \Omega, \\ \nabla\cdot(d_2\nabla v + \chi v\nabla u) + \frac{\delta_2 vw}{v+w} - \frac{\beta_2 vu}{u+v} - \gamma_2 v = 0, & \mathbf{x} \in \Omega, \\ d_3\triangle w + w(1-w) - \frac{\delta_1 vw}{v+w} = 0, & \mathbf{x} \in \Omega, \\ \frac{\partial u}{\partial \nu} = \frac{\partial v}{\partial \nu} = \frac{\partial w}{\partial \nu} = 0, & \mathbf{x} \in \partial\Omega, \end{cases} \tag{5.1}$$

where u, v, w are functions of variable $\mathbf{x} \in \Omega \subseteq \mathbb{R}^2$ and all the parameters are the same as those in (1.3). We assume that $(\mathbf{A_1})$ is satisfied so that $E_* = (u_*, v_*, w_*)$ is the unique positive equilibrium to (4.1).

In the following, to find non-constant positive solutions to (5.1), we will give steady state bifurcation analysis at E_*. We fix $\beta_1, \beta_2, \gamma_1, \gamma_2, \delta_1, \delta_2, d_1, d_2, d_3$ and choose χ to be a bifurcation parameter. We also assume that $(\mathbf{A_2})$ is satisfied so that the unique positive equilibrium E_* is locally asymptotically stable for the non-spatial system (4.1). Then we want to determine the threshold value of the predator-taxis χ^S_{mn} such that non-constant positive steady state of system (1.3) bifurcates from E_* as the parameter χ crosses its threshold value χ^S_{mn}, and also study its stability to obtain some spatially inhomogeneous patterns.

Steady state bifurcation. In order to apply the abstract bifurcation theory of Crandall-Rabinowitz [50], we give the following spaces:

$$\mathbb{X} = \left\{ u \in H^2(\Omega) \Big| \frac{\partial u}{\partial \nu} = 0, \mathbf{x} \in \partial\Omega \right\}, \quad \mathbb{Y} = L^2(\Omega).$$

Then system (5.1) can be converted into the following abstract equation

$$\begin{cases} \mathcal{A}(\mathbf{u}, \chi) = 0,\ (\mathbf{u}, \chi) \in \mathbb{X}^3 \times \mathbb{R}_+, & \mathbf{x} \in \Omega, \\ \frac{\partial \mathbf{u}}{\partial \nu} = 0, & \mathbf{x} \in \partial\Omega, \end{cases} \tag{5.2}$$

where

$$\mathcal{A}(\mathbf{u}, \chi) = \begin{pmatrix} d_1\Delta u + \frac{\beta_1 vu}{v+u} - \gamma_1 u \\ d_2\Delta v + \chi\nabla v\cdot\nabla u + \chi v\Delta u + \frac{\delta_2 vw}{v+w} - \frac{\beta_2 vu}{u+v} - \gamma_2 v \\ d_3\triangle w + w(1-w) - \frac{\delta_1 vw}{v+w} \end{pmatrix}.$$

Define

$$\mathcal{D}_1(\mathbf{u}) = \begin{pmatrix} d_1 & 0 & 0 \\ \chi v & d_2 & 0 \\ 0 & 0 & d_3 \end{pmatrix}, \quad \mathcal{F}(\mathbf{u}, \nabla\mathbf{u}, \chi) = -\begin{pmatrix} \frac{\beta_1 vu}{v+u} - \gamma_1 u \\ \chi\nabla v\cdot\nabla u + \frac{\delta_2 vw}{v+w} - \frac{\beta_2 vu}{u+v} - \gamma_2 v \\ w(1-w) - \frac{\delta_1 vw}{v+w} \end{pmatrix},$$

and for $i, j = 1, 2$, $a_{ij}(\mathbf{u}, \chi) = \mathcal{D}_1(\mathbf{u})\delta_{ij}, b_i(\mathbf{x}) = a_{ij}(\mathbf{u}, \chi)\nu_j(\mathbf{x}), b_0(\mathbf{x}) = 0, c(\mathbf{x}) = \delta(\mathbf{x}) = I$, where δ_{ij} is the Kronecker symbol and I is a unit matrix. Then (5.2) is equivalent to

$$\begin{cases} \mathcal{A}(\mathbf{u}, \chi) = -a_{ij}(\mathbf{u}, \chi)\partial_i\partial_j\mathbf{u} + \mathcal{F}(\mathbf{u}, \nabla\mathbf{u}, \chi) = 0, & \mathbf{x} \in \Omega, \\ \mathcal{B}\mathbf{u} = \delta(x)[b_i(\mathbf{x})\partial_i\mathbf{u} + b_0(\mathbf{x})\mathbf{u}] + (I - \delta(\mathbf{x}))c(\mathbf{x})\mathbf{u} = 0, & \mathbf{x} \in \partial\Omega, \end{cases} \tag{5.3}$$

where $\partial_i = \frac{\partial}{\partial x_i}$ and the summation convention is used.

Since $a_{ij}(\mathbf{u}, \chi) = \mathcal{D}_1(\mathbf{u})\delta_{ij}$, we can conveniently write (5.3) as

$$\begin{cases} \mathcal{A}(\mathbf{u}, \chi) = -\mathcal{D}_1(\mathbf{u})\Delta\mathbf{u} + \mathcal{F}(\mathbf{u}, \nabla\mathbf{u}, \chi) = 0, & \mathbf{x} \in \Omega, \\ \mathcal{B}\mathbf{u} = \delta(\mathbf{x})[b_i(\mathbf{x})\partial_i\mathbf{u} + b_0(\mathbf{x})\mathbf{u}] + (I - \delta(\mathbf{x}))c(\mathbf{x})\mathbf{u} = 0, & \mathbf{x} \in \partial\Omega. \end{cases} \tag{5.4}$$

Moreover, for any fixed $\hat{\mathbf{u}} = (\hat{u}, \hat{v}, \hat{w}) \in \mathbb{X}^3$, the Fré*chet* derivative of $\mathcal{A}$ is given by ($\mathbf{z} = (z_1, z_2, z_3) \in \mathbb{X}^3$)

$$D_{\mathbf{u}}\mathcal{A}(\hat{\mathbf{u}}, \chi)[\mathbf{z}] = -\mathcal{D}_1(\hat{\mathbf{u}})\Delta\mathbf{z} - \Delta\hat{\mathbf{u}}\mathcal{D}_2(\mathbf{z}) - \mathcal{D}_3(\nabla\hat{\mathbf{u}}) \cdot \nabla\mathbf{z} - J(\hat{\mathbf{u}})\mathbf{z}, \tag{5.5}$$

where

$$\mathcal{D}_2(\mathbf{z}) = \begin{pmatrix} 0 & 0 & 0 \\ \chi z_2 & 0 & 0 \\ 0 & 0 & 0 \end{pmatrix}, \ \mathcal{D}_3(\nabla\hat{\mathbf{u}}) = \begin{pmatrix} 0 & 0 & 0 \\ \chi\nabla\hat{v} & \chi\nabla\hat{u} & 0 \\ 0 & 0 & 0 \end{pmatrix},$$

and

$$J(\hat{\mathbf{u}}) = \begin{pmatrix} \hat{f}_u & \hat{f}_v & \hat{f}_w \\ \hat{g}_u & \hat{g}_v & \hat{g}_w \\ \hat{h}_u & \hat{h}_v & \hat{h}_w \end{pmatrix} = \begin{pmatrix} \frac{\beta_1\hat{v}^2}{(\hat{u}+\hat{v})^2} - \gamma_1 & \frac{\beta_1\hat{u}^2}{(\hat{u}+\hat{v})^2} & 0 \\ -\frac{\beta_2\hat{v}^2}{(\hat{u}+\hat{v})^2} & \frac{\delta_2\hat{w}^2}{(\hat{v}+\hat{w})^2} - \frac{\beta_2\hat{u}^2}{(\hat{u}+\hat{v})^2} - \gamma_2 & \frac{\delta_2\hat{v}^2}{(\hat{v}+\hat{w})^2} \\ 0 & -\frac{\delta_1\hat{w}^2}{(\hat{v}+\hat{w})^2} & 1 - 2\hat{w} - \frac{\delta_1\hat{v}^2}{(\hat{v}+\hat{w})^2} \end{pmatrix}.$$

In view of [49, Proposition 3.1], we have

$$D_{\mathbf{u}}\mathcal{B}(\hat{\mathbf{u}}, \chi)[\mathbf{z}] = \delta(\mathbf{x})[b_i(\mathbf{x})\partial_i\mathbf{z} + b_0(\mathbf{x})\mathbf{z}] + (I - \delta(\mathbf{x}))c(\mathbf{x})\mathbf{z}.$$

Lemma 5.1 $D_{\mathbf{u}}\mathcal{A}(\hat{\mathbf{u}}, \chi) : \mathbb{X}^3 \to \mathbb{Y}^3$ *is a Fredholm operator with zero index.*

Proof Clearly for $\hat{\mathbf{u}} \in \mathbb{X}^3$, Trace$(\mathcal{D}_1(\hat{\mathbf{u}})) > 0$ and Det$(\mathcal{D}_1(\hat{\mathbf{u}})) > 0$. So operator $D_{\mathbf{u}}\mathcal{A}(\hat{\mathbf{u}}, \chi)$ is elliptic. In addition, according to **Case 3** of Remark 2.5.5 in [49], here we see that $i = j = 2$, $\alpha_{ij}(\mathbf{x}) = \delta_{ij}$ (the Kronecker symbol), $c(\mathbf{x}) = I$ and $a(\mathbf{x}) = \mathcal{D}_1(\hat{\mathbf{u}})$ with positive eigenvalues d_1, d_2 and d_3, $b_i(\mathbf{x}) = a(\mathbf{x})\alpha_{ij}(\mathbf{x})\nu_j(\mathbf{x})$ with $\nu(\mathbf{x}) := (\nu_1(\mathbf{x}), \nu_2(\mathbf{x}))$ is the outer unit normal vector field on $\partial\Omega$. Then the Neumann boundary condition can be written as

$$\mathbf{0} = a(\mathbf{x})(\nabla z_1 \quad \nabla z_2 \quad \nabla z_3)^{\mathbb{T}}\nu(\mathbf{x}) = b_i(\mathbf{x})\partial_i\mathbf{z}$$

with $\delta(\mathbf{x}) = I_{3\times 3}$ and $b_0(\mathbf{x}) = 0$ at $\partial\Omega$. Since $\delta(\mathbf{x}) = I_{3\times 3}$ at $x \in \partial\Omega$, the condition $(I - \delta(x))a(x)\delta(x) = 0$ for $x \in \partial\Omega$ in **Case 3** of [49, Remark 2.5.5] is satisfied. Note that the eigenvalues of $a(\mathbf{x})$ are positive, so the condition (2.6) with $\sigma = 0$ in **Case 3** of [49, Remark 2.5.5] is satisfied. Therefore, by Remark 2.5.5 of [49], for any $\chi \in \mathbb{R}_+$, $(D_{\mathbf{u}}\mathcal{A}(\hat{\mathbf{u}}, \chi), D_{\mathbf{u}}\mathcal{B}(\hat{\mathbf{u}}, \chi))$ satisfies Agmon's condition for arbitrary angles $\theta \in [-\frac{\pi}{2}, \frac{\pi}{2}]$ (see Definition 2.4 in [49]). Furthermore, by Remark 3.4.1 of [49], $D_{\mathbf{u}}\mathcal{A}(\hat{\mathbf{u}}, \chi) : \mathbb{X}^3 \to \mathbb{Y}^3$ is Fredholm with index 0, which implies that the proof of the lemma is complete. ∎

To look for non-constant positive solutions of (5.1) that bifurcate from the spatially homogeneous steady state $\mathbf{u}_* = (u_*, v_*, w_*)$ we need to check the following necessary condition

$$\mathcal{N}(D_{\mathbf{u}}\mathcal{A}(\mathbf{u}_*, \chi)) \neq \mathbf{0}, \tag{5.6}$$

where $\mathcal{N}$ represents the null space. Picking $\hat{\mathbf{u}} = \mathbf{u}_*$ in (5.5), it is easy to see that the null space in (5.6) consists of some solutions to the following elliptic equations

$$\begin{cases} d_1\Delta u + J_{11}u + J_{12}v = 0, & \mathbf{x} = (\tilde{x}, \tilde{y}) \in \Omega, \\ d_2\Delta v + \chi v_*\Delta u + J_{21}u + J_{22}v + J_{23}w = 0, & \mathbf{x} = (\tilde{x}, \tilde{y}) \in \Omega, \\ d_3\Delta w + J_{32}v + J_{33}w = 0, & \mathbf{x} = (\tilde{x}, \tilde{y}) \in \Omega, \\ \frac{\partial u}{\partial \nu} = \frac{\partial v}{\partial \nu} = \frac{\partial w}{\partial \nu} = 0, & \mathbf{x} = (\tilde{x}, \tilde{y}) \in \partial\Omega. \end{cases} \tag{5.7}$$

To verify (5.6), i.e. find the non-zero solution of (5.7), we substitute the following eigen-expansion in two-dimensional domain $[0, L] \times [0, L]$ with Nuemann boundary conditions

$$\begin{aligned} u(\tilde{x}, \tilde{y}) &= \sum_{(m,n)\in\mathbb{N}^2} a_{mn} \cos(\frac{m\pi\tilde{x}}{L}) \cos(\frac{n\pi\tilde{y}}{L}), \\ v(\tilde{x}, \tilde{y}) &= \sum_{(m,n)\in\mathbb{N}^2} b_{mn} \cos(\frac{m\pi\tilde{x}}{L}) \cos(\frac{n\pi\tilde{y}}{L}), \\ w(\tilde{x}, \tilde{y}) &= \sum_{(m,n)\in\mathbb{N}^2} c_{mn} \cos(\frac{m\pi\tilde{x}}{L}) \cos(\frac{n\pi\tilde{y}}{L}), \end{aligned}$$

where $\mathbb{N} = \{0, 1, 2, \cdots\}$ is nonnegative integer set and a_{mn}, b_{mn}, c_{mn} are the Fourier coefficients, into (5.7) which yields

$$\begin{pmatrix} -d_1k^2 + J_{11} & J_{12} & 0 \\ -\chi v_*k^2 + J_{21} & -d_2k^2 + J_{22} & J_{23} \\ 0 & J_{32} & -d_3k^2 + J_{33} \end{pmatrix} \begin{pmatrix} a_{mn} \\ b_{mn} \\ c_{mn} \end{pmatrix} = \begin{pmatrix} 0 \\ 0 \\ 0 \end{pmatrix}, \tag{5.8}$$

where $k^2 = (\frac{m\pi}{L})^2 + (\frac{n\pi}{L})^2, m, n \in \mathbb{N}$. Clearly $(m, n) = (0, 0)$ can be ruled out because the assumption $(\mathbf{A_2})$ is satisfied. For each pair $(m, n) \in \mathbb{N}^2 \setminus \{(0, 0)\}$, (5.7) has nonzero solution

(u, v, w) if and only if the coefficient matrix of (5.8) is singular or equivalently

$$\begin{aligned}\chi = \chi_{mn}^S =& \frac{(d_1 d_2 J_{33} + d_1 d_3 J_{22} + d_2 d_3 J_{11})k^4 - d_1 d_2 d_3 k^6}{J_{12}(d_3 k^2 - J_{33}) v_* k^2} - \\ & \frac{(d_1 J_{22} J_{33} - d_1 J_{23} J_{32} + d_2 J_{11} J_{33} + d_3 J_{11} J_{22} - d_3 J_{12} J_{21})k^2 + s_3}{J_{12}(d_3 k^2 - J_{33}) v_* k^2},\end{aligned} \tag{5.9}$$

where s_3 is given in (4.4).

So if $\chi = \chi_{mn}^S$ then condition (5.6) is satisfied. Since the rank of coefficient matrix of Eq. (5.8) equals two when $\chi = \chi_{mn}^S$, we conclude that $\dim(\mathcal{N}(D_{\mathbf{u}}\mathcal{A}(\mathbf{u}_*, \chi))) = 1$. When $\chi = \chi_{mn}^S$, solving (5.8) yields

$$a_{mn} = \frac{(d_3 k^2 - J_{33}) J_{12}}{(d_1 k^2 - J_{11}) J_{32}}, \quad b_{mn} = \frac{d_3 k^2 - J_{33}}{J_{32}}, \quad c_{mn} = 1,$$

which is a set of basis vector of the null space $\mathcal{N}(D_{\mathbf{u}}\mathcal{A}(\mathbf{u}_*, \chi))$. Thus we get

$$\mathcal{N}(D_{\mathbf{u}}\mathcal{A}(\mathbf{u}_*, \chi_{mn}^S)) = \operatorname{span}\{(\bar{u}_{mn}, \bar{v}_{mn}, \bar{w}_{mn})\}, \tag{5.10}$$

and

$$\bar{u}_{mn} = a_{mn} \cos(\frac{m\pi\tilde{x}}{L}) \cos(\frac{n\pi\tilde{y}}{L}),\ \bar{v}_{mn} = b_{mn} \cos(\frac{m\pi\tilde{x}}{L}) \cos(\frac{n\pi\tilde{y}}{L}),\ \bar{w}_{mn} = \cos(\frac{m\pi\tilde{x}}{L}) \cos(\frac{n\pi\tilde{y}}{L}). \tag{5.11}$$

Applying the Crandall-Rabinowitz local theory in [50], we now prove in the following theorem that the steady state bifurcation occurs at $(\bar{u}, \bar{v}, \bar{w}, \chi_{mn}^S)$ for each pair $(m, n) \in \mathbb{N}^2 \setminus \{(0, 0)\}$, which establishes the existence of nonconstant positive steady states to (5.1).

Theorem 5.2 *Assume that* $(\mathbf{A_1})$ *and* $(\mathbf{A_2})$ *are satisfied. Furthermore suppose that for arbitrary two pairs of integers* $(m, n), (\tilde{m}, \tilde{n}) \in \mathbb{N}^2 \setminus \{(0, 0)\}$,

$$\chi_{mn}^S \neq \chi_{\tilde{m}\tilde{n}}^S,\ \forall\ (m, n) \neq (\tilde{m}, \tilde{n}) \text{ and } m^2 + n^2 \neq \tilde{m}^2 + \tilde{n}^2. \tag{5.12}$$

Let $\mathcal{Z}$ *be any closed complement of* $\mathcal{N}(D_{\mathbf{u}}\mathcal{A}(\mathbf{u}_*, \chi_{mn}^S)) = \operatorname{span}\{(\bar{u}_{mn}, \bar{v}_{mn}, \bar{w}_{mn})\}$ *in* $\mathbb{X}^3$ *defined by*

$$\mathcal{Z} = \left\{ (u, v, w) \in \mathbb{X} \times \mathbb{X} \times \mathbb{X} \Big| \int_\Omega u\bar{u}_{mn} + v\bar{v}_{mn} + w\bar{w}_{mn} d\tilde{x} d\tilde{y} = 0 \right\}. \tag{5.13}$$

Then for each pair $(m, n) \in \mathbb{N}^2 \setminus \{(0, 0)\}$, *there exist an open interval* $\mathbb{I} = (-\kappa, \kappa)$ *and two continuously differentiable functions* $\chi_{mn}(s) : \mathbb{I} \to \mathbb{R}$ *satisfying* $\chi_{mn}(0) = \chi_{mn}^S$ *and* $(\xi_{mn}(s, \tilde{x}, \tilde{y}), \zeta_{mn}(s, \tilde{x}, \tilde{y}), \eta_{mn}(s, \tilde{x}, \tilde{y})) : \mathbb{I} \to \mathcal{Z}$ *with* $(\xi_{mn}(0, \tilde{x}, \tilde{y}), \zeta_{mn}(0, \tilde{x}, \tilde{y}), \eta_{mn}(0, \tilde{x}, \tilde{y})) = (0, 0, 0)$ *and a unique one-parameter curve* $\Gamma_{mn}(s) = \{(u_{mn}(s, \tilde{x}, \tilde{y}), v_{mn}(s, \tilde{x}, \tilde{y}), w_{mn}(s, \tilde{x}, \tilde{y}),$ $\chi_{mn}(s)) \big| s \in (-\kappa, \kappa)\}$ *of non-constant positive steady states to (5.1) that bifurcate from* (u_*, v_*, w_*)

at $\chi = \chi^S_{mn}$. Furthermore, the solutions are continuously differentiable of s and can be written as follows

$$
\begin{aligned}
&\chi_{mn}(s) = \chi^S_{mn} + O(s),\ \ s \in (-\kappa, \kappa),\\
&(u_{mn}(s,\tilde{x},\tilde{y}), v_{mn}(s,\tilde{x},\tilde{y}), w_{mn}(s,\tilde{x},\tilde{y})) = (u_*, v_*, w_*) + s(\bar{u}_{mn}, \bar{v}_{mn}, \bar{w}_{mn}) + \\
&\qquad\qquad s(\xi_{mn}(s,\tilde{x},\tilde{y}), \zeta_{mn}(s,\tilde{x},\tilde{y}), \eta_{mn}(s,\tilde{x},\tilde{y})), s \in (-\kappa, \kappa)
\end{aligned}
\tag{5.14}
$$

where $(\bar{u}_{mn}, \bar{v}_{mn}, \bar{w}_{mn})$ is given by (5.11).

Proof According to Crandall-Rabinowitz local theory in [50], all necessary conditions except the following have been verified

$$D_{\chi\mathbf{u}}\mathcal{A}(\mathbf{u}_*, \chi)[\bar{u}_{mn}, \bar{v}_{mn}, \bar{w}_{mn}]\ |_{\chi=\chi^S_{mn}} \notin \mathrm{Im}(D_{\mathbf{u}}\mathcal{A}(\mathbf{u}_*, \chi^S_{mn})). \tag{5.15}$$

We'll prove by contradiction that (5.15) is satisfied. For this purpose, we suppose that condition (5.15) fails, then there exists a nontrivial solution (u, v, w) which satisfies

$$
\begin{cases}
d_1\Delta u + J_{11}u + J_{12}v = 0, & (\tilde{x},\tilde{y}) \in \Omega,\\
\chi^S_{mn} v_*\Delta u + d_2\Delta v + J_{21}u + J_{22}v + J_{23}w = k^2 v_* a_{mn}\cos(\frac{m\pi\tilde{x}}{L})\cos(\frac{n\pi\tilde{y}}{L}), & (\tilde{x},\tilde{y}) \in \Omega,\\
d_3\Delta w + J_{32}v + J_{33}w = 0, & (\tilde{x},\tilde{y}) \in \Omega,\\
\frac{\partial u}{\partial \nu} = \frac{\partial v}{\partial \nu} = \frac{\partial w}{\partial \nu} = 0, & (\tilde{x},\tilde{y}) \in \partial\Omega.
\end{cases}
\tag{5.16}
$$

Multiplying the first three equations in (5.16) by $\cos(\frac{m\pi\tilde{x}}{L})\cos(\frac{n\pi\tilde{y}}{L})$ and integrating them over Ω by parts and noting that the Neumann boundary conditions, we have

$$
\begin{aligned}
&\begin{pmatrix}
-d_1k^2 + J_{11} & J_{12} & 0\\
-\chi^S_{mn} v_* k^2 + J_{21} & -d_2k^2 + J_{22} & J_{23}\\
0 & J_{32} & -d_3k^2 + J_{33}
\end{pmatrix}
\begin{pmatrix}
\int_\Omega u\cos(\frac{m\pi\tilde{x}}{L})\cos(\frac{n\pi\tilde{y}}{L})d\tilde{x}d\tilde{y}\\
\int_\Omega v\cos(\frac{m\pi\tilde{x}}{L})\cos(\frac{n\pi\tilde{y}}{L})d\tilde{x}d\tilde{y}\\
\int_\Omega w\cos(\frac{m\pi\tilde{x}}{L})\cos(\frac{n\pi\tilde{y}}{L})d\tilde{x}d\tilde{y}
\end{pmatrix}\\
&= (0, \frac{k^2L^2v_*a_{mn}}{4}, 0)^{\mathbb{T}}.
\end{aligned}
\tag{5.17}
$$

The coefficient matrix of Eq. (5.17) is singular and the rank is equal to two because of (5.9), while the rank of the augmented matrix of Eq. (5.17) is equal to three, then this leads to a contradiction, which manifests condition (5.15) is satisfied. Moreover, from (5.12), we get the uniqueness of the bifurcating nonconstant steady state. In view of Theorem 1.7 of [50], the proof of the theorem is completed. ■

5.2 Stability of the non-constant positive steady state

Here the stability or instability refers to that of the bifurcated inhomogeneous steady state regarded as an equilibrium solution to model (1.3). Based on the arguments in Corollary 1.13 of [51], In what follows, we shall derive criterion and explicit formulas to determine the direction of steady state bifurcation and stability of the bifurcating solution for the predator-taxis system (1.3). Since the operator $\mathcal{A}$ is C^4-smooth, according to Theorem 1.18 in [50], $(u_{mn}(s,\tilde{x},\tilde{y}), v_{mn}(s,\tilde{x},\tilde{y}), w_{mn}(s,\tilde{x},\tilde{y}), \chi_{mn}(s))$ are C^3-smooth functions of s, and therefore we can expand them as follows:

$$\begin{cases} u_{mn}(s,\tilde{x},\tilde{y}) = u_* + sa_{mn}\cos(\frac{m\pi}{L}\tilde{x})\cos(\frac{n\pi}{L}\tilde{y}) + s^2\phi_1(\tilde{x},\tilde{y}) + s^3\phi_2(\tilde{x},\tilde{y}) + o(s^3), \\ v_{mn}(s,\tilde{x},\tilde{y}) = v_* + sb_{mn}\cos(\frac{m\pi}{L}\tilde{x})\cos(\frac{n\pi}{L}\tilde{y}) + s^2\psi_1(\tilde{x},\tilde{y}) + s^3\psi_2(\tilde{x},\tilde{y}) + o(s^3), \\ w_{mn}(s,\tilde{x},\tilde{y}) = w_* + s\cos(\frac{m\pi}{L}\tilde{x})\cos(\frac{n\pi}{L}\tilde{y}) + s^2\rho_1(\tilde{x},\tilde{y}) + s^3\rho_2(\tilde{x},\tilde{y}) + o(s^3), \\ \chi_{mn}(s) = \chi_{mn}^S + s\mathcal{K}_1 + s^2\mathcal{K}_2 + o(s^2), \end{cases} \tag{5.18}$$

where $(\phi_i,\psi_i,\rho_i) \in \mathcal{Z}$ and $\mathcal{K}_i$ are constants for $i=1,2$, $o(s^3)$ terms in $u_{mn}(s,\tilde{x},\tilde{y}), v_{mn}(s,\tilde{x},\tilde{y})$ and $w_{mn}(s,\tilde{x},\tilde{y})$ are taken in $\mathbb{X}$-topology, $o(s^2)$ in term $\chi_{mn}(s)$ is a constant. It is easy to see

$$\begin{cases} d_1\Delta u_{mn}(s,\tilde{x},\tilde{y}) = -sa_{mn}d_1k^2\cos(\frac{m\pi}{L}\tilde{x})\cos(\frac{n\pi}{L}\tilde{y}) + s^2d_1\Delta\phi_1 + s^3d_1\Delta\phi_2 + o(s^3), \\ d_2\Delta v_{mn}(s,\tilde{x},\tilde{y}) = -sb_{mn}d_2k^2\cos(\frac{m\pi}{L}\tilde{x})\cos(\frac{n\pi}{L}\tilde{y}) + s^2d_2\Delta\psi_1 + s^3d_2\Delta\psi_2 + o(s^3), \\ d_3\Delta w_{mn}(s,\tilde{x},\tilde{y}) = -sd_3k^2\cos(\frac{m\pi}{L}\tilde{x})\cos(\frac{n\pi}{L}\tilde{y}) + s^2d_3\Delta\rho_1 + s^3d_3\Delta\rho_2 + o(s^3). \end{cases} \tag{5.19}$$

Moreover, from the Taylor's expansion, we have

$$\begin{aligned} & f(u_{mn}(s,\tilde{x},\tilde{y}), v_{mn}(s,\tilde{x},\tilde{y}), w_{mn}(s,\tilde{x},\tilde{y})) \\ & = \bar{f} + s\Big(\big(\bar{f}_u a_{mn} + \bar{f}_v b_{mn} + \bar{f}_w\big)\cos(\frac{m\pi\tilde{x}}{L})\cos(\frac{n\pi\tilde{y}}{L})\Big) + s^2\Big(\bar{f}_u\phi_1 + \bar{f}_v\psi_1 + \bar{f}_w\rho_1 + \\ & \frac{1}{2}\big(\bar{f}_{uu}a_{mn}^2 + \bar{f}_{vv}b_{mn}^2 + \bar{f}_{ww} + 2\bar{f}_{uv}a_{mn}b_{mn} + 2\bar{f}_{uw}a_{mn} + 2\bar{f}_{vw}b_{mn}\big)\cos^2(\frac{m\pi\tilde{x}}{L})\cos^2(\frac{n\pi\tilde{y}}{L})\Big) \\ & + s^3\Big(\bar{f}_u\phi_2 + \bar{f}_v\psi_2 + \bar{f}_w\rho_2 + (\bar{f}_{uu}a_{mn} + \bar{f}_{uv}b_{mn})\phi_1\cos(\frac{m\pi\tilde{x}}{L})\cos(\frac{n\pi\tilde{y}}{L}) + \\ & (\bar{f}_{uv}a_{mn} + \bar{f}_{vv}b_{mn})\psi_1\cos(\frac{m\pi\tilde{x}}{L})\cos(\frac{n\pi\tilde{y}}{L}) + (\bar{f}_{ww} + \bar{f}_{uw}a_{mn} + \bar{f}_{vw}b_{mn})\rho_1\times \\ & \cos(\frac{m\pi\tilde{x}}{L})\cos(\frac{n\pi\tilde{y}}{L}) + (\bar{f}_{vw}\psi_1 + \bar{f}_{uw}\phi_1)\cos(\frac{m\pi\tilde{x}}{L})\cos(\frac{n\pi\tilde{y}}{L}) + \frac{1}{6}\big(\bar{f}_{uuu}a_{mn}^3 + 3\bar{f}_{uuv}a_{mn}^2b_{mn} \\ & + 3\bar{f}_{uvv}a_{mn}b_{mn}^2 + \bar{f}_{vvv}b_{mn}^3 + \bar{f}_{www} + 3\bar{f}_{vvw}b_{mn}^2 + 3\bar{f}_{vww}b_{mn} + 3\bar{f}_{uuw}a_{mn}^2 + 3\bar{f}_{uww}a_{mn} + \\ & 6\bar{f}_{uvw}a_{mn}b_{mn}\big)\cos^3(\frac{m\pi\tilde{x}}{L})\cos^3(\frac{n\pi\tilde{y}}{L})\Big) + o(s^3), \end{aligned} \tag{5.20}$$

where $\bar{f}_u = \frac{\partial f}{\partial u}\big|_{(u,v,w)=(u_*,v_*,w_*)}$, $\bar{f}_{uu} = \frac{\partial^2 f}{\partial u^2}\big|_{(u,v,w)=(u_*,v_*,w_*)}$, $\bar{f}_{uuu} = \frac{\partial^3 f}{\partial u^3}\big|_{(u,v,w)=(u_*,v_*,w_*)}$. Similar meanings for $\bar{f}_v, \bar{f}_w, \bar{f}_{uv}, \bar{f}_{vv}, \bar{f}_{uw}, \bar{f}_{vw}, \bar{f}_{ww}, \bar{f}_{uuv}, \bar{f}_{uvv}, \bar{f}_{vvv}, \bar{f}_{www}, \bar{f}_{vvw}, \bar{f}_{vww}, \bar{f}_{uuw}, \bar{f}_{uww}, \bar{f}_{uvw}$.

For g and h, we also use this kind of denotation. Similarly, we can obtain the Taylor expressions of $g(u_{mn}(s,\tilde{x},\tilde{y}),v_{mn}(s,\tilde{x},\tilde{y}),w_{mn}(s,\tilde{x},\tilde{y}))$ and $h(u_{mn}(s,\tilde{x},\tilde{y}),v_{mn}(s,\tilde{x},\tilde{y}),w_{mn}(s,\tilde{x},\tilde{y}))$.

$$\begin{aligned}&\nabla\cdot(v_{mn}(s,\tilde{x},\tilde{y})\nabla u_{mn}(s,\tilde{x},\tilde{y}))\\&=s\big(-v_*a_{mn}k^2\cos(\frac{m\pi\tilde{x}}{L})\cos(\frac{n\pi\tilde{y}}{L})\big)+s^2\Big((\frac{m\pi}{L})^2a_{mn}b_{mn}\sin^2(\frac{m\pi\tilde{x}}{L})\cos^2(\frac{n\pi\tilde{y}}{L})+\\&(\frac{n\pi}{L})^2a_{mn}b_{mn}\cos^2(\frac{m\pi\tilde{x}}{L})\sin^2(\frac{n\pi\tilde{y}}{L})-k^2a_{mn}b_{mn}\cos^2(\frac{m\pi\tilde{x}}{L})\cos^2(\frac{n\pi\tilde{y}}{L})+v_*\Delta\phi_1\Big)+\\&s^3\Big(-\frac{m\pi}{L}\big(a_{mn}\frac{\partial\psi_1}{\partial\tilde{x}}+b_{mn}\frac{\partial\phi_1}{\partial\tilde{x}}\big)\sin(\frac{m\pi\tilde{x}}{L})\cos(\frac{n\pi\tilde{y}}{L})-\frac{n\pi}{L}\big(a_{mn}\frac{\partial\psi_1}{\partial\tilde{y}}+b_{mn}\frac{\partial\phi_1}{\partial\tilde{y}}\big)\times\\&\cos(\frac{m\pi\tilde{x}}{L})\sin(\frac{n\pi\tilde{y}}{L})+v_*\Delta\phi_2+b_{mn}\Delta\phi_1\cos(\frac{m\pi\tilde{x}}{L})\cos(\frac{n\pi\tilde{y}}{L})-k^2a_{mn}\psi_1\times\\&\cos(\frac{m\pi\tilde{x}}{L})\cos(\frac{n\pi\tilde{y}}{L})\Big)+o(s^3).\end{aligned}\tag{5.21}$$

By evaluating $\mathcal{K}_1$ in the fourth equation of (5.18), we have

Lemma 5.3 *Suppose that all conditions in Theorem 5.2 are satisfied. Then for each pair $(m,n)\in\mathbb{N}^2\setminus\{(0,0)\}$, $\mathcal{K}_1=0$ and the bifurcation curve $\Gamma_{mn}(s)$ is pitch-fork.*

Proof Substituting (5.18)-(5.21) into the second equation of (5.1) and collecting s^2-terms yields the following equality:

$$\begin{cases}d_2\Delta\psi_1+\bar{g}_u\phi_1+\bar{g}_v\psi_1+\bar{g}_w\rho_1+\frac{1}{2}\big(\bar{g}_{uu}a_{mn}^2+\bar{g}_{vv}b_{mn}^2+\bar{g}_{ww}+\\2\bar{g}_{uv}a_{mn}b_{mn}+2\bar{g}_{uw}a_{mn}+2\bar{g}_{vw}b_{mn}\big)\cos^2(\frac{m\pi\tilde{x}}{L})\cos^2(\frac{n\pi\tilde{y}}{L})\\\quad=-\chi_{mn}^S\Big((\frac{m\pi}{L})^2a_{mn}b_{mn}\sin^2(\frac{m\pi\tilde{x}}{L})\cos^2(\frac{n\pi\tilde{y}}{L})+v_*\Delta\phi_1+\\\quad(\frac{n\pi}{L})^2a_{mn}b_{mn}\cos^2(\frac{m\pi\tilde{x}}{L})\sin^2(\frac{n\pi\tilde{y}}{L})-k^2a_{mn}b_{mn}\cos^2(\frac{m\pi\tilde{x}}{L})\cos^2(\frac{n\pi\tilde{y}}{L})\Big)+\\\quad\mathcal{K}_1v_*a_{mn}k^2\cos(\frac{m\pi\tilde{x}}{L})\cos(\frac{n\pi\tilde{y}}{L}),\quad(\tilde{x},\tilde{y})\in\Omega,\\\frac{\partial\phi_1}{\partial\nu}=\frac{\partial\psi_1}{\partial\nu}=\frac{\partial\rho_1}{\partial\nu}=0,\quad(\tilde{x},\tilde{y})\in\partial\Omega.\end{cases}\tag{5.22}$$

Multiplying the first equation in (5.22) by $\cos(\frac{m\pi\tilde{x}}{L})\cos(\frac{n\pi\tilde{y}}{L})$ and integrating it over Ω by noting that Neumann boundary conditions yields

$$\begin{aligned}\mathcal{K}_1=&\frac{4}{a_{mn}v_*k^2}\Big(\big(\bar{g}_u-\chi_{mn}^Sv_*k^2\big)\int_\Omega\phi_1\cos(\frac{m\pi\tilde{x}}{L})\cos(\frac{n\pi\tilde{y}}{L})d\tilde{x}d\tilde{y}+\big(\bar{g}_v-d_2k^2\big)\times\\&\int_\Omega\psi_1\cos(\frac{m\pi\tilde{x}}{L})\cos(\frac{n\pi\tilde{y}}{L})d\tilde{x}d\tilde{y}+\bar{g}_w\int_\Omega\rho_1\cos(\frac{m\pi\tilde{x}}{L})\cos(\frac{n\pi\tilde{y}}{L})d\tilde{x}d\tilde{y}\Big).\end{aligned}\tag{5.23}$$

Substituting (5.18)-(5.21) into the first and third equations of (5.1) and collecting their s^2-terms give us

$$\begin{cases} d_1\Delta\phi_1 + \bar{f}_u\phi_1 + \bar{f}_v\psi_1 + \bar{f}_w\rho_1 + \frac{1}{2}\big(\bar{f}_{uu}a_{mn}^2 + \bar{f}_{vv}b_{mn}^2 + \bar{f}_{ww} + \\ 2\bar{f}_{uv}a_{mn}b_{mn} + 2\bar{f}_{uw}a_{mn} + 2\bar{f}_{vw}b_{mn}\big)\cos^2(\frac{m\pi\tilde{x}}{L})\cos^2(\frac{n\pi\tilde{y}}{L}) = 0, \qquad (\tilde{x},\tilde{y})\in\Omega, \\ d_3\Delta\rho_1 + \bar{h}_u\phi_1 + \bar{h}_v\psi_1 + \bar{h}_w\rho_1 + \frac{1}{2}\big(\bar{h}_{uu}a_{mn}^2 + \bar{h}_{vv}b_{mn}^2 + \bar{h}_{ww} + \\ 2\bar{h}_{uv}a_{mn}b_{mn} + 2\bar{h}_{uw}a_{mn} + 2\bar{h}_{vw}b_{mn}\big)\cos^2(\frac{m\pi\tilde{x}}{L})\cos^2(\frac{n\pi\tilde{y}}{L}) = 0, \qquad (\tilde{x},\tilde{y})\in\Omega, \\ \frac{\partial\phi_1}{\partial\nu} = \frac{\partial\psi_1}{\partial\nu} = \frac{\partial\rho_1}{\partial\nu} = 0, \qquad (\tilde{x},\tilde{y})\in\partial\Omega. \end{cases} \tag{5.24}$$

Multiplying the first two equations in (5.24) by $\cos(\frac{m\pi\tilde{x}}{L})\cos(\frac{n\pi\tilde{y}}{L})$ and noting that Neumann boundary conditions and integrating them over Ω by parts yield

$$\begin{aligned} &\Big(-d_1k^2+\bar{f}_u\Big)\int_\Omega \phi_1\cos(\frac{m\pi\tilde{x}}{L})\cos(\frac{n\pi\tilde{y}}{L})d\tilde{x}d\tilde{y} + \bar{f}_v\int_\Omega \psi_1\cos(\frac{m\pi\tilde{x}}{L})\cos(\frac{n\pi\tilde{y}}{L})d\tilde{x}d\tilde{y} + \\ &\bar{f}_w\int_\Omega \psi_1\cos(\frac{m\pi\tilde{x}}{L})\cos(\frac{n\pi\tilde{y}}{L})d\tilde{x}d\tilde{y} = 0, \\ &\bar{h}_u\int_\Omega \phi_1\cos(\frac{m\pi\tilde{x}}{L})\cos(\frac{n\pi\tilde{y}}{L})d\tilde{x}d\tilde{y} + \bar{h}_v\int_\Omega \psi_1\cos(\frac{m\pi\tilde{x}}{L})\cos(\frac{n\pi\tilde{y}}{L})d\tilde{x}d\tilde{y} + \\ &\Big(-d_3k^2+\bar{h}_w\Big)\int_\Omega \rho_1\cos(\frac{m\pi\tilde{x}}{L})\cos(\frac{n\pi\tilde{y}}{L})d\tilde{x}d\tilde{y} = 0. \end{aligned} \tag{5.25}$$

Noting that $(\phi_1,\psi_1,\rho_1)\in\mathcal{Z}$ as defined in (5.13), we have

$$\begin{aligned} &a_{mn}\int_\Omega \phi_1\cos(\frac{m\pi\tilde{x}}{L})\cos(\frac{n\pi\tilde{y}}{L})d\tilde{x}d\tilde{y} + b_{mn}\int_\Omega \psi_1\cos(\frac{m\pi\tilde{x}}{L})\cos(\frac{n\pi\tilde{y}}{L})d\tilde{x}d\tilde{y} + \\ &\int_\Omega \rho_1\cos(\frac{m\pi\tilde{x}}{L})\cos(\frac{n\pi\tilde{y}}{L})d\tilde{x}d\tilde{y} = 0. \end{aligned} \tag{5.26}$$

From (5.25) and (5.26), we arrive at the following equations:

$$\begin{pmatrix} -d_1k^2+\bar{f}_u & \bar{f}_v & \bar{f}_w \\ \bar{h}_u & \bar{h}_v & -d_3k^2+\bar{h}_w \\ a_{mn} & b_{mn} & 1 \end{pmatrix}\begin{pmatrix} \int_\Omega \phi_1\cos(\frac{m\pi\tilde{x}}{L})\cos(\frac{n\pi\tilde{y}}{L})d\tilde{x}d\tilde{y} \\ \int_\Omega \psi_1\cos(\frac{m\pi\tilde{x}}{L})\cos(\frac{n\pi\tilde{y}}{L})d\tilde{x}d\tilde{y} \\ \int_\Omega \rho_1\cos(\frac{m\pi\tilde{x}}{L})\cos(\frac{n\pi\tilde{y}}{L})d\tilde{x}d\tilde{y} \end{pmatrix} = \begin{pmatrix} 0 \\ 0 \\ 0 \end{pmatrix}. \tag{5.27}$$

Noting that $\bar{f}_w = J_{13} = 0$ and $\bar{h}_u = J_{31} = 0$. The determinant of the coefficient matrix $\mathcal{M}$ in system (5.27) is

$$\begin{aligned} Det(\mathcal{M}) &= (-d_1k^2+\bar{f}_u)\bar{h}_v + \bar{f}_v(-d_3k^2+\bar{h}_w)a_{mn} - (-d_1k^2+\bar{f}_u)(-d_3k^2+\bar{h}_w)b_{mn} \\ &= (-d_1k^2+\bar{f}_u)\bar{h}_v + \bar{f}_v(-d_3k^2+\bar{h}_w)\frac{(d_3k^2-\bar{h}_w)\bar{f}_v}{(d_1k^2-\bar{f}_u)\bar{h}_v} - (d_1k^2-\bar{f}_u)(d_3k^2-\bar{h}_w)\frac{d_3k^2-\bar{h}_w}{\bar{h}_v} > 0. \end{aligned}$$

Hence we have

$$\int_\Omega \phi_1\cos(\frac{m\pi\tilde{x}}{L})\cos(\frac{n\pi\tilde{y}}{L}) = \int_\Omega \psi_1\cos(\frac{m\pi\tilde{x}}{L})\cos(\frac{n\pi\tilde{y}}{L}) = \int_\Omega \rho_1\cos(\frac{m\pi\tilde{x}}{L})\cos(\frac{n\pi\tilde{y}}{L}) = 0,$$

which implies that $\mathcal{K}_1 = 0$ and thus we finish the proof of the lemma. ■

Next, we present another version stability result about the unique positive spatially homogeneous steady state E_* in this subsection, which is useful for analyzing the stability of the bifurcating non-constant steady states.

Lemma 5.4 *Assume that* $(\mathbf{A_1})$ *and* $(\mathbf{A_2})$ *hold. Furthermore suppose that* $\delta_1 v_* < (v_* + w_*)^2$ *and* $\frac{(\beta_2-\beta_1)u_*}{(u_*+v_*)^2} < \frac{\delta_2 w_*}{(v_*+w_*)^2}$ *are satisfied. Denote*

$$\chi_0 = \max_{(m,n)\in\mathbb{N}^2\setminus\{(0,0)\}} \{\chi_{mn}^S, \chi_{mn}^H\}, \tag{5.28}$$

where χ_{mn}^S *is given in* (5.9) *and* χ_{mn}^H *is given in* (5.29) *which specified within the proof. Then the unique positive spatially homogeneous steady state* $E_*(u_*, v_*, w_*)$ *is locally asymptotically stable if* $\chi > \chi_0$ *and it is unstable if* $\chi < \chi_0$.

Proof From the assumptions $\delta_1 v_* < (v_* + w_*)^2$ and $\frac{(\beta_2-\beta_1)u_*}{(u_*+v_*)^2} < \frac{\delta_2 w_*}{(v_*+w_*)^2}$, we have $\frac{\delta_1 v_* w_*}{(v_*+w_*)^2} - w_* < 0$ and $\frac{(\beta_2-\beta_1)u_* v_*}{(u_*+v_*)^2} - \frac{\delta_2 v_* w_*}{(v_*+w_*)^2} < 0$. A direct calculation yields that

$$r_3(\chi, k) > 0 \text{ if and only if } \chi > \chi_{mn}^S,$$
$$r_1(\chi, k) r_2(\chi, k) - r_3(\chi, k) > 0 \text{ if and only if } \chi > \chi_{mn}^H,$$

where χ_{mn}^S is given in (5.9) and

$$\begin{aligned}\chi_{mn}^H = &-\frac{(d_1(d_1d_2 + d_1d_3) + (d_2 + d_3)(d_1d_2 + d_2d_3 + d_3d_1))k^6}{(d_1 + d_2)v_*J_{12}k^4 - (J_{11} + J_{22})k^2} + \\ &\frac{((d_1 + d_2 + d_3)d_1(J_{22} + J_{33}) + d_1d_2J_{11} + d_2^2(J_{11} + J_{33}) + d_2d_3J_{33} + d_1d_3J_{11})k^4}{(d_1 + d_2)v_*J_{12}k^4 - (J_{11} + J_{22})k^2} \\ &+ \frac{((d_2 + d_3)d_3(J_{11} + J_{22}) - (d_1d_2 + d_2d_3 + d_3d_1)s_1)k^4}{(d_1 + d_2)v_*J_{12}k^4 - (J_{11} + J_{22})k^2} \\ &+ \frac{(d_1s_1(J_{22} + J_{33}) - (d_1 + d_2 + d_3)s_2 + d_2s_1(J_{11} + J_{33}) + d_3s_1(J_{11} + J_{22}))k^2}{(d_1 + d_2)v_*J_{12}k^4 - (J_{11} + J_{22})k^2} \\ &+ \frac{(d_1(J_{22}J_{33} - J_{23}J_{32}) + d_2J_{11}J_{33} + d_3(J_{11}J_{22} - J_{12}J_{21}))k^2 - s_1s_2 + s_3}{(d_1 + d_2)v_*J_{12}k^4 - (J_{11} + J_{22})k^2},\end{aligned} \tag{5.29}$$

where J_{ij} with $i, j = 1, 2, 3$ are given in (4.2). Therefore (u_*, v_*, w_*) is locally asymptotically stable if for each pair $(m, n) \in \mathbb{N}^2 \setminus \{(0, 0)\}$ such that $\chi > \chi_0$, while is unstable if there exists one pair $(m, n) \in \mathbb{N}^2 \setminus \{(0, 0)\}$ such that $\chi < \chi_{mn}^S$ or $\chi < \chi_{mn}^H$, that is, if $\chi < \chi_0$ over $(m, n) \in \mathbb{N}^2 \setminus \{(0, 0)\}$. This completes the proof. ■

Remark 5.5 *From Lemma 5.4, we know that system* (1.3) *undergoes Turing instability when the chemotactic factor* χ *crosses the critical value* χ^S_{mn}. *On the other hand, Theorem 5.2 says that there exists a unique one-parameter curve* $\Gamma_{mn}(s)$, $s \in (-\kappa, \kappa)$ *corresponding to the non-constant positive steady states of system* (1.3) *bifurcates from* $E_*(u_*, v_*, w_*)$ *at* $\chi = \chi^S_{mn}$, *which shows that the existence of non-constant positive steady state is close related to Turing instability and pattern formation.*

Remark 5.6 *Lemma 5.4 also implies that the predator-taxis may annihilate the spatial patterns and induce the unique coexistence steady state even thought the chemotaxis coefficient is sufficiently large, which is also illustrated in [31] and [32]. This phenomenon is possibly occurs in predator-prey interactive population models because some predators know how to hunt evasive prey. For example, fish predators know how to pursue and capture evasive prey once they find, which have been disclosed recently by Matthew J. McHenry in [52].*

We proceed to the stability analysis of the bifurcating solutions $(u_{mn}(s, \tilde{x}, \tilde{y}), v_{mn}(s, \tilde{x}, \tilde{y}), w_{mn}(s, \tilde{x}, \tilde{y}), \chi_{mn}(s))$ with $s \in (-\kappa, \kappa)$. Since 0 is a simple eigenvalue of operator $D_{(u,v,w)}\mathcal{A}(u_*, v_*, w_*, \chi^S_{mn})$ with one-dimensional eigenspace $\mathcal{N}(D_{(u,v,w)}\mathcal{A}(u_*, v_*, w_*, \chi^S_{mn})) = \text{span}\{(\bar{u}_{mn}, \bar{v}_{mn}, \bar{w}_{mn})\}$ given in (5.10). According to the arguments in [51, Corollary1.13], this branch of solutions will be asymptotically stable if the real part of any eigenvalue λ of the following linearized system of (5.1) around $(u_{mn}(s, \tilde{x}, \tilde{y}), v_{mn}(s, \tilde{x}, \tilde{y}), w_{mn}(s, \tilde{x}, \tilde{y}), \chi_{mn}(s))$ is negative:

$$D_{(u,v,w)}\mathcal{A}(u_{mn}(s, \tilde{x}, \tilde{y}), v_{mn}(s, \tilde{x}, \tilde{y}), w_{mn}(s, \tilde{x}, \tilde{y}), \chi_{mn}(s))(u, v, w) = \lambda(s)(u, v, w), \quad (5.30)$$

for $(u, v, w) \in \mathbb{X} \times \mathbb{X} \times \mathbb{X}$. We now give the following stability results of the bifurcating non-constant positive steady states.

Theorem 5.7 *Assume that all conditions in Theorem 5.2 and Lemma 5.4 are satisfied. Let* $\Gamma_{mn}(s) = \{(u_{mn}(s, \tilde{x}, \tilde{y}), v_{mn}(s, \tilde{x}, \tilde{y}), w_{mn}(s, \tilde{x}, \tilde{y}), \chi_{mn}(s))\}$, $s \in (-\kappa, \kappa)$ *be the bifurcation branch given by* (5.14). *Denote* $\chi_0 = \max\limits_{(m,n)\in\mathbb{N}^2\setminus\{(0,0)\}} \{\chi^S_{mn}, \chi^H_{mn}\}$ *which is the same as given in* (5.28), *and assume that* $\chi^S_{mn} \neq \chi^H_{mn}$ *for all* $(m, n) \in \mathbb{N}^2 \setminus \{(0, 0)\}$ *holds. Then the following statements hold:*

(i) If $\chi_0 = \chi^H_{m_1 n_1} > \max\limits_{(m,n)\in\mathbb{N}^2\setminus\{(0,0)\}} \chi^S_{mn}$, *then* $\Gamma_{mn}(s)$ *near* $(u_*, v_*, w_*, \chi^S_{mn})$ *is always unstable for each pair* $(m, n) \in \mathbb{N}^2 \setminus \{(0, 0)\}$.

(ii) *If* $\chi_0 = \chi^S_{m_0n_0} > \max_{(m,n)\in\mathbb{N}^2\setminus\{(0,0)\}} \chi^H_{mn}$*, then we have the following results*

(ii.a) when $\Xi_0 = 1 + \frac{J_{23}J_{32}}{(J_{33}-d_3k_0^2)^2} + \frac{J_{12}(J_{21}-\chi^S_{m_0n_0}v_*k_0^2)}{(J_{11}-d_1k_0^2)^2} > 0$, $\Gamma_{m_0n_0}(s), s \in (-\kappa,\kappa)$ *near* $(u_*, v_*, w_*, \chi^S_{m_0n_0})$ *is locally asymptotically stable when* $\mathcal{K}_2 < 0$ *and it is unstable when* $\mathcal{K}_2 > 0$*;*

(ii.b) when $\Xi_0 = 1 + \frac{J_{23}J_{32}}{(J_{33}-d_3k_0^2)^2} + \frac{J_{12}(J_{21}-\chi^S_{m_0n_0}v_*k_0^2)}{(J_{11}-d_1k_0^2)^2} < 0$, $\Gamma_{m_0n_0}(s), s \in (-\kappa,\kappa)$ *near* $(u_*, v_*, w_*, \chi^S_{m_0n_0})$ *is locally asymptotically stable when* $\mathcal{K}_2 > 0$ *and it is unstable when* $\mathcal{K}_2 < 0$*;*

(ii.c) $\Gamma_{mn}(s)$ *near* $(u_*, v_*, w_*, \chi^S_{mn})$ *is always unstable for pairs of integers* $(m,n) \in \mathbb{N}^2 \setminus \{(0,0)\}$ *satisfying* $(m,n) \neq (m_0,n_0)$ *and* $m^2+n^2 \neq m_0^2+n_0^2$*;*

Proof To prove (i), according to the standard eigenvalue perturbation theory in [53], we shall study the limit of eigenvalue system (5.30) for each pair $(m,n) \in \mathbb{N}^2 \setminus \{(0,0)\}$ as $s \to 0$, that is, the following eigenvalue problem

$$\begin{cases} d_1\Delta u + J_{11}u + J_{12}v = \hat{\lambda}u, & \mathbf{x} = (\tilde{x},\tilde{y}) \in \Omega, \\ d_2\Delta v + \chi^S_{mn}v_*\Delta u + J_{21}u + J_{22}v + J_{23}w = \hat{\lambda}v, & \mathbf{x} = (\tilde{x},\tilde{y}) \in \Omega, \\ d_3\Delta w + J_{32}v + J_{33}w = \hat{\lambda}w, & \mathbf{x} = (\tilde{x},\tilde{y}) \in \Omega, \\ \frac{\partial u}{\partial \nu} = \frac{\partial v}{\partial \nu} = \frac{\partial w}{\partial \nu} = 0, & \mathbf{x} = (\tilde{x},\tilde{y}) \in \partial\Omega. \end{cases} \tag{5.31}$$

Multiplying (5.31) the first three equations by $\cos(\frac{m\pi\tilde{x}}{L})\cos(\frac{n\pi\tilde{y}}{L})$ and then integrating them over Ω by parts and noting Neumann boundary conditions, we obtain

$$\begin{pmatrix} -d_1k^2 + J_{11} - \hat{\lambda} & J_{12} & 0 \\ -\chi^S_{mn}v_*k^2 + J_{21} & -d_2k^2 + J_{22} - \hat{\lambda} & J_{23} \\ 0 & J_{32} & -d_3k^2 + J_{33} - \hat{\lambda} \end{pmatrix} \begin{pmatrix} \int_\Omega u\cos(\frac{m\pi}{L}\tilde{x})\cos(\frac{n\pi}{L}\tilde{y})d\tilde{x}d\tilde{y} \\ \int_\Omega v\cos(\frac{m\pi}{L}\tilde{x})\cos(\frac{n\pi}{L}\tilde{y})d\tilde{x}d\tilde{y} \\ \int_\Omega w\cos(\frac{m\pi}{L}\tilde{x})\cos(\frac{n\pi}{L}\tilde{y})d\tilde{x}d\tilde{y} \end{pmatrix}$$
$$= (0,0,0)^{\mathbb{T}}. \tag{5.32}$$

Clearly $\hat{\lambda}$ is an eigenvalue of (5.31) if and only if the coefficient determinant of (5.32) is equal to zero, i.e.,

$$\begin{vmatrix} -d_1k^2 + J_{11} - \hat{\lambda} & J_{12} & 0 \\ -\chi^S_{mn}v_*k^2 + J_{21} & -d_2k^2 + J_{22} - \hat{\lambda} & J_{23} \\ 0 & J_{32} & -d_3k^2 + J_{33} - \hat{\lambda} \end{vmatrix} = 0,$$

which gives the following characteristic equation

$$\hat{\lambda}^3 + r_1(\chi^S_{mn},k)\hat{\lambda}^2 + r_2(\chi^S_{mn},k)\hat{\lambda} + r_3(\chi^S_{mn},k) = 0, \tag{5.33}$$

where the coefficients $r_i(\chi^S_{mn},k), i=1,2,3$ are the coefficients $r_i(\chi,k)\, i=1,2,3$ defined in (4.7) evaluated at $\chi=\chi^S_{mn}$. It is easy to see that characteristic eq. (5.33) has a root with positive real part if $r_3(\chi^S_{mn},k)<0$ or $r_1(\chi^S_{mn},k)r_2(\chi^S_{mn},k)-r_3(\chi^S_{mn},k)<0$, which means if $\chi^S_{mn}<\max\limits_{(m,n)\in\mathbb{N}^2\setminus\{(0,0)\}}\{\chi^S_{mn},\chi^H_{mn}\}=\chi_0=\chi^H_{m_1n_1}$ for $(m,n)\in\mathbb{N}^2\setminus\{(0,0)\}$ or $\chi_0=\chi^S_{m_0n_0}>\max\limits_{(m,n)\in\mathbb{N}^2\setminus\{(0,0)\}}\chi^H_{mn}$ satisfying $(m,n)\neq(m_0,n_0)$ and $m^2+n^2\neq m_0^2+n_0^2$, we infer from Lemma 5.4 that the characteristic Eq. (5.33) always has at least an eigenvalue with positive real part. According to the standard eigenvalue perturbation theory (see, for example [53]), the linearized system (5.30) has a corresponding eigenvalue with positive real part when s is sufficiently small, which implies the non-constant steady state Γ^s_{mn} is always unstable near $(u_*,v_*,w_*,\chi^S_{mn})$. Therefore, the proof of (i) and $(ii.c)$ are completed.

Next, we proceed to investigate the stability result about the bifurcating nonconstant steady state $(u_{m_0n_0}(s,\tilde{x},\tilde{y}),v_{m_0n_0}(s,\tilde{x},\tilde{y}),w_{m_0n_0}(s,\tilde{x},\tilde{y}))$ of (ii). In view of Corollary 1.13 in [51], there exist an interval $\hat{\mathbb{I}}$ with $\chi^S_{m_0n_0}\in\hat{\mathbb{I}}$ and two continuously differentiable functions $\lambda:\mathbb{I}=(-\kappa,\kappa)\to\mathbb{R}$, $\mu:\hat{\mathbb{I}}\to\mathbb{R}$ with $\lambda(0)=0$ and $\mu(\chi^S_{m_0n_0})=0$ such that $\lambda(s)$ is an eigenvalue of (5.30) and $\mu(\chi)$ is an eigenvalue of the following eigenvalue problem

$$D_{(u,v,w)}\mathcal{A}(u_*,v_*,w_*,\chi)(u,v,w)=\mu(\chi)(u,v,w),\ (u,v,w)\in\mathbb{X}\times\mathbb{X}\times\mathbb{X}. \tag{5.34}$$

Furthermore we know from [51] that the eigenfunction of (5.34) can be represented by $\mathbf{u}(\chi,\tilde{x},\tilde{y})=(u(\chi,\tilde{x},\tilde{y}),v(\chi,\tilde{x},\tilde{y}),w(\chi,\tilde{x},\tilde{y}))$, which depends on χ continuously differentiable and is uniquely determined by

$$\begin{aligned}&(u(\chi^S_{m_0n_0},\tilde{x},\tilde{y}),v(\chi^S_{m_0n_0},\tilde{x},\tilde{y}),w(\chi^S_{m_0n_0},\tilde{x},\tilde{y}))\\&=(a_{m_0n_0}\cos(\frac{m_0\pi\tilde{x}}{L})\cos(\frac{n_0\pi\tilde{y}}{L}),b_{m_0n_0}\cos(\frac{m_0\pi\tilde{x}}{L})\cos(\frac{n_0\pi\tilde{y}}{L}),\cos(\frac{m_0\pi\tilde{x}}{L})\cos(\frac{n_0\pi\tilde{y}}{L}))\end{aligned}$$

and $\mathbf{u}(\chi,\tilde{x},\tilde{y})-(u(\chi_{m_0n_0},\tilde{x},\tilde{y}),v(\chi_{m_0n_0},\tilde{x},\tilde{y}),w(\chi_{m_0n_0},\tilde{x},\tilde{y}))\in\mathcal{Z}$, where $a_{m_0n_0},b_{m_0n_0}$ and $\mathcal{Z}$ are defined in (5.11) and (5.13) respectively. It follows from (5.34) that

$$\begin{cases}d_1\Delta u+J_{11}u+J_{12}v=\mu u, & (\tilde{x},\tilde{y})\in\Omega,\\ d_2\Delta v+\chi v_*\Delta u+J_{21}u+J_{22}v+J_{23}w=\mu v, & (\tilde{x},\tilde{y})\in\Omega,\\ d_3\Delta w+J_{32}v+J_{33}w=\mu w, & (\tilde{x},\tilde{y})\in\Omega,\\ \frac{\partial u}{\partial\nu}=\frac{\partial v}{\partial\nu}=\frac{\partial w}{\partial\nu}=0, & (\tilde{x},\tilde{y})\in\partial\Omega.\end{cases} \tag{5.35}$$

Differentiating (5.35) with respect to χ and then letting $\chi = \chi^S_{m_0n_0}$, we have

$$\begin{cases} d_1\Delta\dot{u} + J_{11}\dot{u} + J_{12}\dot{v} = \dot{\mu}(\chi^S_{m_0n_0})a_{m_0n_0}\cos(\frac{m_0\pi\tilde{x}}{L})\cos(\frac{n_0\pi\tilde{y}}{L}), & (\tilde{x},\tilde{y}) \in \Omega, \\ d_2\Delta\dot{v} - v_*a_{m_0n_0}k_0^2\cos(\frac{m_0\pi\tilde{x}}{L})\cos(\frac{n_0\pi\tilde{y}}{L}) + \chi^S_{m_0n_0}v_*\Delta\dot{u} + J_{21}\dot{u} + J_{22}\dot{v} + J_{23}\dot{w} & \\ \qquad\qquad = \dot{\mu}(\chi^S_{mn})b_{m_0n_0}\cos(\frac{m_0\pi\tilde{x}}{L})\cos(\frac{n_0\pi\tilde{y}}{L}), & (\tilde{x},\tilde{y}) \in \Omega, \\ d_3\Delta\dot{w} + J_{32}\dot{v} + J_{33}\dot{w} = \dot{\mu}(\chi^S_{mn})\cos(\frac{m_0\pi\tilde{x}}{L})\cos(\frac{n_0\pi\tilde{y}}{L}), & (\tilde{x},\tilde{y}) \in \Omega, \\ \frac{\partial u}{\partial\nu} = \frac{\partial v}{\partial\nu} = \frac{\partial w}{\partial\nu} = 0, & (\tilde{x},\tilde{y}) \in \partial\Omega, \end{cases} \tag{5.36}$$

where $k_0^2 = (\frac{m_0\pi}{L})^2 + (\frac{n_0\pi}{L})^2$, the dot sign $\dot{}$ in (5.36) denotes the differentiation with respect to χ evaluated at $\chi = \chi^S_{m_0n_0}$, that is, $\dot{u} = \frac{\partial u(\chi,\tilde{x},\tilde{y})}{\partial\chi}\big|_{\chi=\chi^S_{m_0n_0}}$, the same meanings for $\dot{v}$ and $\dot{w}$. Multiplying the first three equations in (5.36) by $\cos(\frac{m_0\pi\tilde{x}}{L})\cos(\frac{n_0\pi\tilde{y}}{L})$ and integrating them we obtain

$$\begin{pmatrix} J_{11} - d_1k_0^2 & J_{12} & 0 \\ J_{21} - \chi^S_{m_0n_0}v_*k_0^2 & J_{22} - d_2k_0^2 & J_{23} \\ 0 & J_{32} & J_{33} - d_3k_0^2 \end{pmatrix} \begin{pmatrix} \int_\Omega \dot{u}\cos(\frac{m\pi}{L}\tilde{x})\cos(\frac{n\pi}{L}\tilde{y})d\tilde{x}d\tilde{y} \\ \int_\Omega \dot{v}\cos(\frac{m\pi}{L}\tilde{x})\cos(\frac{n\pi}{L}\tilde{y})d\tilde{x}d\tilde{y} \\ \int_\Omega \dot{w}\cos(\frac{m\pi}{L}\tilde{x})\cos(\frac{n\pi}{L}\tilde{y})d\tilde{x}d\tilde{y} \end{pmatrix} \tag{5.37}$$
$$= (\dot{\mu}(\chi^S_{m_0n_0})a_{m_0n_0}\frac{L^2}{4},\ \dot{\mu}(\chi^S_{m_0n_0})b_{m_0n_0}\frac{L^2}{4} + \frac{k_0^2v_*a_{m_0n_0}L^2}{4},\ \dot{\mu}(\chi^S_{m_0n_0})\frac{L^2}{4})^{\mathbb{T}}.$$

We denote by $\hat{A}$ the augmented matrix of the algebraic system (5.37). Then we have

$$\begin{aligned} \hat{A} = & \begin{pmatrix} J_{11} - d_1k_0^2 & J_{12} & 0 & \dot{\mu}(\chi^S_{m_0n_0})a_{m_0n_0}\frac{L^2}{4} \\ J_{21} - \chi^S_{m_0n_0}v_*k_0^2 & J_{22} - d_2k_0^2 + & J_{23} & \dot{\mu}(\chi^S_{m_0n_0})b_{m_0n_0}\frac{L^2}{4} + \frac{k_0^2v_*a_{m_0n_0}L^2}{4} \\ 0 & J_{32} & J_{33} - d_3k_0^2 & \dot{\mu}(\chi^S_{m_0n_0})\frac{L^2}{4} \end{pmatrix} \\ \to & \begin{pmatrix} J_{11} - d_1k_0^2 & J_{12} & 0 & \dot{\mu}(\chi^S_{m_0n_0})a_{m_0n_0}\frac{L^2}{4} \\ 0 & J_{32} & J_{33} - d_3k_0^2 & \dot{\mu}(\chi^S_{m_0n_0})\frac{L^2}{4} \\ J_{21} - \chi^S_{m_0n_0}v_*k_0^2 & J_{22} - d_2k_0^2 & J_{23} & \dot{\mu}(\chi^S_{m_0n_0})b_{m_0n_0}\frac{L^2}{4} + \frac{k_0^2v_*a_{m_0n_0}L^2}{4} \end{pmatrix} \\ \to & \begin{pmatrix} J_{11} - d_1k_0^2 & J_{12} & 0 & \dot{\mu}(\chi^S_{m_0n_0})a_{m_0n_0}\frac{L^2}{4} \\ 0 & J_{32} & J_{33} - d_3k_0^2 & \dot{\mu}(\chi^S_{m_0n_0})\frac{L^2}{4} \\ 0 & \Theta_1 & J_{23} & \Theta_2 \end{pmatrix}, \end{aligned} \tag{5.38}$$

where $\Theta_1 = J_{22} - d_2k_0^2 - \frac{J_{21}-\chi^S_{m_0n_0}v_*k_0^2}{J_{11}-d_1k_0^2}J_{12}$ and $\Theta_2 = \dot{\mu}(\chi^S_{m_0n_0})b_{m_0n_0}\frac{L^2}{4} + k_0^2v_*a_{m_0n_0}\frac{L^2}{4} - \frac{J_{21}-\chi^S_{m_0n_0}v_*k_0^2}{J_{11}-d_1k_0^2}\dot{\mu}(\chi^S_{m_0n_0})a_{m_0n_0}\frac{L^2}{4}$. From (5.37), we know that the coefficient matrix is singular. Since the algebraic system (5.37) is solvable, it follows from (5.38) that

$$\frac{J_{32}}{\Theta_1} = \frac{J_{33} - d_3k_0^2}{J_{23}} = \frac{\dot{\mu}(\chi^S_{m_0n_0})\frac{L^2}{4}}{\Theta_2}. \tag{5.39}$$

Solving the second equality in (5.39) gives us

$$\varpi\dot{\mu}(\chi^S_{m_0n_0}) = \upsilon,$$

where

$$\begin{aligned}\varpi =&(J_{11}-d_1k_0^2)^2(J_{33}-d_3k_0^2)^2+J_{23}J_{32}(J_{11}-d_1k_0^2)^2+\\ &J_{12}(J_{33}-d_3k_0^2)^2(J_{21}-\chi^S_{m_0n_0}v_*k_0^2))\\ =&(J_{11}-d_1k_0^2)^2(J_{33}-d_3k_0^2)^2\Big(1+\frac{J_{23}J_{32}}{(J_{33}-d_3k_0^2)^2}+\frac{J_{12}(J_{21}-\chi^S_{m_0n_0}v_*k_0^2)}{(J_{11}-d_1k_0^2)^2}\Big),\end{aligned} \tag{5.40}$$

and

$$\upsilon = J_{12}(J_{11}-d_1k_0^2)(J_{33}-d_3k_0^2)^2k_0^2v_* < 0. \tag{5.41}$$

So if we denote

$$\Xi_0 = 1+\frac{J_{23}J_{32}}{(J_{33}-d_3k_0^2)^2}+\frac{J_{12}(J_{21}-\chi^S_{m_0n_0}v_*k_0^2)}{(J_{11}-d_1k_0^2)^2},$$

then we have $\dot{\mu}(\chi^S_{m_0n_0})<0$ if $\Xi_0>0$ while $\dot{\mu}(\chi^S_{m_0n_0})>0$ if $\Xi_0<0$. In view of Theorem 1.16 in [51], near $s=0$ the two functions $\lambda(s)$ and $-s\dot{\chi}_{m_0n_0}(s)\dot{\mu}(\chi^S_{m_0n_0})$ have the same sign. More precisely, we have

$$\lim_{s\to 0}\frac{-s\dot{\chi}_{m_0n_0}(s)\dot{\mu}(\chi^S_{m_0n_0})}{\lambda(s)} = 1. \tag{5.42}$$

Therefore, if $\Xi_0>0$, then $\mathrm{sgn}(\lambda(s)) = \mathrm{sgn}(\mathcal{K}_2)$ because of $\mathcal{K}_1=0$; while if $\Xi_0<0$, then $\mathrm{sgn}(\lambda(s)) = -\mathrm{sgn}(\mathcal{K}_2)$. Here $\mathcal{K}_2$ can be evaluated in terms of system parameters and we include the details in **Appendix B**. This completes the proof of part (*ii.a*) and (*ii.b*). ■

6 Numerical simulations

In this section, we devote to the numerical studies of dynamic behavior of system (1.3) in a two-dimensional bounded domain $\Omega\subseteq\mathbb{R}^2$ and want to investigate the effect of predator-taxis χ on the formation of two kinds of nontrivial patterns, that is, stationary Turing pattern and oscillatory pattern, emerging from bifurcations χ_c^T, χ_c^H, respectively. Here the finite-difference simulations use forward time and centred spatial differences for the interior points with appropriate care at the boundary to accommodate Neumann boundary conditions in two dimensional space domain [55]. For this purpose, we discrete in time, with time stepsize $\delta t=\tau>0$ and space stepsizes $\delta x=\delta y=h>0$, using the following explicit-forward difference

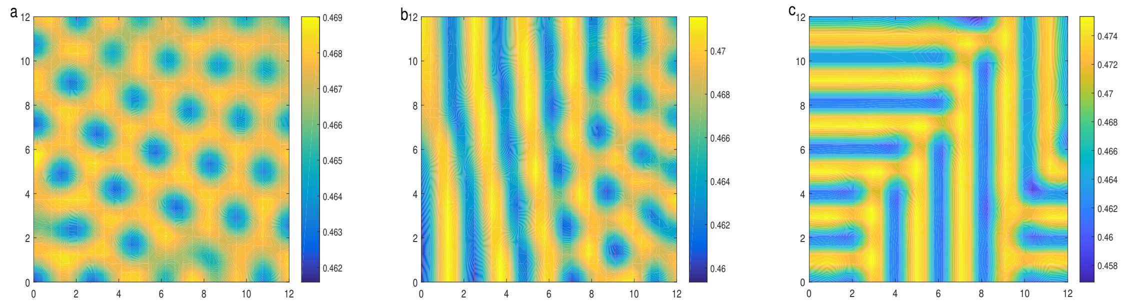

Figure 3: Formation of stationary Turing pattern of system (1.3) with different predator-taxis rates for top-predator species u: **a** $\chi = 1.6$; **b** $\chi = 1.23$; **c** $\chi = 0.53$. The other system parameters are the same as those in Figure 1 (left).

Euler scheme:

$$\begin{aligned}
u_{i,j}^{k+1} &= u_{i,j}^{k} + \tau d_1 \Delta u_{i,j}^{k} + \tau f_1(u_{i,j}^{k}, v_{i,j}^{k}, w_{i,j}^{k}),\\
v_{i,j}^{k+1} &= v_{i,j}^{k} + \tau d_2 \Delta v_{i,j}^{k} + \tau \chi v_{i,j}^{k} \Delta u_{i,j}^{k} + \tau \chi \bigtriangledown v_{i,j}^{k} \cdot \bigtriangledown u_{i,j}^{k} + \tau f_2(u_{i,j}^{k}, v_{i,j}^{k}, w_{i,j}^{k}),\\
w_{i,j}^{k+1} &= w_{i,j}^{k} + \tau d_3 \Delta w_{i,j}^{k} + \tau f_3(u_{i,j}^{k}, v_{i,j}^{k}, w_{i,j}^{k}),
\end{aligned}$$

where the discretization of the gradient term and the Laplacian term take the following form

$$\begin{aligned}
\bigtriangledown u_{i,j}^{k} &= \frac{1}{h}(a_r(i,j)u_{i+1,j}^{k} - u_{i,j}^{k}, a_u(i,j)u_{i,j+1}^{k} - u_{i,j}^{k})^{\mathbb{T}},\\
\Delta u_{i,j}^{k} &= \frac{1}{h^2}[a_l(i,j)u_{i-1,j}^{k} + a_r(i,j)u_{i+1,j}^{k} + a_d(i,j)u_{i,j-1}^{k} + a_u(i,j)u_{i,j+1}^{k} - 4u_{i,j}^{k}].
\end{aligned}$$

Here (i,j) denote the lattice sites and h is the lattice constant. The matrix elements of a_l, a_r, a_d, a_u are unity except at the boundary. When (i,j) is at the left boundary, that is $i = 0$, we define $a_l(i,j)u_{i-1,j}^{k} = u_{i+1,j}^{k}$, which guarantees zero-flux of individuals in the left boundary. Similarly, we define $a_r(i,j), a_d(i,j), a_u(i,j)$ such that the no-flux boundary is satisfied. Here to ensure the stability of numerical computation, the selected stepsize, space stepsize and diffusion coefficients should satisfy the Courant-Friedrichs-Lewy stability criterion, i.e., $\left(d_i\left(\frac{1}{(\delta x)^2} + \frac{1}{(\delta y)^2}\right)\delta t \leq \frac{1}{2}\right)$ for $i = 1, 2, 3$.

Also it is well known that the system dynamics depends on the choice of the initial conditions. If the initial spatial distribution of the two species is spatially homogenous, then the distribution of species would stay homogeneous for any time, and no spatial pattern can emerge, which is not interesting. To get a nontrivial spatiotemporal dynamics, the initial condition has been taken as a small random perturbation to the homogeneous steady state of the system for the subsequent simulations if we don't make a special statement. It is to be

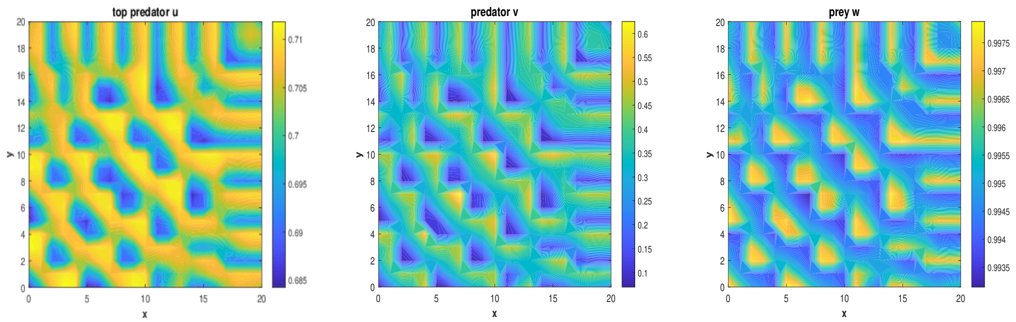

Figure 4: Formation of stationary pattern of system (1.3) in two-dimensional domains for the three species u, v, w by steady-state bifurcation near the unique spatially homogeneous steady state $(0.6999, 0.3, 0.9954)$. Here $\chi = 1.5 < \chi_0 = \chi_{7,7}^S \approx 1.9544$. The other system parameters are given as $\beta_1 = 10/3, \beta_2 = 9, \gamma_1 = 1, \gamma_2 = 1, \delta_1 = 0.02, \delta_2 = 9.5, d_1 = 10, d_2 = 0.02, d_3 = 0.1$. Initial datas are $(u_0, v_0, w_0) = (0.6999 + 0.01\cos\frac{7\pi x}{L}\cos\frac{7\pi y}{L}, 0.3 + 0.01\cos\frac{7\pi x}{L}\cos\frac{7\pi y}{L}, 0.9954 + 0.01\cos\frac{7\pi x}{L}\cos\frac{7\pi y}{L})$ with $L = 20$.

noted here that, the time at which we stopped the simulations is sufficient to assume that the patters attained the stationary state and they do not change further with time.

6.1 Stationary Turing pattern

The results are shown in Figure 3 and as expected, we obtain a stationary Turing pattern. The system parameters are chosen the same as those used in Figure 1(left), which located in the Turing domain II of Figure 1(right). With these parameters, it is easy to check that all assumptions in Theorem 4.5(ii) are satisfied. As can be seen from Figure 3, the unique spatially homogeneous steady state $(u_*, v_*, w_*) = (0.4667, 0.2000, 0.8000)$ loses its stability to Turing bifurcation when the predator-taxis rate χ crosses its threshold value $\chi_c^T = \chi_1^c \approx 1.6563$. These numerical simulations support the related results obtained in Theorem 4.5(ii). Moreover, we also find that the Turing pattern undergoes pattern transition from spot pattern to long stripe pattern via the mixture of spots and short strips as the decreases of the chemotaxis rate χ, which can be interpreted by the amplitude equations of pattern. Here we choose time stepsize $\delta t = 0.01$ and space stepsizes $\delta x = \delta y = 0.4$ to satisfy the Courant-Friedrichs-Lewy stability conditions.

Figure 4 is devoted to verify the effectiveness of our Theorem 5.7. It is easy to check that all conditions in Theorem 5.7 are satisfied under this set of parameters. By calculation, we find $Q(\chi, k) > 0$ for all $\chi > 0$ and $k > 0$, which means that $\chi_0 = \max\limits_{(m,n)\in\mathbb{N}^2\setminus(0,0)}\{\chi_{mn}^S, \chi_{mn}^H\} =$

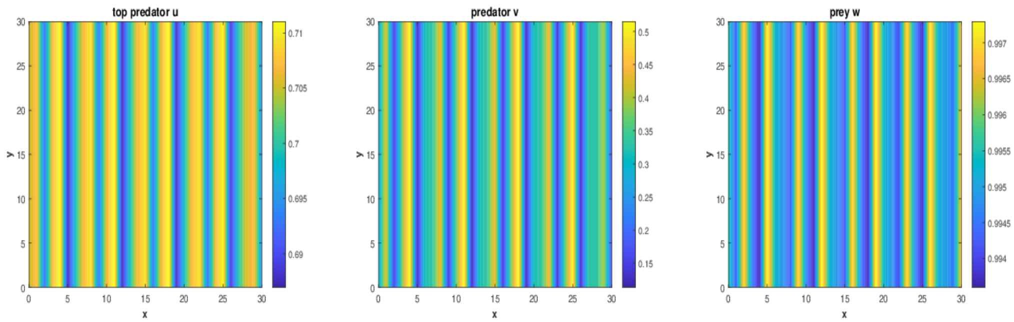

Figure 5: Formation of stationary pattern of system (1.3) in two-dimensional domains for the three species u, v, w by steady-state bifurcation near the unique spatially homogeneous steady state $(0.6999, 0.3, 0.9954)$ with $L = 30$. Here all the system parameters and the initial datas are the same as in Figure 4.

$\max\limits_{(m,n)\in\mathbb{N}^2\setminus(0,0)}\{\chi^S_{mn}\}$. Furthermore, from the expression of χ^S_{mn}, we find that the value of χ^S_{mn} varies from nonnegative to positive at first and then to nonnegative again as the increase of wavenumber k, so it will attain maximum at some finite wavenumber k. By calculation, we obtain $\max\limits_{(m,n)\in\mathbb{N}^2\setminus(0,0)}\{\chi^S_{mn}\} = \chi^S_{7,7} = 1.9544$. Moreover, $\Xi_0 = 0.9986 > 0$ and $\mathcal{K}_2 = -3.3213 \times 10^8 < 0$ when $\chi_0 = \chi^S_{7,7} = 1.9544$ and $L = 20$. Therefore a bunch of stable spatially inhomogeneous steady states $\Gamma_{7,7}(s)$ for $s \in (-\kappa, \kappa)$ bifurcates from $(0.6999, 0.3, 0.9954)$ as χ is close to its critical value χ_0 according to Theorem 5.7. Numerical simulations in Figure 4 support the theoretical findings about the stability of the bifurcating steady states. Here the time stepsize and the space stepsizes are chosen as $\delta t = 0.01$ and $\delta x = \delta y = 1$ to satisfy the Courant-Friedrichs-Lewy stability criterion. In Figure 5, we observe different kinds of stable stationary Turing patterns with different spatial size $L = 30$ via steady state bifurcation near $E_*(u_*, v_*, w_*)$, here the system parameters and initial conditions are chosen the same as in Figure 4. This shows that spatial size L can affect pattern structure.

6.2 Oscillatory pattern

Our next set of numerical simulations are devoted to demonstrate that system (1.3) admits oscillatory patterns through spatiotemporal Hopf bifurcations. Here the system parameters are chosen in Turing spatio-temporal Hopf bifurcation domain IV of Figure 2 (right). We shall show that the spatially homogeneous steady state $(u_*, v_*, w_*) = (0.35, 0.4325, 0.9368)$ loses its stability to time-periodic orbits under this set of parameter values. As is shown in Figure 6, we observe oscillatory pattern formation as the chemotaxis rate $\chi = 4.0$ crosses the

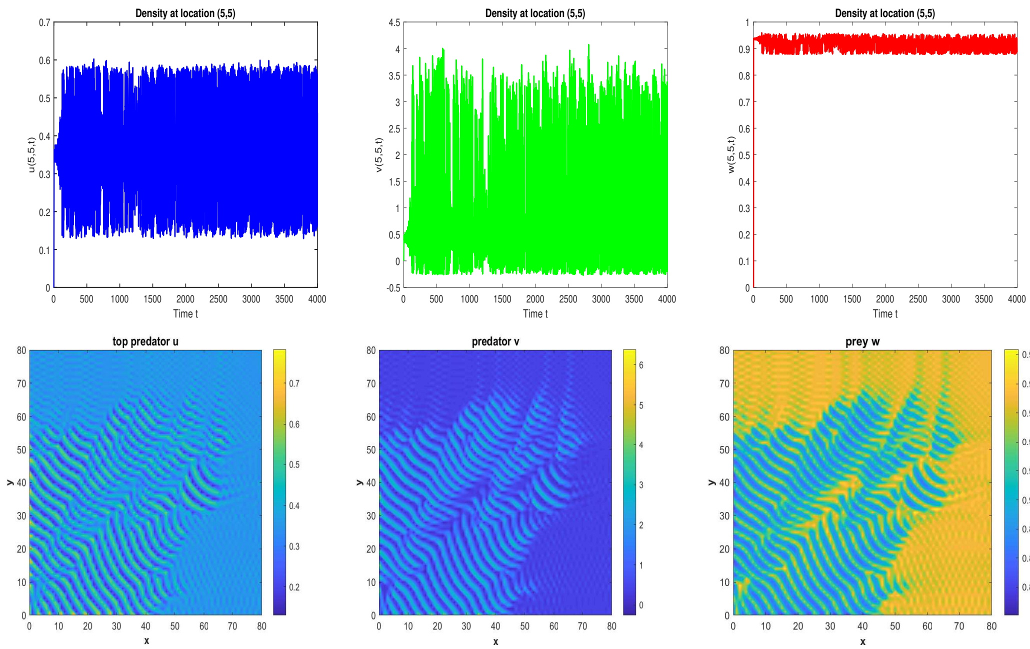

Figure 6: Formation of oscillatory pattern of system (1.3) for the three species u, v, w over $\Omega = (0, 80) \times (0, 80)$ (bottom) and the time history of three populations $\mathring{u}$, $\mathring{v}$ and $\mathring{w}$ (top), where $\mathring{u} := u(5, 5, t), \mathring{v} := v(5, 5, t), \mathring{w} := w(5, 5, t)$. Here $\chi = 4.0 > \chi_c^H = 3.5609$ and the other system parameters are the same as in Figure 2 (left).

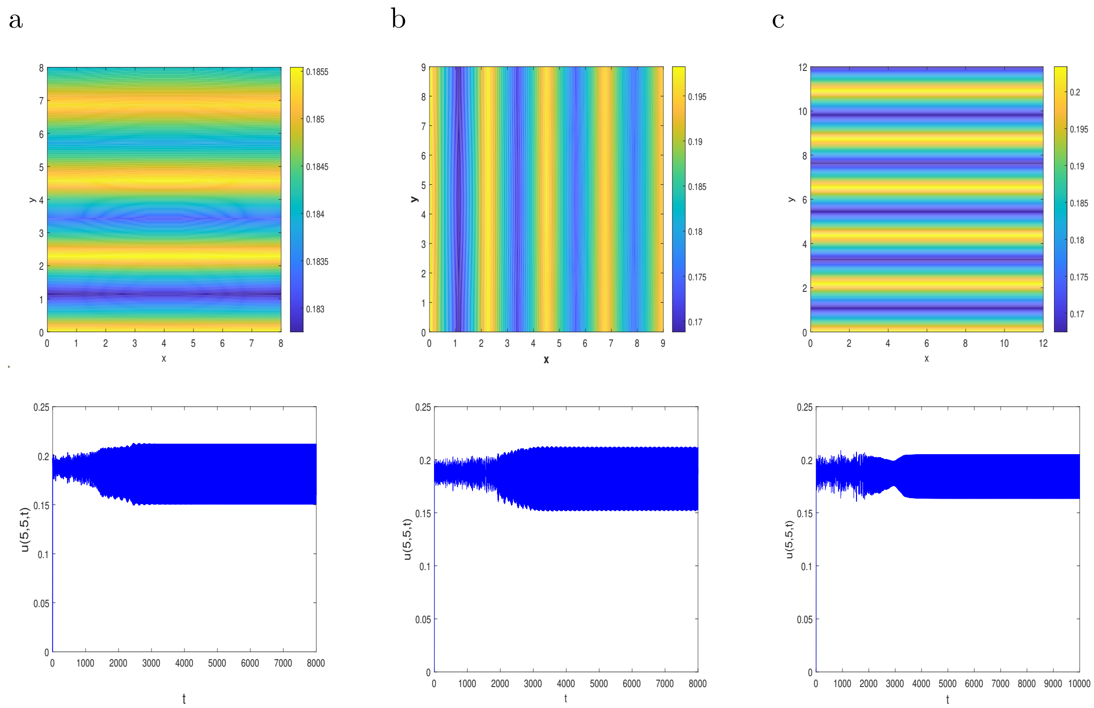

Figure 7: Formation of oscillatory pattern of system (1.3) in two-dimensional domains with different lengths for top-predator species u (top) and the corresponding time history (bottom): **a** $L = 8$, **b** $L = 9$, **c** $L = 12$. The system parameters are $\gamma 2 = 1, \gamma 1 = 1.5, \beta 1 = 2, \beta 2 = 10, \delta 1 = 0.5, \delta 2 = 6, \chi = 10, d1 = 0.002, d2 = 0.01, d3 = 0.001$. Here $\chi_c^H = 0.384$.

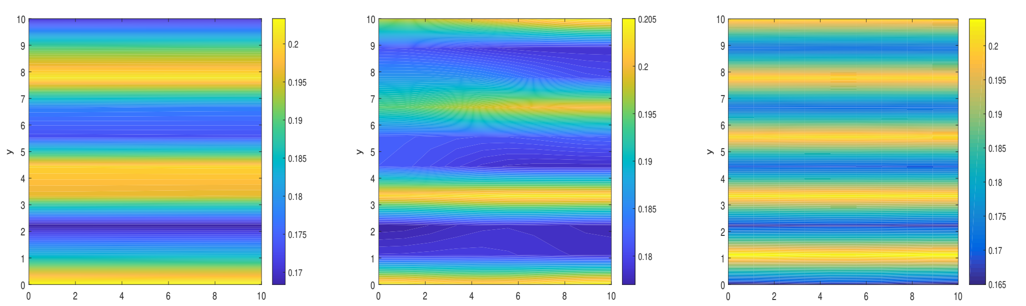

Figure 8: Formation of oscillatory pattern of system (1.3) in two-dimensional domains with different chemotactic factors for top-predator species u: $\chi = 8$ (left), $\chi = 8.8$ (middle), $\chi = 9.5$ (right). The other system parameters are the same as in Figure 7.

critical value $\chi_c^H = 3.5609$, which is oscillatory not only in space but also periodic in time. We also observe different kinds of oscillatory patterns in two-dimensional domains with different lengths in Figure 7 and different chemotactic factors in Figure 8. Here the time stepsize $\delta t = 0.01$ and space stepsizes $\delta x = \delta y = 1$ are chosen to satisfy the Courant-Friedrichs-Lewy stability conditions. As can be seen from Figure 7 and Figure 8, the change of spatial size L or the chemotactic factor χ has an important effect on the bandwidth of the periodic oscillatory pattern.

6.3 Non-Turing pattern

In this subsection, we investigate non-Turing pattern through numerical simulation. For this purpose, the parameters are chosen in the temporal Hopf bifurcation region which is a non-Turing domain. As we know, the type of model dynamics depends on the choice of initial data. If we choose a purely homogeneous initial conditions then the system stays homogeneous forever and no spatial pattern emerges, if we choose a weakly perturbed initial conditions then the pattern also evolves to the homogeneous distribution eventually. To get a inhomogeneous spatial pattern, following [11, 54], here we choose a strongly perturbed unsymmetrical initial species distribution as follows:

$$(IC)_{Stro.Pert.}: \begin{cases} u(\tilde{x}, \tilde{y}, 0) = u_* - \epsilon_1(\tilde{x} - 100) - \epsilon_2(\tilde{y} - 100), \\ v(\tilde{x}, \tilde{y}, 0) = v_* - \epsilon_3(\tilde{x} - 150) - \epsilon_4(\tilde{y} - 50), \\ w(\tilde{x}, \tilde{y}, 0) = w_* - \epsilon_5(\tilde{x} - 0.1\tilde{y} - 125)(\tilde{x} - 0.1\tilde{y} - 275), \end{cases}$$

where $\epsilon_1 = 1.5 \times 10^{-4}, \epsilon_2 = 1.0 \times 10^{-5}, \epsilon_3 = 1.0 \times 10^{-5}, \epsilon_4 = 2.0 \times 10^{-4}, \epsilon_5 = 1.5 \times 10^{-7}$. Snapshots of the spatial distribution under the initial conditions $(IC)_{Stro.Pert.}$ as time evolution are shown in Figure 9, where the parameter are chosen as: $\gamma_1 = 1, \gamma_2 = 1$, $\beta_1 = 10/3$, $\beta_2 = 10$, $\delta_1 = 3.2$, $\delta_2 = 10$, $\chi = 0.1$, $d_1 = 0.01$, $d_2 = 0.02$ and $d_3 = 0.03$. It is easy to check that this set of parameter set belongs to a Non-Turing domain because the equilibrium E_* of the corresponding ODE system (4.1) is unstable according to Theorem 4.1 (ii). As can be seen from Figure 9, at the beginning, the spiral wave grows steadily as the time evolution (cf. Figures 9**a** and 9**b**). After a period of time, the center of spiral wave loses its stability and results in some irregular spatial structures grow steadily at its center (cf. Figure 9**d**). Then the destruction of center also triggers the spirals lose their stability on the boundary as time further evolution (cf. Figure 9**e**). Furthermore, the new spirals emerge in the center of the domain (cf. Figures 9**f**) and persist for some while (cf. Figures 9**g** and 9**h**). Finally the irregular spatial pattern occupies the whole domain (cf. Figure 9**i**). Here the evolution process

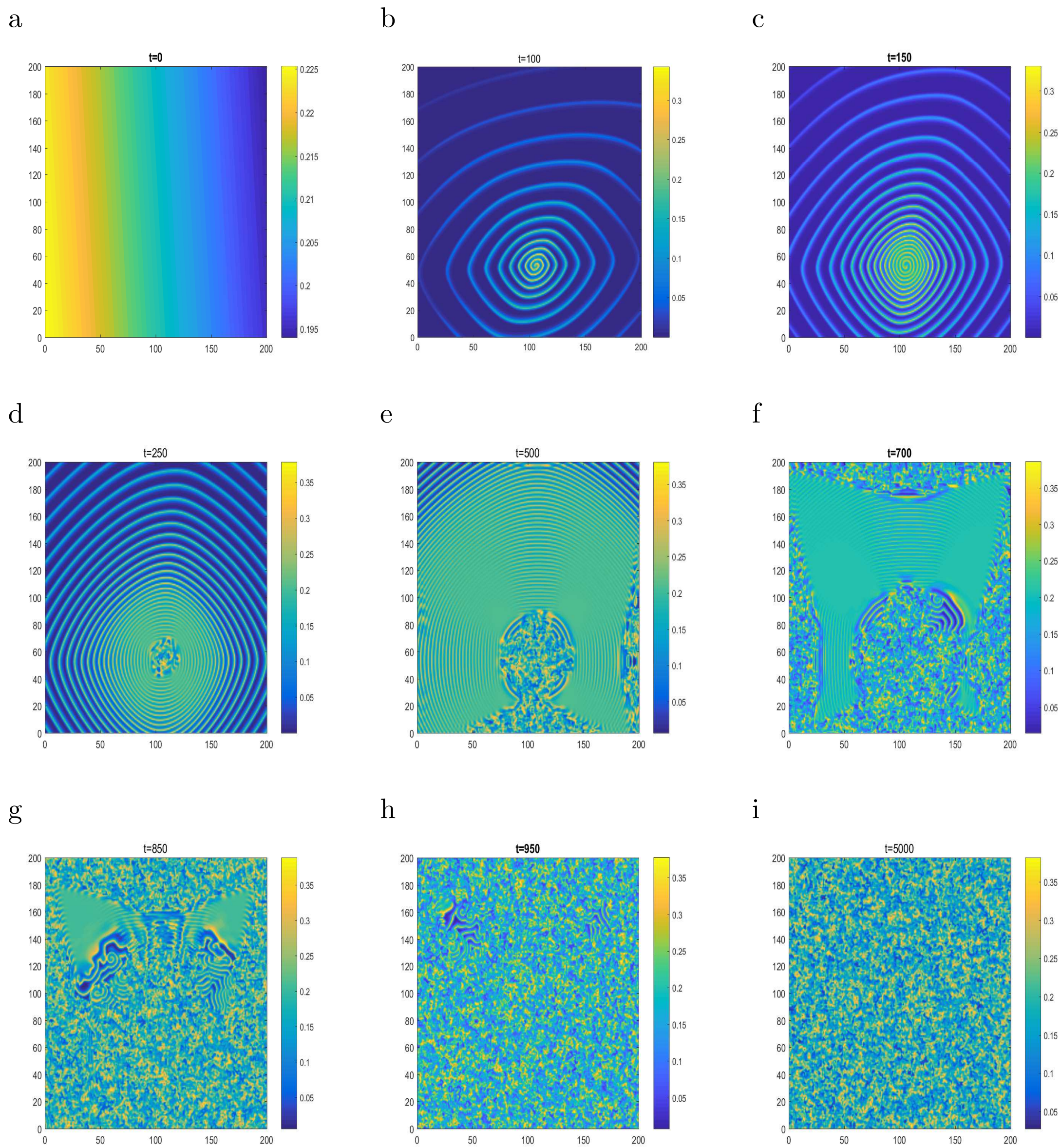

Figure 9: Non-Turing pattern evolution of top-predator species u of system (1.3) for different times. The system parameters are given in the text.

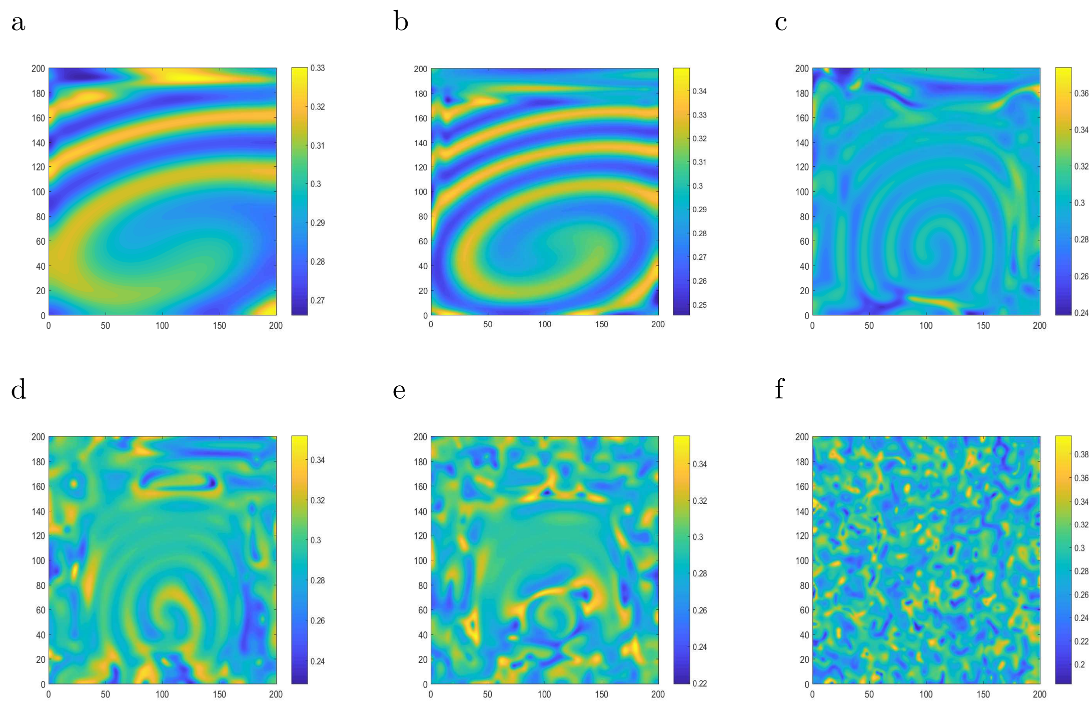

Figure 10: Non-Turing pattern transition of system (1.3) with different parameter values δ_1 for the top-predator species u: **a** $\delta_1 = 2.445$, **b** $\delta_1 = 2.45$, **c** $\delta_1 = 2.455$, **d** $\delta_1 = 2.46$, **e** $\delta_1 = 2.465$ and **f** $\delta_1 = 2.5$. The other system parameters are given in the text.

of spatial pattern is slightly different from the observation in [54] because the destruction of spiral waves not only occurs in their centers but also in their boundary and some new spirals emerge in the center of domain accompanying time evolution.

To further investigate the effect of parameter δ_1 on Non-Turing pattern formation, we choose a set of different parameter values $\delta_1 = 2.445$, 2.45, 2.455, 2.46, 2.465, 2.5 and the other parameters are fixed. As can be seen from Figure 10, when parameter δ_1 is very close to its Hopf bifurcation critical value $\delta_1^H = 2.4271$, spiral wave pattern grows steadily as the slight increase of parameter value δ_1 (cf. Figures 10**a** and 10**b**). However, as δ_1 goes further beyond its critical value, the spiral wave structure is very sensitive to the change of parameter value δ_1 and results in losing its stability gradually and surrounded by irregular spatial structures (cf. Figures 10**c** and 10**d**); the irregular spatial structures gradually occupy the majority domain as the value of parameter δ_1 further increases (cf. Figure 10**e**), and finally the irregular spatial pattern prevails over the whole domain (cf. Figure 10**f**). In a word, the parameter value δ_1 controls the appearance or disappearance of the spirals.

7 Conclusion and discussion

In this investigation, we explore a reaction-diffusion-chemotaxis food chain model with predator-taxis effect, where the predator is top predator. By virtue of the theory of semigroups of linear operators and some important embedding inequalities, we have established the global existence and boundedness of solution of the original system with arbitrary spatial dimension N. Then by choose predator-taxis rate as bifurcation parameter, we study two types of primary instability: Turing bifurcation and Turing-spatiotemporal Hopf bifurcation. According to our theoretical analyses, two kinds of important patterns are observed by numerical simulations. Finally, we also investigate the existence of non-constant positive steady state by using abstract bifurcation theory. From the obtained results, we find chemotaxis can induce non-constant positive steady state bifurcates from the spatially homogeneous steady state via steady state bifurcation.

On the other hand, although from the stationary Turing pattern generating analysis, specified in Section 4, the conditions admitting Turing bifurcation and stimulating stationary Turing pattern formation for system (1.3) have been achieved, it is still not easy to find out how to select the proper Turing pattern structures with Neumannn boundary conditions. As a consequence, in coming future, one can derive the amplitude equations of Turing patterns close to the onset of some significant system parameter, which will probably interpret the stability of diverse forms of Turing patterns with the structural transitions among them. In addition, we only consider the anti-predator behavior of the intermediate predator v to the top predator u. However, most of the bottom prey w possesses the ability to escape the risk of being preyed by the predator v. Then it is difficult to prove the global existence of the solution mathematically because the w-equation involving the gradient term ∇v. We leave it for future work.

Appendix A: The coefficients of Eq. (4.10) and Eq. (4.11)

$$
\begin{aligned}
P_0 =& d_1 d_2 d_3, \qquad P_3 = s_3,\\
P_1 =& \left(w_* - \frac{\delta_1 v_* w_*}{(v_*+w_*)^2}\right) d_1 d_2 + \left(\frac{\delta_2 v_* w_*}{(v_*+w_*)^2} - \frac{\beta_2 u_* v_*}{(u_*+v_*)^2}\right) d_1 d_3 + \frac{\beta_1 u_* v_* d_2 d_3}{(u_*+v_*)^2} + \frac{\chi \beta_1 u_*^2 v_* d_3}{(u_*+v_*)^2},\\
P_2 =& \left(w_* - \frac{\delta_1 v_* w_*}{(v_*+w_*)^2}\right)\left(d_1\left(\frac{\delta_2 v_* w_*}{(v_*+w_*)^2} - \frac{\beta_2 u_* v_*}{(u_*+v_*)^2}\right) + d_2 \frac{\beta_1 u_* v_*}{(u_*+v_*)^2}\right)\\
&+ \frac{d_1 \delta_1 \delta_2 v_*^2 w_*^2}{(v_*+w_*)^4} + \frac{\beta_1 \delta_2 u_* v_*^2 w_* d_3}{(u_*+v_*)^2 (v_*+w_*)^2} + \frac{\chi \beta_1 u_*^2 v_*}{(u_*+v_*)^2}\left(w_* - \frac{\delta_1 v_* w_*}{(v_*+w_*)^2}\right).\\
Q_0 =& d_1(d_1 d_2 + d_1 d_3) + (d_2 + d_3)(d_1 d_2 + d_2 d_3 + d_3 d_1), \quad Q_3 = s_1 s_2 - s_3, \qquad \text{(A.1)}\\
Q_1 =& (d_1+d_2+d_3) d_1 \left(w_* + \frac{(\delta_2-\delta_1) v_* w_*}{(v_*+w_*)^2} - \frac{\beta_2 u_* v_*}{(u_*+v_*)^2}\right) + d_1 d_2 \frac{\beta_1 u_* v_*}{(u_*+v_*)^2} +\\
& d_2^2 \left(w_* - \frac{\delta_1 v_* w_*}{(v_*+w_*)^2} + \frac{\beta_1 u_* v_*}{(u_*+v_*)^2}\right) + d_2 d_3 \left(w_* - \frac{\delta_1 v_* w_*}{(v_*+w_*)^2}\right) + d_1 d_3 \frac{\beta_1 u_* v_*}{(u_*+v_*)^2}\\
&+ (d_2+d_3) d_3 \left(\frac{(\beta_1-\beta_2) u_* v_*}{(u_*+v_*)^2} + \frac{\delta_2 v_* w_*}{(v_*+w_*)^2}\right) + (d_1 d_2 + d_2 d_3 + d_3 d_1) s_1 +\\
& \chi (d_1+d_2) \frac{\beta_1 u_*^2 v_*}{(u_*+v_*)^2},\\
Q_2 =& (d_1+d_2+d_3) s_2 + d_1 s_1 \left(w_* + \frac{(\delta_2-\delta_1) v_* w_*}{(v_*+w_*)^2} - \frac{\beta_2 u_* v_*}{(u_*+v_*)^2}\right) +\\
& d_2 s_1 \left(w_* - \frac{\delta_1 v_* w_*}{(v_*+w_*)^2} + \frac{\beta_1 u_* v_*}{(u_*+v_*)^2}\right) + d_3 s_1 \left(\frac{(\beta_1-\beta_2) u_* v_*}{(u_*+v_*)^2} + \frac{\delta_2 v_* w_*}{(v_*+w_*)^2}\right)\\
&- d_1 \left(\frac{\delta_1 \delta_2 v_*^2 w_*^2}{(v_*+w_*)^4} + \left(w_* - \frac{\delta_1 v_* w_*}{(v_*+w_*)^2}\right)\left(\frac{\delta_2 v_* w_*}{(v_*+w_*)^2} - \frac{\beta_2 u_* v_*}{(u_*+v_*)^2}\right)\right)\\
&- d_2 \frac{\beta_1 u_* v_*}{(u_*+v_*)^2}\left(w_* - \frac{\delta_1 v_* w_*}{(v_*+w_*)^2}\right) - d_3 \frac{\beta_1 \delta_2 u_* v_*^2 w_*}{(u_*+v_*)^2 (v_*+w_*)^2}\\
&+ \chi \left(\frac{\delta_2 v_* w_*}{(v_*+w_*)^2} + \frac{(\beta_1-\beta_2) u_* v_*}{(u_*+v_*)^2}\right). \qquad \text{(A.2)}
\end{aligned}
$$

Appendix B: The calculation of $\mathcal{K}_2$

First of all, substituting the asymptotic expressions (5.18)-(5.21) into the second equation of (5.1) and collecting s^3-terms yields the following equality:

$$
\begin{aligned}
&d_2\Delta\psi_2+\bar g_u\phi_2+\bar g_v\psi_2+\bar g_w\rho_2+(\bar g_{uu}a_{mn}+\bar g_{uv}b_{mn})\phi_1\cos(\frac{m\pi\tilde x}{L})\cos(\frac{n\pi\tilde y}{L})+\\
&(\bar g_{uv}a_{mn}+\bar g_{vv}b_{mn})\psi_1\cos(\frac{m\pi\tilde x}{L})\cos(\frac{n\pi\tilde y}{L})+(\bar g_{ww}+\bar g_{uw}a_{mn}+\bar g_{vw}b_{mn})\times\\
&\rho_1\cos(\frac{m\pi\tilde x}{L})\cos(\frac{n\pi\tilde y}{L})+(\bar g_{vw}\psi_1+\bar g_{uw}\phi_1)\cos(\frac{m\pi\tilde x}{L})\cos(\frac{n\pi\tilde y}{L})+\\
&\frac{1}{6}\big(\bar g_{uuu}a_{mn}^3+3\bar g_{uuv}a_{mn}^2b_{mn}+3\bar g_{uvv}a_{mn}b_{mn}^2+\bar g_{vvv}b_{mn}^3+\bar g_{www}+3\bar g_{vvw}b_{mn}^2+\\
&3\bar g_{vww}b_{mn}+3\bar g_{uuw}a_{mn}^2+3\bar g_{uww}a_{mn}+6\bar g_{uvw}a_{mn}b_{mn}\big)\cos^3(\frac{m\pi\tilde x}{L})\cos^3(\frac{n\pi\tilde y}{L})\\
&=\chi_{mn}^S\Big(\frac{m\pi}{L}\big(a_{mn}\frac{\partial\psi_1}{\partial\tilde x}+b_{mn}\frac{\partial\phi_1}{\partial\tilde x}\big)\sin(\frac{m\pi\tilde x}{L})\cos(\frac{n\pi\tilde y}{L})+\frac{n\pi}{L}\big(a_{mn}\frac{\partial\psi_1}{\partial\tilde y}+b_{mn}\frac{\partial\phi_1}{\partial\tilde y}\big)\times\\
&\cos(\frac{m\pi\tilde x}{L})\sin(\frac{n\pi\tilde y}{L})-v_*\Delta\phi_2-b_{mn}\Delta\phi_1\cos(\frac{m\pi\tilde x}{L})\cos(\frac{n\pi\tilde y}{L})+k^2a_{mn}\psi_1\times\\
&\cos(\frac{m\pi\tilde x}{L})\cos(\frac{n\pi\tilde y}{L})\Big)+\mathcal{K}_2v_*a_{mn}k^2\cos(\frac{m\pi\tilde x}{L})\cos(\frac{n\pi\tilde y}{L}),\quad(\tilde x,\tilde y)\in\Omega,\\
&\frac{\partial\phi_i}{\partial\nu}=\frac{\partial\psi_i}{\partial\nu}=\frac{\partial\rho_i}{\partial\nu}=0,\quad(\tilde x,\tilde y)\in\partial\Omega,\quad i=1,2.
\end{aligned}\tag{B.1}
$$

Multiplying the first equation in (B.1) by $\cos(\frac{m\pi\tilde x}{L})\cos(\frac{n\pi\tilde y}{L})$ and integrating it over Ω yields

$$
\begin{aligned}
\frac{v_*a_{mn}k^2}{4}\mathcal{K}_2=&(\bar g_v-d_2k^2)\int_\Omega\psi_2\cos(\frac{m\pi\tilde x}{L})\cos(\frac{n\pi\tilde y}{L})d\tilde xd\tilde y+(\bar g_u-v_*k^2\chi_{mn}^S)\times\\
&\int_\Omega\phi_2\cos(\frac{m\pi\tilde x}{L})\cos(\frac{n\pi\tilde y}{L})d\tilde xd\tilde y+\bar g_w\int_\Omega\rho_2\cos(\frac{m\pi\tilde x}{L})\cos(\frac{n\pi\tilde y}{L})d\tilde xd\tilde y-\chi_{mn}^Sb_{mn}k^2\times\\
&\int_\Omega\phi_1\cos(\frac{2m\pi\tilde x}{L})\cos(\frac{2n\pi\tilde y}{L})d\tilde xd\tilde y+\frac{\bar g_{uv}a_{mn}+\bar g_{vv}b_{mn}+\bar g_{vw}-\chi_{mn}^Sk^2a_{mn}}{4}\times\\
&\int_\Omega\psi_1d\tilde xd\tilde y+\frac{\bar g_{uu}a_{mn}+\bar g_{uv}b_{mn}+\bar g_{uw}}{4}\int_\Omega\phi_1d\tilde xd\tilde y+\frac{\bar g_{ww}+\bar g_{uw}a_{mn}+\bar g_{vw}b_{mn}}{4}\int_\Omega\rho_1\\
&+\chi_{mn}^S\frac{m\pi}{L}\Big(\frac{m\pi a_{mn}}{2L}\big(\int_\Omega\psi_1\cos(\frac{2m\pi\tilde x}{L})d\tilde xd\tilde y+\int_\Omega\psi_1\cos(\frac{2m\pi\tilde x}{L})\cos(\frac{2n\pi\tilde y}{L})d\tilde xd\tilde y\big)\\
&+\frac{m\pi b_{mn}}{2L}\big(\int_\Omega\phi_1\cos(\frac{2m\pi\tilde x}{L})d\tilde xd\tilde y+\int_\Omega\phi_1\cos(\frac{2m\pi\tilde x}{L})\cos(\frac{2n\pi\tilde y}{L})d\tilde xd\tilde y\big)\Big)+\\
&\chi_{mn}^S\frac{n\pi}{L}\Big(\frac{n\pi a_{mn}}{2L}\big(\int_\Omega\psi_1\cos(\frac{2n\pi\tilde y}{L})d\tilde xd\tilde y+\int_\Omega\psi_1\cos(\frac{2m\pi\tilde x}{L})\cos(\frac{2n\pi\tilde y}{L})d\tilde xd\tilde y\big)\\
&+\frac{n\pi b_{mn}}{2L}\big(\int_\Omega\phi_1\cos(\frac{2n\pi\tilde y}{L})d\tilde xd\tilde y+\int_\Omega\phi_1\cos(\frac{2m\pi\tilde x}{L})\cos(\frac{2n\pi\tilde y}{L})d\tilde xd\tilde y\big)\Big)-
\end{aligned}
$$

$$
\begin{aligned}
&\chi^S_{mn} b_{mn} (\frac{n\pi}{L})^2 \int_\Omega \phi_1 \cos(\frac{2n\pi\tilde{y}}{L}) d\tilde{x}d\tilde{y} - \chi^S_{mn} b_{mn} (\frac{m\pi}{L})^2 \int_\Omega \phi_1 \cos(\frac{2m\pi\tilde{x}}{L}) d\tilde{x}d\tilde{y} + \\
&\frac{3L^2}{128} \big(\bar{g}_{uuu} a^3_{mn} + 3\bar{g}_{uuv} a^2_{mn} b_{mn} + 3\bar{g}_{uvv} a_{mn} b^2_{mn} + \bar{g}_{vvv} b^3_{mn} + \bar{g}_{www} + 3\bar{g}_{vvw} b^2_{mn} \\
&+ 3\bar{g}_{vww} b_{mn} + 3\bar{g}_{uuw} a^2_{mn} + 3\bar{g}_{uww} a_{mn} + 6\bar{g}_{uvw} a_{mn} b_{mn} \big).
\end{aligned} \tag{B.2}
$$

Similarly, Substituting (5.18)-(5.19) into the first and third equation in (5.1) and collecting their s^3-terms yield

$$
\begin{aligned}
&d_1 \Delta\phi_2 + \bar{f}_u \phi_2 + \bar{f}_v \psi_2 + \bar{f}_w \rho_2 + (\bar{f}_{uu} a_{mn} + \bar{f}_{uv} b_{mn}) \phi_1 \cos(\tfrac{m\pi\tilde{x}}{L}) \cos(\tfrac{n\pi\tilde{y}}{L}) + \\
&(\bar{f}_{uv} a_{mn} + \bar{f}_{vv} b_{mn}) \psi_1 \cos(\tfrac{m\pi\tilde{x}}{L}) \cos(\tfrac{n\pi\tilde{y}}{L}) + (\bar{f}_{ww} + \bar{f}_{uw} a_{mn} + \bar{f}_{vw} b_{mn}) \rho_1 \times \\
&\cos(\tfrac{m\pi\tilde{x}}{L}) \cos(\tfrac{n\pi\tilde{y}}{L}) + (\bar{f}_{vw}\psi_1 + \bar{f}_{uw}\phi_1) \cos(\tfrac{m\pi\tilde{x}}{L}) \cos(\tfrac{n\pi\tilde{y}}{L}) + \tfrac{1}{6} \big(\bar{f}_{uuu} a^3_{mn} + 3\bar{f}_{uuv} a^2_{mn} b_{mn} \\
&+ 3\bar{f}_{uvv} a_{mn} b^2_{mn} + \bar{f}_{vvv} b^3_{mn} + \bar{f}_{www} + 3\bar{f}_{vvw} b^2_{mn} + 3\bar{f}_{vww} b_{mn} + 3\bar{f}_{uuw} a^2_{mn} + 3\bar{f}_{uww} a_{mn} + \\
&6\bar{f}_{uvw} a_{mn} b_{mn} \big) \cos^3(\tfrac{m\pi\tilde{x}}{L}) \cos^3(\tfrac{n\pi\tilde{y}}{L}) = 0, \quad (\tilde{x},\tilde{y}) \in \Omega, \\
&d_3 \Delta\rho_2 + \bar{h}_u \phi_2 + \bar{h}_v \psi_2 + \bar{h}_w \rho_2 + (\bar{h}_{uu} a_{mn} + \bar{h}_{uv} b_{mn}) \phi_1 \cos(\tfrac{m\pi\tilde{x}}{L}) \cos(\tfrac{n\pi\tilde{y}}{L}) + \\
&(\bar{h}_{uv} a_{mn} + \bar{h}_{vv} b_{mn}) \psi_1 \cos(\tfrac{m\pi\tilde{x}}{L}) \cos(\tfrac{n\pi\tilde{y}}{L}) + (\bar{h}_{ww} + \bar{h}_{uw} a_{mn} + \bar{h}_{vw} b_{mn}) \rho_1 \times \\
&\cos(\tfrac{m\pi\tilde{x}}{L}) \cos(\tfrac{n\pi\tilde{y}}{L}) + (\bar{h}_{vw}\psi_1 + \bar{h}_{uw}\phi_1) \cos(\tfrac{m\pi\tilde{x}}{L}) \cos(\tfrac{n\pi\tilde{y}}{L}) + \tfrac{1}{6} \big(\bar{h}_{uuu} a^3_{mn} + 3\bar{h}_{uuv} a^2_{mn} b_{mn} \\
&+ 3\bar{h}_{uvv} a_{mn} b^2_{mn} + \bar{h}_{vvv} b^3_{mn} + \bar{h}_{www} + 3\bar{h}_{vvw} b^2_{mn} + 3\bar{h}_{vww} b_{mn} + 3\bar{h}_{uuw} a^2_{mn} + 3\bar{h}_{uww} a_{mn} + \\
&6\bar{h}_{uvw} a_{mn} b_{mn} \big) \cos^3(\tfrac{m\pi\tilde{x}}{L}) \cos^3(\tfrac{n\pi\tilde{y}}{L}) = 0, \quad (\tilde{x},\tilde{y}) \in \Omega.
\end{aligned} \tag{B.3}
$$

Noting that Neumann boundary conditions $\frac{\partial \phi_i}{\partial \nu} = \frac{\partial \psi_i}{\partial \nu} = \frac{\partial \rho_i}{\partial \nu} = 0$, $(\tilde{x},\tilde{y}) \in \partial\Omega$, we multiply the two equations in (B.3) by $\cos(\frac{m\pi\tilde{x}}{L})\cos(\frac{n\pi\tilde{y}}{L})$ and integrate them over Ω, which implies that

$$
\begin{aligned}
0 =& (\bar{f}_u - d_1 k^2) \int_\Omega \phi_2 \cos(\frac{m\pi\tilde{x}}{L}) \cos(\frac{n\pi\tilde{y}}{L}) d\tilde{x}d\tilde{y} + \bar{f}_v \int_\Omega \psi_2 \cos(\frac{m\pi\tilde{x}}{L}) \cos(\frac{n\pi\tilde{y}}{L}) d\tilde{x}d\tilde{y} \\
&+ \bar{f}_w \int_\Omega \rho_2 \cos(\frac{m\pi\tilde{x}}{L}) \cos(\frac{n\pi\tilde{y}}{L}) d\tilde{x}d\tilde{y} + \frac{\bar{f}_{uv} a_{mn} + \bar{f}_{vv} b_{mn} + \bar{f}_{vw}}{4} \int_\Omega \psi_1 d\tilde{x}d\tilde{y} + \\
&\frac{\bar{f}_{uu} a_{mn} + \bar{f}_{uv} b_{mn} + \bar{f}_{uw}}{4} \int_\Omega \phi_1 d\tilde{x}d\tilde{y} + \frac{\bar{f}_{ww} + \bar{f}_{uw} a_{mn} + \bar{f}_{vw} b_{mn}}{4} \int_\Omega \rho_1 d\tilde{x}d\tilde{y} + \frac{3L^2}{128} \times \\
&\big(\bar{f}_{uuu} a^3_{mn} + 3\bar{f}_{uuv} a^2_{mn} b_{mn} + 3\bar{f}_{uvv} a_{mn} b^2_{mn} + \bar{f}_{vvv} b^3_{mn} + \bar{f}_{www} + \\
&3\bar{f}_{vvw} b^2_{mn} + 3\bar{f}_{vww} b_{mn} + 3\bar{f}_{uuw} a^2_{mn} + 3\bar{f}_{uww} a_{mn} + 6\bar{f}_{uvw} a_{mn} b_{mn} \big),
\end{aligned} \tag{B.4}
$$

$$
\begin{aligned}
0 =& \bar{h}_u \textstyle\int_\Omega \phi_2 \cos(\frac{m\pi\tilde{x}}{L}) \cos(\frac{n\pi\tilde{y}}{L}) d\tilde{x}d\tilde{y} + \bar{h}_v \int_\Omega \psi_2 \cos(\frac{m\pi\tilde{x}}{L}) \cos(\frac{n\pi\tilde{y}}{L}) d\tilde{x}d\tilde{y} + \\
&(\bar{h}_w - d_3 k^2) \textstyle\int_\Omega \rho_2 \cos(\frac{m\pi\tilde{x}}{L}) \cos(\frac{n\pi\tilde{y}}{L}) d\tilde{x}d\tilde{y} + \frac{\bar{h}_{uv} a_{mn} + \bar{h}_{vv} b_{mn} + \bar{h}_{vw}}{4} \int_\Omega \psi_1 d\tilde{x}d\tilde{y} + \\
&\tfrac{\bar{h}_{uu} a_{mn} + \bar{h}_{uv} b_{mn} + \bar{h}_{uw}}{4} \textstyle\int_\Omega \phi_1 d\tilde{x}d\tilde{y} + \frac{\bar{h}_{ww} + \bar{h}_{uw} a_{mn} + \bar{h}_{vw} b_{mn}}{4} \int_\Omega \rho_1 d\tilde{x}d\tilde{y} + \frac{3L^2}{128} \times \\
&\big(\bar{h}_{uuu} a^3_{mn} + 3\bar{h}_{uuv} a^2_{mn} b_{mn} + 3\bar{h}_{uvv} a_{mn} b^2_{mn} + \bar{h}_{vvv} b^3_{mn} + \bar{h}_{www} + \\
&3\bar{h}_{vvw} b^2_{mn} + 3\bar{h}_{vww} b_{mn} + 3\bar{h}_{uuw} a^2_{mn} + 3\bar{h}_{uww} a_{mn} + 6\bar{h}_{uvw} a_{mn} b_{mn} \big).
\end{aligned} \tag{B.5}
$$

Since $(\phi_2, \psi_2, \rho_2) \in \mathcal{Z}$ as defined in (5.13), we get

$$\begin{aligned}&a_{mn}\int_\Omega \phi_2 \cos(\tfrac{m\pi\tilde{x}}{L})\cos(\tfrac{n\pi\tilde{y}}{L})d\tilde{x}d\tilde{y} + b_{mn}\int_\Omega \psi_2 \cos(\tfrac{m\pi\tilde{x}}{L})\cos(\tfrac{n\pi\tilde{y}}{L})d\tilde{x}d\tilde{y} +\\ &\int_\Omega \rho_2 \cos(\tfrac{m\pi\tilde{x}}{L})\cos(\tfrac{n\pi\tilde{y}}{L})d\tilde{x}d\tilde{y} = 0.\end{aligned} \tag{B.6}$$

Combining (B.4)-(B.6), we have that

$$\begin{pmatrix} \bar{f}_u - d_1k^2 & \bar{f}_v & \bar{f}_w \\ \bar{h}_u & \bar{h}_v & \bar{h}_w - d_3k^2 \\ a_{mn} & b_{mn} & 1 \end{pmatrix}\begin{pmatrix} \int_\Omega \phi_2 \cos(\frac{m\pi\tilde{x}}{L})\cos(\frac{n\pi\tilde{y}}{L})d\tilde{x}d\tilde{y} \\ \int_\Omega \psi_2 \cos(\frac{m\pi\tilde{x}}{L})\cos(\frac{n\pi\tilde{y}}{L})d\tilde{x}d\tilde{y} \\ \int_\Omega \rho_2 \cos(\frac{m\pi\tilde{x}}{L})\cos(\frac{n\pi\tilde{y}}{L})d\tilde{x}d\tilde{y} \end{pmatrix} = \begin{pmatrix} \mathcal{C}_1 \\ \mathcal{C}_2 \\ 0 \end{pmatrix}, \tag{B.7}$$

where

$$\begin{aligned}\mathcal{C}_1 = &-\frac{\bar{f}_{uv}a_{mn} + \bar{f}_{vv}b_{mn} - \bar{f}_{vw}}{4}\int_\Omega \psi_1 d\tilde{x}d\tilde{y} - \frac{\bar{f}_{uu}a_{mn} + \bar{f}_{uv}b_{mn} + \bar{f}_{uw}}{4}\int_\Omega \phi_1 d\tilde{x}d\tilde{y} -\\ &\frac{\bar{f}_{ww} + \bar{f}_{uw}a_{mn} - \bar{f}_{vw}b_{mn}}{4}\int_\Omega \rho_1 d\tilde{x}d\tilde{y} - \frac{3L^2}{128}\Big(\bar{f}_{uuu}a_{mn}^3 + 3\bar{f}_{uuv}a_{mn}^2 b_{mn} +\\ &3\bar{f}_{uvv}a_{mn}b_{mn}^2 + \bar{f}_{vvv}b_{mn}^3 + \bar{f}_{www} + 3\bar{f}_{vvw}b_{mn}^2 + 3\bar{f}_{vww}b_{mn} + 3\bar{f}_{uuw}a_{mn}^2 +\\ &3\bar{f}_{uww}a_{mn} + 6\bar{f}_{uvw}a_{mn}b_{mn}\Big),\end{aligned}$$

$$\begin{aligned}\mathcal{C}_2 = &-\frac{\bar{h}_{uv}a_{mn} + \bar{h}_{vv}b_{mn} - \bar{f}_{vw}}{4}\int_\Omega \psi_1 d\tilde{x}d\tilde{y} - \frac{\bar{h}_{uu}a_{mn} + \bar{h}_{uv}b_{mn} + \bar{h}_{uw}}{4}\int_\Omega \phi_1 d\tilde{x}d\tilde{y} -\\ &\frac{\bar{h}_{ww} + \bar{h}_{uw}a_{mn} - \bar{h}_{vw}b_{mn}}{4}\int_\Omega \rho_1 d\tilde{x}d\tilde{y} - \frac{3L^2}{128}\Big(\bar{h}_{uuu}a_{mn}^3 + 3\bar{h}_{uuv}a_{mn}^2 b_{mn} +\\ &3\bar{h}_{uvv}a_{mn}b_{mn}^2 + \bar{h}_{vvv}b_{mn}^3 + \bar{h}_{www} + 3\bar{h}_{vvw}b_{mn}^2 + 3\bar{h}_{vww}b_{mn} + 3\bar{h}_{uuw}a_{mn}^2 +\\ &3\bar{h}_{uww}a_{mn} + 6\bar{h}_{uvw}a_{mn}b_{mn}\Big).\end{aligned}$$

Since the coefficient determinant $\det(\mathcal{M}) > 0$, solving (B.7) by Cramer's rule, we obtain that

$$\begin{gathered}\int_\Omega \phi_2 \cos(\frac{m\pi\tilde{x}}{L})\cos(\frac{n\pi\tilde{y}}{L})d\tilde{x}d\tilde{y} = \frac{\mathcal{D}_1}{\mathcal{D}_0},\\ \int_\Omega \psi_2 \cos(\frac{m\pi\tilde{x}}{L})\cos(\frac{n\pi\tilde{y}}{L})d\tilde{x}d\tilde{y} = \frac{\mathcal{D}_2}{\mathcal{D}_0}, \quad \int_\Omega \rho_2 \cos(\frac{m\pi\tilde{x}}{L})\cos(\frac{n\pi\tilde{y}}{L})d\tilde{x}d\tilde{y} = \frac{\mathcal{D}_3}{\mathcal{D}_0},\end{gathered} \tag{B.8}$$

where

$$\mathcal{D}_1 = \begin{vmatrix} \mathcal{C}_1 & \bar{f}_v & \bar{f}_w \\ \mathcal{C}_2 & \bar{h}_v & \bar{h}_w - d_3k^2 \\ 0 & b_{mn} & 1 \end{vmatrix}, \mathcal{D}_2 = \begin{vmatrix} \bar{f}_u - d_1k^2 & \mathcal{C}_1 & \bar{f}_w \\ \bar{h}_u & \mathcal{C}_2 & \bar{h}_w - d_3k^2 \\ a_{mn} & 0 & 1 \end{vmatrix},$$

$$\mathcal{D}_3 = \begin{vmatrix} \bar{f}_u - d_1k^2 & \bar{f}_v & \mathcal{C}_1 \\ \bar{h}_u & \bar{h}_v & \mathcal{C}_2 \\ a_{mn} & b_{mn} & 0 \end{vmatrix}, \mathcal{D}_0 = \begin{vmatrix} \bar{f}_u - d_1k^2 & \bar{f}_v & \bar{f}_w \\ \bar{h}_u & \bar{h}_v & \bar{h}_w - d_3k^2 \\ a_{mn} & b_{mn} & 1 \end{vmatrix}.$$

Next, to evaluate $\mathcal{K}_2$, we need to evaluate the following integrals:

$$\int_\Omega \phi_1 d\tilde{x}d\tilde{y}, \int_\Omega \psi_1 d\tilde{x}d\tilde{y}, \int_\Omega \rho_1 d\tilde{x}d\tilde{y}, \int_\Omega \phi_1 \cos(\frac{2m\pi\tilde{x}}{L})\cos(\frac{2n\pi\tilde{y}}{L})d\tilde{x}d\tilde{y},$$
$$\int_\Omega \psi_1 \cos(\frac{2m\pi\tilde{x}}{L})\cos(\frac{2n\pi\tilde{y}}{L})d\tilde{x}d\tilde{y}, \int_\Omega \phi_1 \cos(\frac{2m\pi\tilde{x}}{L})d\tilde{x}d\tilde{y},$$
$$\int_\Omega \psi_1 \cos(\frac{2m\pi\tilde{x}}{L})d\tilde{x}d\tilde{y}, \int_\Omega \phi_1 \cos(\frac{2n\pi\tilde{y}}{L})d\tilde{x}d\tilde{y}, \int_\Omega \psi_1 \cos(\frac{2n\pi\tilde{y}}{L})d\tilde{x}d\tilde{y}.$$

Noting that $\mathcal{K}_1 = 0$ and the Neumann boundary conditions, integrating (5.22) and (5.24) over Ω by parts yields

$$\begin{pmatrix} \bar{f}_u & \bar{f}_v & \bar{f}_w \\ \bar{g}_u & \bar{g}_v & \bar{g}_w \\ \bar{h}_u & \bar{h}_v & \bar{h}_w \end{pmatrix} \begin{pmatrix} \int_\Omega \phi_1 d\tilde{x}d\tilde{y} \\ \int_\Omega \psi_1 d\tilde{x}d\tilde{y} \\ \int_\Omega \rho_1 d\tilde{x}d\tilde{y} \end{pmatrix} = \begin{pmatrix} \mathcal{C}_3 \\ \mathcal{C}_4 \\ \mathcal{C}_5 \end{pmatrix}, \tag{B.9}$$

where

$$\mathcal{C}_3 = -\frac{L^2}{8}\big(\bar{f}_{uu}a_{mn}^2 + \bar{f}_{vv}b_{mn}^2 + \bar{f}_{ww} + 2\bar{f}_{uv}a_{mn}b_{mn} + 2\bar{f}_{uw}a_{mn} + 2\bar{f}_{vw}b_{mn}\big),$$
$$\mathcal{C}_4 = -\frac{L^2}{8}\big(\bar{g}_{uu}a_{mn}^2 + \bar{g}_{vv}b_{mn}^2 + \bar{g}_{ww} + 2\bar{g}_{uv}a_{mn}b_{mn} + 2\bar{g}_{uw}a_{mn} + 2\bar{g}_{vw}b_{mn}\big),$$
$$\mathcal{C}_5 = -\frac{L^2}{8}\big(\bar{h}_{uu}a_{mn}^2 + \bar{h}_{vv}b_{mn}^2 + \bar{h}_{ww} + 2\bar{h}_{uv}a_{mn}b_{mn} + 2\bar{h}_{uw}a_{mn} + 2\bar{h}_{vw}b_{mn}\big).$$

Solving (B.9) gives us

$$\int_\Omega \phi_1 d\tilde{x}d\tilde{y} = \frac{\mathcal{E}_1}{\mathcal{E}_0}, \quad \int_\Omega \psi_1 d\tilde{x}d\tilde{y} = \frac{\mathcal{E}_2}{\mathcal{E}_0}, \quad \int_\Omega \rho_1 d\tilde{x}d\tilde{y} = \frac{\mathcal{E}_3}{\mathcal{E}_0}, \tag{B.10}$$

where

$$\mathcal{E}_1 = \begin{vmatrix} \mathcal{C}_3 & \bar{f}_v & \bar{f}_w \\ \mathcal{C}_4 & \bar{g}_v & \bar{g}_w \\ \mathcal{C}_5 & \bar{h}_v & \bar{h}_w \end{vmatrix}, \ \mathcal{E}_2 \begin{vmatrix} \bar{f}_u & \mathcal{C}_3 & \bar{f}_w \\ \bar{g}_u & \mathcal{C}_4 & \bar{g}_w \\ \bar{h}_u & \mathcal{C}_5 & \bar{h}_w \end{vmatrix}, \ \mathcal{E}_3 = \begin{vmatrix} \bar{f}_u & \bar{f}_v & \mathcal{C}_3 \\ \bar{g}_u & \bar{g}_v & \mathcal{C}_4 \\ \bar{h}_u & \bar{h}_v & \mathcal{C}_5 \end{vmatrix}, \ \mathcal{E}_0 = \begin{vmatrix} \bar{f}_u & \bar{f}_v & \bar{f}_w \\ \bar{g}_u & \bar{g}_v & \bar{g}_w \\ \bar{h}_u & \bar{h}_v & \bar{h}_w \end{vmatrix}.$$

Multiplying the equations in (5.22) and (5.24) by $\cos(\frac{2m\pi\tilde{x}}{L})$ and then integrating them over Ω by parts yields

$$\begin{pmatrix} -d_1(\frac{2m\pi}{L})^2 + \bar{f}_u & \bar{f}_v & \bar{f}_w \\ \bar{g}_u - \chi_{mn}^S v_*(\frac{2m\pi}{L})^2 & -d_2(\frac{2m\pi}{L})^2 + \bar{g}_v & \bar{g}_w \\ \bar{h}_u & \bar{h}_v & -d_3(\frac{2m\pi}{L})^2 + \bar{h}_w \end{pmatrix} \begin{pmatrix} \int_\Omega \phi_1 \cos(\frac{2m\pi\tilde{x}}{L})d\tilde{x}d\tilde{y} \\ \int_\Omega \psi_1 \cos(\frac{2m\pi\tilde{x}}{L})d\tilde{x}d\tilde{y} \\ \int_\Omega \rho_1 \cos(\frac{2m\pi\tilde{x}}{L})d\tilde{x}d\tilde{y} \end{pmatrix}$$
$$= (\mathcal{C}_6,\ \mathcal{C}_7,\ \mathcal{C}_8)^{\mathbb{T}}, \tag{B.11}$$

where

$$\mathcal{C}_6 = -\frac{L^2}{16}\big(\bar{f}_{uu}a_{mn}^2 + \bar{f}_{vv}b_{mn}^2 + \bar{f}_{ww} + 2\bar{f}_{uv}a_{mn}b_{mn} + 2\bar{f}_{uw}a_{mn} + 2\bar{f}_{vw}b_{mn}\big),$$
$$\mathcal{C}_7 = -\frac{L^2}{16}\big(\bar{g}_{uu}a_{mn}^2 + \bar{g}_{vv}b_{mn}^2 + \bar{g}_{ww} + 2\bar{g}_{uv}a_{mn}b_{mn} + 2\bar{g}_{uw}a_{mn} + 2\bar{g}_{vw}b_{mn}\big)+ \frac{m^2\pi^2}{4}\chi_{mn}^S a_{mn}b_{mn},$$
$$\mathcal{C}_8 = -\frac{L^2}{16}\big(\bar{h}_{uu}a_{mn}^2 + \bar{h}_{vv}b_{mn}^2 + \bar{h}_{ww} + 2\bar{h}_{uv}a_{mn}b_{mn} + 2\bar{h}_{uw}a_{mn} + 2\bar{h}_{vw}b_{mn}\big).$$

Solving (B.11) yields

$$\int_\Omega \phi_1 \cos(\frac{2m\pi\tilde{x}}{L}) = \frac{\mathcal{F}_1}{\mathcal{F}_0},\ \int_\Omega \psi_1 \cos(\frac{2m\pi\tilde{x}}{L}) = \frac{\mathcal{F}_2}{\mathcal{F}_0},\ \int_\Omega \rho_1 \cos(\frac{2m\pi\tilde{x}}{L}) = \frac{\mathcal{F}_3}{\mathcal{F}_0}, \tag{B.12}$$

with

$$\mathcal{F}_1 = \begin{vmatrix} \mathcal{C}_6 & \bar{f}_v & \bar{f}_w \\ \mathcal{C}_7 & -d_2(\frac{2m\pi}{L})^2 + \bar{g}_v & \bar{g}_w \\ \mathcal{C}_8 & \bar{h}_v & -d_3(\frac{2m\pi}{L})^2 + \bar{h}_w \end{vmatrix},$$

$$\mathcal{F}_2 = \begin{vmatrix} -d_1(\frac{2m\pi}{L})^2 + \bar{f}_u & \mathcal{C}_6 & \bar{f}_w \\ \bar{g}_u - \chi_{mn}^S v_*(\frac{2m\pi}{L})^2 & \mathcal{C}_7 & \bar{g}_w \\ \bar{h}_u & \mathcal{C}_8 & -d_3(\frac{2m\pi}{L})^2 + \bar{h}_w \end{vmatrix},$$

$$\mathcal{F}_3 = \begin{vmatrix} -d_1(\frac{2m\pi}{L})^2 + \bar{f}_u & \bar{f}_v & \mathcal{C}_6 \\ \bar{g}_u - \chi_{mn}^S v_*(\frac{2m\pi}{L})^2 & -d_2(\frac{2m\pi}{L})^2 + \bar{g}_v & \mathcal{C}_7 \\ \bar{h}_u & \bar{h}_v & \mathcal{C}_8 \end{vmatrix},$$

$$\mathcal{F}_0 = \begin{vmatrix} -d_1(\frac{2m\pi}{L})^2 + \bar{f}_u & \bar{f}_v & \bar{f}_w \\ \bar{g}_u - \chi_{mn}^S v_*(\frac{2m\pi}{L})^2 & -d_2(\frac{2m\pi}{L})^2 + \bar{g}_v & \bar{g}_w \\ \bar{h}_u & \bar{h}_v & -d_3(\frac{2m\pi}{L})^2 + \bar{h}_w \end{vmatrix}.$$

Multiplying the equations in (5.22) and (5.24) by $\cos(\frac{2n\pi\tilde{x}}{L})$ and then integrating them over Ω by parts yields

$$\begin{pmatrix} -d_1(\frac{2n\pi}{L})^2 + \bar{f}_u & \bar{f}_v & \bar{f}_w \\ \bar{g}_u - \chi_{mn}^S v_*(\frac{2n\pi}{L})^2 & -d_2(\frac{2n\pi}{L})^2 + \bar{g}_v & \bar{g}_w \\ \bar{h}_u & \bar{h}_v & -d_3(\frac{2n\pi}{L})^2 + \bar{h}_w \end{pmatrix} \begin{pmatrix} \int_\Omega \phi_1 \cos(\frac{2n\pi\tilde{y}}{L}) d\tilde{x}d\tilde{y} \\ \int_\Omega \psi_1 \cos(\frac{2n\pi\tilde{y}}{L}) d\tilde{x}d\tilde{y} \\ \int_\Omega \rho_1 \cos(\frac{2n\pi\tilde{y}}{L}) d\tilde{x}d\tilde{y} \end{pmatrix}$$
$$= (\mathcal{C}_9,\ \mathcal{C}_{10},\ \mathcal{C}_{11})^{\mathbb{T}} \tag{B.13}$$

where

$$\begin{aligned}
\mathcal{C}_9 =& -\frac{L^2}{16}\big(\bar f_{uu}a_{mn}^2+\bar f_{vv}b_{mn}^2+\bar f_{ww}+2\bar f_{uv}a_{mn}b_{mn}+2\bar f_{uw}a_{mn}+2\bar f_{vw}b_{mn}\big),\\
\mathcal{C}_{10} =& -\frac{L^2}{16}\big(\bar g_{uu}a_{mn}^2+\bar g_{vv}b_{mn}^2+\bar g_{ww}+2\bar g_{uv}a_{mn}b_{mn}+2\bar g_{uw}a_{mn}+2\bar g_{vw}b_{mn}\big)+\\
&\frac{n^2\pi^2}{4}\chi_{mn}^S a_{mn}b_{mn},\\
\mathcal{C}_{11} =& -\frac{L^2}{16}\big(\bar h_{uu}a_{mn}^2+\bar h_{vv}b_{mn}^2+\bar h_{ww}+2\bar h_{uv}a_{mn}b_{mn}+2\bar h_{uw}a_{mn}+2\bar h_{vw}b_{mn}\big).
\end{aligned}$$

Solving (B.13) yields

$$\int_\Omega \phi_1\cos(\frac{2n\pi\tilde y}{L})=\frac{\mathcal{G}_1}{\mathcal{G}_0},\quad \int_\Omega \psi_1\cos(\frac{2n\pi\tilde y}{L})=\frac{\mathcal{G}_2}{\mathcal{G}_0},\quad \int_\Omega \rho_1\cos(\frac{2n\pi\tilde y}{L})=\frac{\mathcal{G}_3}{\mathcal{G}_0}, \tag{B.14}$$

$$\mathcal{G}_1=\begin{vmatrix} \mathcal{C}_9 & \bar f_v & \bar f_w \\ \mathcal{C}_{10} & -d_2(\frac{2n\pi}{L})^2+\bar g_v & \bar g_w \\ \mathcal{C}_{11} & \bar h_v & -d_3(\frac{2n\pi}{L})^2+\bar h_w \end{vmatrix},$$

$$\mathcal{G}_2=\begin{vmatrix} -d_1(\frac{2n\pi}{L})^2+\bar f_u & \mathcal{C}_9 & \bar f_w \\ \bar g_u-\chi_{mn}^S v_*(\frac{2n\pi}{L})^2 & \mathcal{C}_{10} & \bar g_w \\ \bar h_u & \mathcal{C}_{11} & -d_3(\frac{2n\pi}{L})^2+\bar h_w \end{vmatrix},$$

$$\mathcal{G}_3=\begin{vmatrix} -d_1(\frac{2n\pi}{L})^2+\bar f_u & \bar f_v & \mathcal{C}_9 \\ \bar g_u-\chi_{mn}^S v_*(\frac{2n\pi}{L})^2 & -d_2(\frac{2n\pi}{L})^2+\bar g_v & \mathcal{C}_{10} \\ \bar h_u & \bar h_v & \mathcal{C}_{11} \end{vmatrix},$$

$$\mathcal{G}_0=\begin{vmatrix} -d_1(\frac{2n\pi}{L})^2+\bar f_u & \bar f_v & \bar f_w \\ \bar g_u-\chi_{mn}^S v_*(\frac{2n\pi}{L})^2 & -d_2(\frac{2n\pi}{L})^2+\bar g_v & \bar g_w \\ \bar h_u & \bar h_v & -d_3(\frac{2n\pi}{L})^2+\bar h_w \end{vmatrix}.$$

Finally, multiplying the equations in (5.22) and (5.24) by $\cos(\frac{2n\pi\tilde x}{L})\cos(\frac{2n\pi\tilde x}{L})$ and then integrating them over Ω by parts yields

$$\begin{aligned}
&\begin{pmatrix} -4d_1k^2+\bar f_u & \bar f_v & \bar f_w \\ \bar g_u-4\chi_{mn}^S v_*k^2 & -4d_2k^2+\bar g_v & \bar g_w \\ \bar h_u & \bar h_v & -4d_3k^2+\bar h_w \end{pmatrix}\begin{pmatrix} \int_\Omega \phi_1\cos(\frac{2n\pi\tilde x}{L})\cos(\frac{2n\pi\tilde y}{L})d\tilde x d\tilde y \\ \int_\Omega \psi_1\cos(\frac{2n\pi\tilde x}{L})\cos(\frac{2n\pi\tilde y}{L})d\tilde x d\tilde y \\ \int_\Omega \rho_1\cos(\frac{2n\pi\tilde x}{L})\cos(\frac{2n\pi\tilde y}{L})d\tilde x d\tilde y \end{pmatrix}\\
&=(\mathcal{C}_{12},\ \mathcal{C}_{13},\ \mathcal{C}_{14})^{\mathbb{T}},
\end{aligned} \tag{B.15}$$

where

$$\mathcal{C}_{12}=-\frac{L^2}{32}\big(\bar{f}_{uu}a_{mn}^2+\bar{f}_{vv}b_{mn}^2+\bar{f}_{ww}+2\bar{f}_{uv}a_{mn}b_{mn}+2\bar{f}_{uw}a_{mn}+2\bar{f}_{vw}b_{mn}\big),$$
$$\mathcal{C}_{13}=-\frac{L^2}{32}\big(\bar{g}_{uu}a_{mn}^2+\bar{g}_{vv}b_{mn}^2+\bar{g}_{ww}+2\bar{g}_{uv}a_{mn}b_{mn}+2\bar{g}_{uw}a_{mn}+2\bar{g}_{vw}b_{mn}\big)+\frac{m^2\pi^2+n^2\pi^2}{8}\chi_{mn}^S a_{mn}b_{mn},$$
$$\mathcal{C}_{14}=-\frac{L^2}{32}\big(\bar{h}_{uu}a_{mn}^2+\bar{h}_{vv}b_{mn}^2+\bar{h}_{ww}+2\bar{h}_{uv}a_{mn}b_{mn}+2\bar{h}_{uw}a_{mn}+2\bar{h}_{vw}b_{mn}\big).$$

Solving (B.15) yields

$$\int_\Omega \phi_1\cos(\frac{2m\pi\tilde{x}}{L})\cos(\frac{2n\pi\tilde{y}}{L})d\tilde{x}d\tilde{y}=\frac{\mathcal{H}_1}{\mathcal{H}_0},\ \int_\Omega \psi_1\cos(\frac{2m\pi\tilde{x}}{L})\cos(\frac{2n\pi\tilde{y}}{L})d\tilde{x}d\tilde{y}=\frac{\mathcal{H}_2}{\mathcal{H}_0},$$
$$\int_\Omega \rho_1\cos(\frac{2m\pi\tilde{x}}{L})\cos(\frac{2n\pi\tilde{y}}{L})d\tilde{x}d\tilde{y}=\frac{\mathcal{H}_3}{\mathcal{H}_0}, \quad \text{(B.16)}$$

where

$$\mathcal{H}_1=\begin{vmatrix}\mathcal{C}_{12} & \bar{f}_v & \bar{f}_w\\ \mathcal{C}_{13} & -4d_2k^2+\bar{g}_v & \bar{g}_w\\ \mathcal{C}_{14} & \bar{h}_v & -4d_3k^2+\bar{h}_w\end{vmatrix},\ \mathcal{H}_2=\begin{vmatrix}-4d_1k^2+\bar{f}_u & \mathcal{C}_{12} & \bar{f}_w\\ \bar{g}_u-4\chi_{mn}^S v_*k^2 & \mathcal{C}_{13} & \bar{g}_w\\ \bar{h}_u & \mathcal{C}_{14} & -4d_3k^2+\bar{h}_w\end{vmatrix},$$

$$\mathcal{H}_3=\begin{vmatrix}-4d_1k^2+\bar{f}_u & \bar{f}_v & \mathcal{C}_{12}\\ \bar{g}_u-4\chi_{mn}^S v_*k^2 & -4d_2k^2+\bar{g}_v & \mathcal{C}_{13}\\ \bar{h}_u & \bar{h}_v & \mathcal{C}_{14}\end{vmatrix},$$

$$\mathcal{H}_0=\begin{vmatrix}-4d_1k^2+\bar{f}_u & \bar{f}_v & \bar{f}_w\\ \bar{g}_u-4\chi_{mn}^S v_*k^2 & -4d_2k^2+\bar{g}_v & \bar{g}_w\\ \bar{h}_u & \bar{h}_v & -4d_3k^2+\bar{h}_w\end{vmatrix}.$$

Finally, In light of (B.8), (B.10), (B.12), (B.14) and (B.16), we are able to evaluate $\mathcal{K}_2$ in (B.2) in terms of system parameters.

Acknowledgments

The first author gratefully acknowledges the financial support from Youth Foundation of Zhejiang University of Science and Technology (Grant No. 2021QN001) and the National Research, Development and Innovation Fund of Hungary grants KKP 129877. The second author was supported by NKFIH FK 124016 and 2020-2.1.1-ED-2020-0000.

Conflict of Interest: We declare that we have no competing interests.

Data accessibility: There is no data for sharing in this article.

References

[1] J. D. Murray, Mathematical Biology I: An Introduction, Spring-Verlag, New York, 2003.

[2] A. Klebanoff, A. Hasings, Chaos in three species food chain, Ecol. 72 (1991) 896.

[3] C.H. Chiu, S.B. Hsu, Exinction of top predator in a three level food-chain model, J. Math. Biol. 37 (1998) 372.

[4] S.B. Hsu, T.W. Hwang, Y. Kuang, A ratio-dependent food chain model and its applications to biological control, Math. Biol. 181 (2003) 55-83.

[5] R.K. Upadhyay, R.K. Naji, Dynamics of a three species food chain model with Crowley-Martin type functional response, Chaos, Solit. and Fract. 42 (2009) 1337-1346.

[6] A. Okubo, S. Levin, Diffusion and Ecological Problems: Modern Perspectives, Springer-Verlag, Berlin, 2001.

[7] R.S. Cantrell, C. Cosner, Spatial Ecology via Reaction-diffusion Equations, Wiley, Chichester, 2003.

[8] J. D. Murray, Mathematical Biology II: Spatial Models and Biomedical Applications, Spring-Verlag, New York, 2003.

[9] H. Malchow, Spatio-temporal pattern formation in nonlinear nonequilibrium plankton dynamics, Proc. R. Soc. Lond. B 251 (1993) 103-109.

[10] H. Malchow, Nonequilibrium structures in plankton dynamics, Ecol. Model. 75 (1994) 123-134.

[11] H. Malchow, B. Radtke, M. Kallache, et al., Spatio-temporal pattern formation in coupled models of plankton dynamics and fish school motion, Nonlin. Anal.: RWA 1 (2000) 53-67.

[12] H.B. Shi, S.G. Ruan, Spatial, temporal and spatiotemporal patterns of diffusive predator-prey models with mutual interference, IMA J. Appl. Math. 80 (2015) 1534-1568.

[13] G. Gambino, M.C. Lombardo, M. Sammartino, Pattern formation driven by cross-diffusion in a 2D domain, Nonlin. Anal.: RWA 14 (2013) 1755-1779.

[14] A. Madzvamuse, H.S. Ndakwo, R. Barreira, Cross-diffusion-driven instability for reaction-diffusion systems: analysis and simulations, J. Math. Biol. 70 (2015) 709-743.

[15] R. Han, B. Dai, Spatiotemporal pattern formation and selection induced by nonlinear cross-diffusion in a toxic-phytoplankton-zooplankton model with Allee effect, Nonlin. Anal.: RWA 45 (2019) 822-853.

[16] R. Han, L.N. Guin, B. Dai, Cross-diffusion-driven pattern formation and selection in a modified Leslie-Gower predator-prey model with fear effect, J. Biol. Syst. 28 (2020) 1-38.

[17] M.A. Fuentes, M.N. Kuperman, V.M. Kenkre, Nonlocal interaction effects on pattern

formation in population dynamics, Phys. Rev. Lett. 91(15) (2003) 158104-1-158104-4.

[18] M.C. Tanzy, V.A. Volpert, A. Bayliss, M.E. Nehrkon, A Nagumo-type model for competing populations with nonlocal coupling, Math. Biosci. 263 (2015) 70-82.

[19] R.A. Satnoianu, J.H. Merkin, S.K. Scott, pattern formation in a differential-flow reactor model, Chem. Eng. Sci. 55 (2000) 461-469.

[20] C. Tian, Delay-driven spatial patterns in a plankton allelopathic system, Chaos 22 (2012) Art. no. 013129-7.

[21] M. Jankovic, S.V. Petrovskii, M. Banerjee, Delay driven spatiotemporal chaos in single population dynamics models, Theor. Popul. Biol. 110 (2016) 51-62.

[22] D. Horstmann, M. Winkler, Boundness vs. blow-up in a chemotaxis system, J. Diff. Eqs. 215 (2005) 52-107.

[23] B.E. Ainseba, M. Bendahmane and A.Noussair, A reaction-diffusion system modeling predator-prey with prey-taxis, Nonlin. Anal.: RWA 9 (2008) 2086-2105.

[24] M. Winkler, Boundedness in the higher-dimensional parabolic-parabolic chemotaxis system with logistic source, Comm. Par. Diff. Eqs. 35 (2010) 1516-1537.

[25] S. Wu, J. Shi, B. Wu, Global existence of solutions and uniform persistence of a diffusive predator-prey model with prey-taxis, J. Diff. Eqs. 260 (2016) 5847-5874.

[26] J.M. Lee, T. Hillen and M.A. Lewis, Pattern formation in prey-taxis system, J. Biol. Dyns. 3 (2009) 551-573.

[27] Y.L. Song, X.S. Tang, Stability, steady-state bifurcations, and Turing patterns in a predator-prey model with herd behavior and prey-taxis, Stud. Appl. Math. 139 (2017) 371-404.

[28] M.J. Ma, C.H. Ou, Z.A. Wang, Stationary solutions of a volume-filling chemotaxis model with logistic growth and their stability, SIAM J. Appl. Math. 72 (2012) 740-766.

[29] Q. Wang, Y. Song, L. Shao, Nonconstant positive steady states and patten formation of 1D prey-taxis systems, J. Nonlin. Sci. 27 (2017) 71-97.

[30] K. Wang, Q. Wang, F. Yu, Stationary and time-periodic patterns of two-predator and one-prey systems with prey-taxis, Discrete Cont. Dyn. Sys. 37 (2017) 505-543.

[31] S. Wu, J. Wang, J.P. Shi, Dynamics and pattern formation of a diffusive predator-prey model with predator-taxis, Math. Models Methods Appl. Sci. 28 (2018) 2275-2312.

[32] X. Wang, X.F. Zou, Pattern formation of predator-prey model with the cost of anti-predator behaviors, Math. Bios. Eng. 15 (2018) 775-805.

[33] F. Dai, B. Liu, Global solution for a general cross-diffusion two-competitive-predator

and one-prey system with predator-taxis, Commun. Nonlinear SCi. Numer. Simulat. 89 (2020) 105336.

[34] H.R. Akcakaya, R. Arditi, L.R. Ginzburg, Ratio-dependent prediction: an abstraction that works, Ecol. 76 (1995) 995.

[35] C. Cosner, D.L. DeAngelis, J.S. Ault, et al., Effects of spatial grouping on the functional response of predators, Theor. Popu. Biol. 56 (1999) 65.

[36] W. Ko, I. Ahn, Analysis of ratio-dependent food chain model, J. Math. Anal. Appl. 335 (2007) 498-523.

[37] W. Ko, I. Ahn, Dynamics of a simple food chain model with a ratio-dependent functional response, Nonlin. Anal.: RWA 12 (2011) 1670-1680.

[38] Z. Xie, Cross-diffusion induced Turing instability for a three species food chain model, J. Math. Anal. Appl. 388 (2012) 539-547.

[39] E.A. Autry, A. Bayliss, V.A. Volpert, Biological control with nonlocal interactions, Math. Biol. 301 (2018) 129-146.

[40] N. Mukherjee, S. Ghorai, M. Banerjee, Detection of turing patterns in a three species food chain model via amplitude equation, Commun. Nonlinear Sci. Numer. Simulat. 69 (2019) 219-236.

[41] N.D. Alikakos, L^p bounds of solutions of reaction-diffusion equations, Comm. Par. Diff. Eqs. 4 (1979) 827-868.

[42] H. Amann, Dynamic theory of quasilinear parabolic equations II. Reaction-diffusion systems, Diff. Int. Eqs. 3 (1990) 13-75.

[43] H. Amann, Dynamic theory of quasilinear parabolic systems III. Global existence, Math. Z. 202 (1989) 219-250.

[44] A. Pazy, Semigroups of linear operators and applications to partial differential equations, Springer-Verlag, NewYork, 1983.

[45] M.I. Rabinovich, A.B. Ezersky, P.D. Weidman, The Dynamics of Patterns, World Scientific, London, 2000.

[46] Q. Ouyang, Pattern Formation in Reaction-Diffusion Systems, Shanghai Scientific and Technological Education Publishing House, Shanghai, 2000.

[47] M. Cross, H. Greenside, Pattern formation and dynamics in nonequilibrium systems, Cambridge University Press, UK, 2009.

[48] Y.A. Kuznetsov, Elements of Applied Bifurcation Theory (3rd edition), Springer-Verlag, NewYork, 2004.

[49] J.P. Shi, X.F. Wang, On global bifurcation for quasilinear elliptic systems on bounded domains, J. Diff. Eqs. 246 (2009) 2788-2812.

[50] M.G. Crandall, P.H. Rabinowitz, Bifurcation from simple eigenvalues, J. Funct. Anal. 8 (1971) 321-340.

[51] M.G. Crandall, P.H. Rabinowitz, Bifurcation, perturbation of simple eigenvalues, and linearized stability, Arch. Rational Mech. Anal. 52 (1973) 161-180.

[52] A.N. Peterson, A.P. Soto, M.J. McHenry, Pursuit and Evasion Strategies in the Predator-prey Interactions of Fishes, Integrative and Comparative Biology, 61 (2) (2021) 668-680.

[53] T. Kato,Functional Analysis, Springer Classics in Mathematics, 1996.

[54] A.B. Medvinsky, S.V. Petrovskii, I.A. Tikhonova et al., Spatiotemporal complexity of plankton and fish dynamics, SIAM Review 44(3) (2002) 311-370.

[55] M. Garvie, Finite-difference schemes for reaction-diffusion equations modeling predator-prey interactions in MATLAB, Bull. Math. Biol. 69 (2007) 931-956.